Detection of Incipient Thermal Damage Of Carbon Fiber/Epoxy Composites Using Fluorescent Thermal Damage Probes

Tucker Layne Howie

A dissertation

submitted in partial fulfillment of the

requirements for the degree of

Doctor of Philosophy

University of Washington

2013

Reading Committee:

Brian D. Flinn, Chair

Alex K-Y. Jen

Peter Pauzauskie

Program Authorized to Offer Degree:

Materials Science and Engineering

University of Washington

Abstract

Detection of Incipient Thermal Damage Of Carbon Fiber/Epoxy Composites Using Fluorescent Thermal Damage Probes

Tucker Layne Howie

Chair of the Supervisory Committee:

Professor Brian D. Flinn

Materials Science and Engineering

Incipient thermal damage (ITD) of carbon fiber/epoxy composites occurs due to short term exposures to temperatures known to cause matrix degradation. ITD is a concern for composite parts because it can significantly reduce mechanical strength of the part, but it cannot be detected by common inspection techniques such as ultrasound and thermography. This paper focuses on using molecular probes whose fluorescence emissions changes irreversibly after thermal exposure as a means to quickly and efficiently detect areas of the composite that have been thermally exposed. These probes are referred to as thermal damage probes. In this research, two fluorescent thermal damage probes were designed and synthesized. These probes

were called AJNDE16 and AJNDE35. The fluorescence emission behavior of these probes in response to thermal exposure was characterized in several epoxy systems with cure temperatures ranging from room temperature to 177 °C. It was found that the fluorescence of both probes changed with thermal exposure as expected indicating there viability of the probes as sensors for thermal exposure.

Several potential issues with utilizing the probes were identified including oxidation of the matrix, temporal stability, the presence of carbon fibers, and the ability to detect localized thermal damage were investigated. Oxidation was found to quench the fluorescence signal, but the signal could easily be restored by removing the oxidation with light sanding. The temporal stability at ambient conditions was found to be excellent with no significant decrease in the signal observed over 18 months. The presence of carbon fibers was found to cause more scattering of the excitation light source, but otherwise did not have much of an effect on the measurements. The probes also exhibited excellent ability to detect a localized thermal exposure.

The activation kinetics of both probes was also measured and the probes were found to exhibit a first order reaction rate. Using the kinetic measurements, models were generated for both probes. It was found that using only one probe could indicate that a significant thermal exposure had occurred, but it was not capable of quantifying the amount of thermal exposure. To solve this issue, probes AJNDE16 and AJNDE35 were combined to form a multiplexed probe system. It was found that the fluorescence response of the multiplexed system to thermal exposure could be modeled as the superposition of the fluorescence emission peaks of the individual probes using the kinetic models. Utilizing ratiometric fluorescence measurements of the peak intensities at 540 and 560 nm, the multiplexed system was found to be capable of acting

as a time-temperature indicator (TTI) with a response on the temperature and time scale of ITD in CFRP. Using the multiplexed system model response curves for temperatures in the range known to cause ITD were generated. Due to difficulty determining the complete thermal history (time and temperature) of part, the responsive curves were utilized by setting a time or temperature of interest and estimating an effective value of the other parameter. To test the accuracy of the multiplexed system as a TTI, it was applied as a coating to a composite panel and exposed to a localized thermal event. Using the response curves it was found that the estimated parameter (time or temperature) matched very well with thermocouple data from the exposure.

TABLE OF CONTENTS

LIST OF FIGURES

LIST OF TABLES

1. INTRODUCTION

1.1 Incipient Thermal Damage of CFRP

Carbon fiber reinforced polymer (CFRP) composite materials have seen increasing usage in aerospace and automotive industries due to their high strength and stiffness, and low weight compared to metals such as steel and aluminum. One of the issues with using composites, however, is that they experience different damage mechanisms than metals and reliable inspection techniques for these new damage mechanisms need to be developed. The focus of this research is on detecting a particular type of damage in CFRP known as incipient thermal damage (ITD). ITD is the term given to thermal damage of CFRP that cannot be visibly detected, but has significantly reduced the mechanical properties of the composite. ITD is of significant concern for CFRP parts because it is not reliably detected by common NDI methods such as ultrasound and thermography.[1] The reason for this is that ITD occurs as a result of thermally-induced chemical changes to the matrix on a molecular scale, which is well below the practical detection limit for the above NDE methods.[2]

This research is particularly focused on detecting ITD in carbon fiber composites with epoxy matrices, which generally occurs in the temperature range of 200 ºC to 290 ºC although there is no definitive temperature range in the literature since the temperatures can be dependent on the epoxy system. ITD is known to be related to degradation of the matrix and fiber-matrix interface as no changes to the carbon fibers are observed in this temperature range.[3] A plot of short beam shear strength retention of a CFRP with an epoxy matrix as a function of thermal exposure time and temperature can be seen in Figure 1.1.

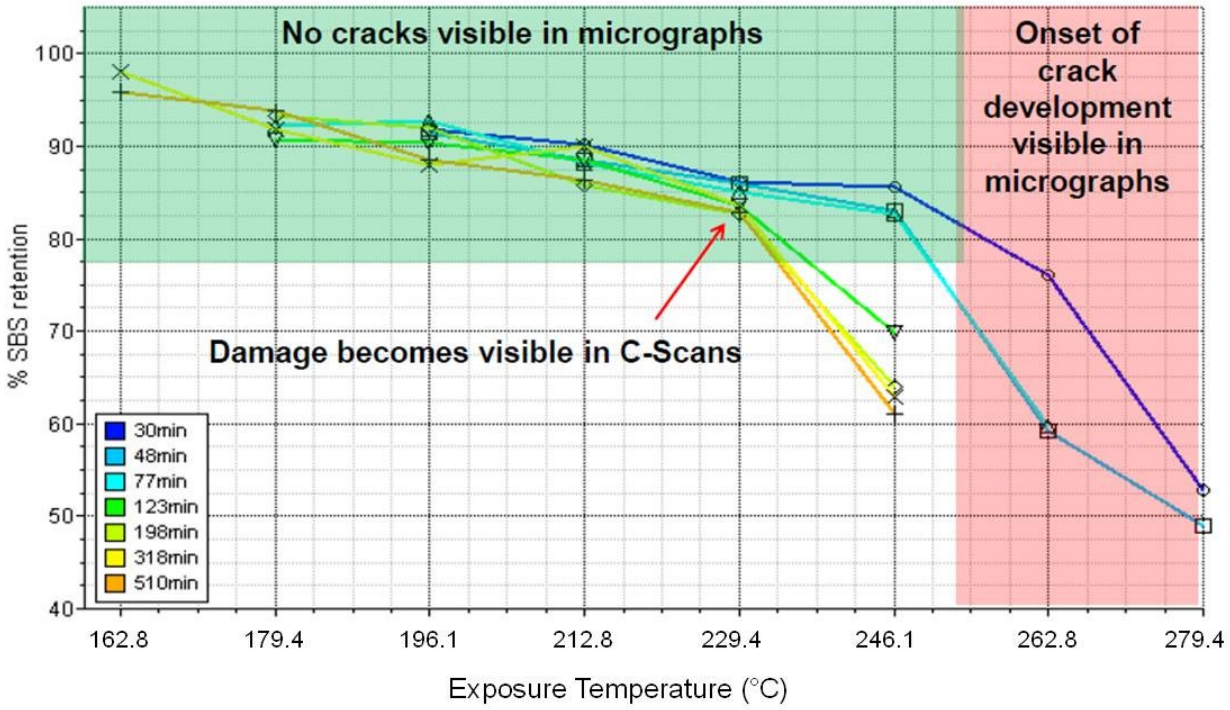

Figure 1.1 SBS strength retention of CF-epoxy composite as a function of time and temperature (chart courtesy of Dennis Roach, Sandia National Laboratory)

Figure 1.1 shows that almost 20 % of the SBS strength of this composite system is lost before the damage can be detected by ultrasound. This level of mechanical property loss can have a significant impact on the safety of flying the aircraft if it has primary structural parts made with CFRP. Without the ability to detect and repair this damage the parts have to be overdesigned such that the part still has enough load bearing capability to safely fly with the damage. This can be costly both in terms of the extra weight which reduces fuel efficiency and also extra material. Thus it is advantageous to have a reliable inspection for ITD, which would allow engineers to reduce the amount of overdesign necessary for the part.

In this chapter a brief discussion of the degradation mechanisms of the matrix and composite that lead to ITD will be presented. This will be followed by a review of current

inspection techniques for ITD. Lastly the project motivation and document organization will be presented.

1.1.1 Thermal Degradation of Epoxy

There is a significant amount of literature available on the thermal degradation mechanisms of epoxy-amine systems. For the most part the degradation studies are performed using thermogravimetric analysis (TGA) and Fourier transform infrared (FTIR) spectroscopy to determine the degradation mechanisms and energies. The studies cover a wide range of epoxy monomers and amine curing agents, but in general the resulting degradation mechanisms and products are similar regardless of the resin system. These degradation mechanisms are discussed below.

TGA has been used to study the degradation of epoxies in many different epoxy-amine monomer combinations. Even though there are quite a few epoxy-curing agent pairs in the literature, the TGA curves all exhibit a similar two-step degradation process. The first large mass loss occurs between 300-350 ºC and is found to occur in both oxidative and nonoxidative environments and has been attributed primarily to dehydration of secondary alcohol groups.[4, 5] The second step is a complete degradation of the epoxy that only occurs in oxidative conditions at higher temperatures.[5] The TGA measurements do not show significant mass loss in the range of 200-290 ºC which is the temperature range where ITD is found to occur though. However, it was found that under vacuum at 250 ºC, that significant mass loss was observed. These losses were attributed to thermolysis of the network that results in chain scission and occurs regardless of the oxidative environment. The difference between the vacuum and air mass losses is believed to be caused by thermolysis degradation products that were volatile under primary

vacuum, but not in air. Although the authors also point out that mass loss in air, may be partially offset by increases in mass from the polymer reacting with oxygen.[6]

Fourier transform infrared (FTIR) spectroscopy studies have provided more meaningful information about epoxy degradation in the ITD temperature range. FTIR studies of the thermal degradation of epoxies have shown that the degradation of epoxies in the temperature range for ITD is complex and involves multiple oxidative pathways.[7] The studies found that thermo-oxidation of the epoxy network resulted in the production of water, hydroperoxides, phenolics, aliphatic and/or aromatic aldehydes and ketones, and amides.[5, 7, 8] The dehydration of the secondary alcohols produces water and an allyl group. The allyic hydrogen generated during the dehydration reaction is relatively easily abstracted by O_2 or hydroperoxides and this eventually leads to chain scission and breakdown of the network. The breakdown of the network has been associated with significant reduction in the glass transition temperature (T_g). Formation and subsequent decomposition of hydroperoxides result in the production of the carbonyl and amide species.[5, 7, 9, 10] FTIR measurements under nonodixative conditions exhibited almost no change for temperatures up to 290 ºC, which can be considered the upper temperature threshold for ITD in composites.[8]

The oxidation of epoxy samples has been found to be diffusion limited.[4, 6, 11] Buch and Shanahan profiled the oxygen content as a function of depth up to 100 μm from the surface in as-cured and aged samples. The as-cured samples showed a relative constant level of oxygen throughout the sample, but after aging for 115 hours at 250 ºC there was a gradient in the oxygen content until about 50 μm. This region was believed to contain products of the thermo-oxidation of the epoxy and was called the thin oxidized layer (TOL). The levels of oxygen in the aged samples below the TOL was lower than that found in the as-cured samples, which the authors

believe was indicative of degradation products containing oxygen intrinsically trapped in the bulk during curing diffusing to closer to the surface.[6]

It should also be noted that several authors reported yellowing or darkening of the matrix was observed for samples heated in air.[6, 7, 9, 12-14] No change in color was observed for samples heated in nitrogen or vacuum environments indicative that the darkening of the matrix is a result of products from the thermo-oxidation of the matrix.[6] The darkening of the matrix has been attributed to the formation of highly conjugated structures during the thermo-oxidation process.[7, 15] UV-Vis absorbance measurements on an epoxy sample heated at 100 ºC for up to 350 hours showed an increase in absorbance at wavelengths between 300 nm and 700 nm with no maximum apparent. The increase in absorbance was found to be greater at shorter wavelengths.[13]

1.1.2 Thermal Degradation of CFRP

Thermal damage of composites can lead to a significant reduction of matrix dominated mechanical properties such as flexural strength, compression after impact (CAI), and interlaminar shear strength (ILSS), and can cause delaminations, fiber-matrix debonding, decreases in T_g and embrittlement and cracking of the matrix.[2, 16, 17] ITD is considered to be the onset of thermal damage to composites and has been to known to decrease the mechanical properties up to 60 %, before damage is detected by ultrasound or other inspection techniques.[2] Very little literature is available on ITD of composites as most of it is focused on long term thermal exposures on the order of hundreds of hours at lower temperatures compared to ITD which generally occurs within a time scale that is better measured in minutes. However, the damage mechanisms are similar between the two types of thermal exposures; the main difference

is the amount of oxidation that occurs. Thus it is possible to discuss the damage mechanisms of ITD based on the literature for longer thermal exposures.

As described in the previous section, epoxy degradation is believed to be mainly caused by thermo-oxidation of the matrix that results in chain scission and breakdown of the network.[18, 19] Although the matrix degradation is mainly responsible for the mechanical property loss, the carbon fibers play an important role in the damage development of composites. In composite parts it was found that oxidation grows faster in the axial direction (along the fibers) than the transverse direction.[20-22] This anisotropic oxidation growth was not observed in bulk resin samples. In composites, local diffusion of oxygen can be affected by factors such as resin shrinkage, residual stresses between plies (interlaminar) and at the fiber-matrix interface, and even the presence of a sizing.[17, 19-21, 23, 24] All these factors can lead to anisotropic growth of the oxidation layer. An example of this is shown by Tandon et al. who determined that neighboring plies affects the oxidation growth. In the study, it was found that oxidation was increased in plies with a 0 º neighbor, while the less oxidation growth was observed in plies next to ply oriented 90 º to the free surface.[20, 21] A good illustration of this oxidation anisotropy can be seen in Figure 1.2. The light parts near the left edge are the oxidation layer.

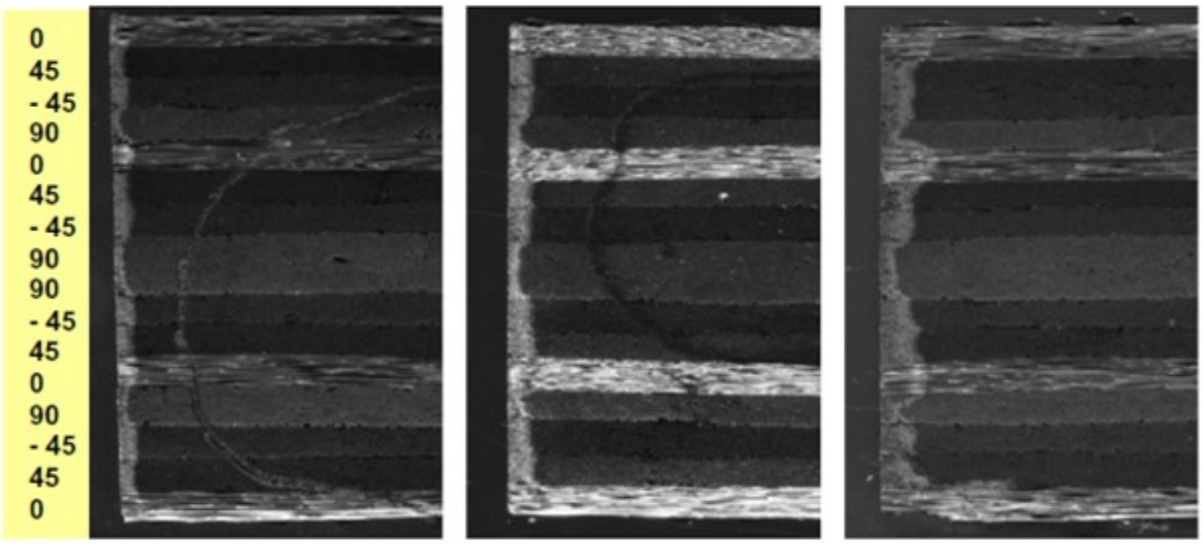

Figure 1.2 Effect of ply orientation on oxidation growth in polyimide-carbon fiber composites aged for various times at 288 ºC[20]

As aging time increases, the stresses due to the shrinkage of the matrix cause debonding at the fiber-matrix interface which leads to the development of cracks. These cracks provide pathways for further oxygen penetration into the composite and thus increasing oxidation as aging continues.

As with the bulk epoxy, a significant difference was observed in the composite samples that were heated in air or nitrogen. Figure 1.3 shows SEM images taken of composite samples that have been subjected to 500 thermal cycles between -50 and 180 ºC in nitrogen and air. The sample treated in N_2 does not exhibit any significant damage due to the thermal cycle. The small differences in the fiber matrix level are caused by polishing of the sample. On the other hand, the sample treated in air exhibits signs of severe matrix shrinkage as seen by the large hollow areas between fibers confirming that oxidation plays a significant role in the thermal degradation of composites.

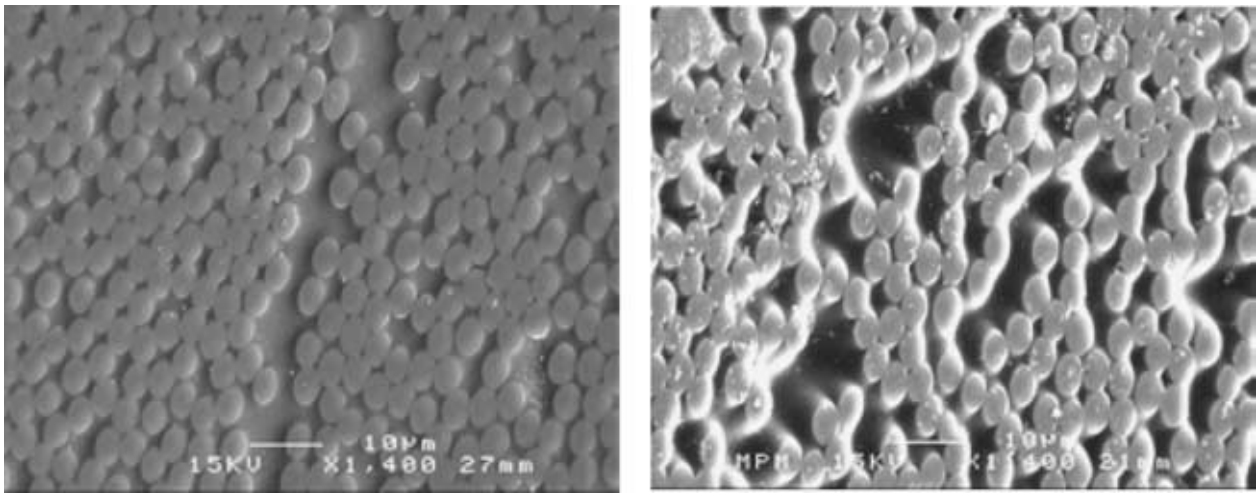

Figure 1.3 SEM images of carbon fiber epoxy composites after 500 thermal cycles between -50 and 180 ºC in (a) nitrogen (b) air[25]

1.1.3 Kinetics of ITD of CFRP

A full study of the kinetics of the degradation of CFRP in the range of ITD was not found in the literature. Some kinetic studies have been done on the degradation of the epoxies using TGA measurements which may be relevant to the discussion though. It is important to note, however, that there some significant differences in the literature for kinetic studies of epoxy degradation even for the same epoxy system. In one case, the reported activation energies for the first stage of epoxy degradation for a certain epoxy ranged from 43-138 kJ/mol.[4] For another epoxy a range of 126-196 kJ/mol was reported.[4, 26, 27] One of the issues with doing analysis of degradation kinetics with TGA is that the results are dependent on the experimental conditions and analysis method.[28, 29] One of the difficulties in analyzing the kinetics of epoxy degradation is that the kinetics due not obey an order reaction model. In fact, it is probable that several different degradations mechanisms which all fit different kinetic models occur simultaneously.[4, 26] The wide range of activation energies reported may be due to parameter distortion by using an inappropriate kinetic model function.[26]

Several authors report an analysis method called the invariant kinetic parameter (IKP) method which is independent of the experimental conditions and does not assume a particular kinetic model function.[4, 27-29] Instead the IKP method compares many different kinetic models and determines the probability that a given model fits the experimental results. Using the IKP method to analyze 18 kinetic models, it was found that the most probable kinetic model for degradation of a TGDDM-DDS epoxy was a diffusion limited model, but that phase boundary reactions and potential law reactions may also be present.[4] Another study on the same epoxy found that a reaction order rate law may be applicable as well.[26]

In one study it was found that the activation energy for the first stage of epoxy degradation was the same in air and nitrogen atmosphere indicating that the first stage of degradation is not dependent on oxygen.[27]

1.2 NDE Techniques for Detecting Incipient Thermal Damage

Although ultrasound techniques are not adequate for reliably detecting ITD, several other NDE techniques have been utilized as potential methods for detecting ITD. Of these techniques Fourier Transform Infrared (FTIR) spectroscopy and laser-induced fluorescence (LIF) have shown the most promise.[30] Thermoelastic characterization of the composite has also recently been proposed as method to detect ITD.[1, 31] A brief discussion on the detection of ITD using these methods will be given in this section.

1.2.1 FTIR

As described in section 1.1.1, thermo-oxidative degradation of the epoxy matrix results in the formation and loss of several different organic functional groups. FTIR is well suited to

measuring these types of chemical changes. There are many different techniques that can be used to collect FTIR spectra of samples including transmission, attenuated total reflectance (ATR), specular reflectance, and diffuse reflectance.[32] For field inspections specular and diffuse reflectance measurements work better because they do not require mechanical contact with the material. Due to the significant scattering of the IR radiation by the carbon fibers, diffuse reflectance is generally preferred when measuring CFRP composites unless the surface is resin rich.[33] Recently handheld FTIR devices based on these reflectance measurements have become commercially available.

Dara et al. studied the relation between the drop in ILSS and changes in the diffuse reflectance infrared Fourier transform (DRIFT) spectra of a composite heated for 30 min at temperatures between 190 and 250 ºC. The data showed good correlation between the changes in the carbonyl and phenyl band integrals. The correlations between the loss in ILSS and the change in the FTIR band integrals is shown in Figure 1.4.

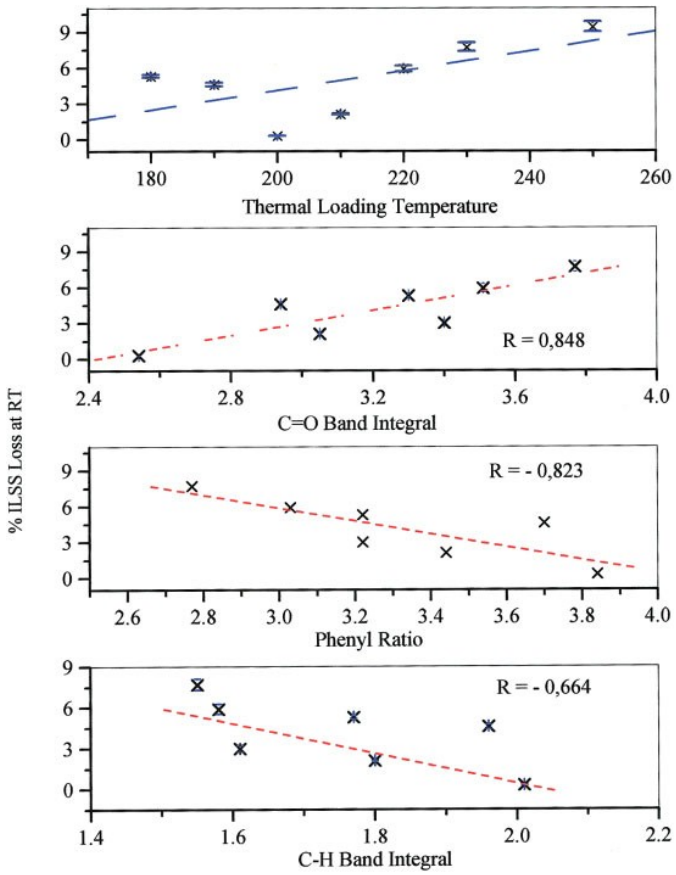

Figure 1.4 Relation of ILSS loss to change in FTIR band integrals as a function of thermal exposure[34]

While FTIR has been shown capable of detecting ITD, it does have some limitations for field inspections. Some of the issues with using FTIR for ITD detection are that FTIR has a relatively limited spot size compared to the potential size of the parts to be inspected. As mentioned previously, one of the characteristics of ITD is that it is not visibly detectable and due to the small spot size of the FTIR devices locating localized thermal damage on large panels is a time consuming process unless the location of the damaged area is already known. Another drawback of using DRIFT is that it is difficult to predict bulk mechanical properties based on surface chemical analysis especially for thicker laminates. In addition, the FTIR signal is

sensitive the amount of resin present so some scatter can be found between samples that are resin rich and resin poor.[35]

1.2.2 Laser-induced Fluorescence

As the name suggests laser-induced fluorescence (LIF) uses a laser to excite fluorescence from the matrix of the composite. Since the fluorescence of molecule is very sensitive to the local environment changes can be observed in the fluorescence spectra of the matrix as the material degrades. The setup for the LIF fluorescence measurement can be seen in Figure 1.5.

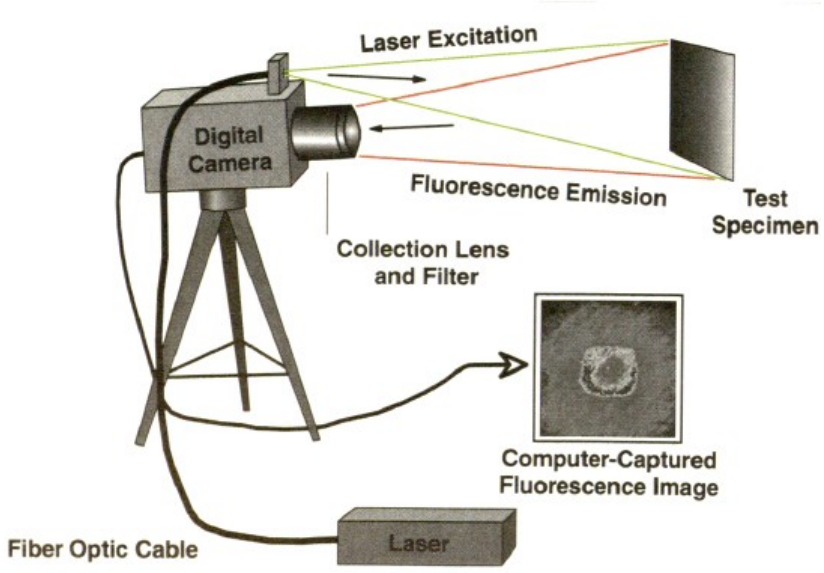

Figure 1.5 Laser-induced fluorescence measurement setup [30]

It has been found that at low levels of damage the fluorescence intensity increases sharply at first, but decreases as the level of damage increases to the point where the fluorescence is quenched. Since the intensity does not increase monotonically with strength loss it is only useful as a qualitative measure to locate damage areas. Bathochromic shifts in the peak wavelength λ_{max} are also observed as the damage level increases. The shift of λ_{max} does correspond monotonically to increase loss of flexural strength and can be used as an estimate of the damage.

However, the measured λ_{max} cannot be directly correlated to mechanical strength since this measurement is only sensitive to the surface and may not correspond to the integrity of the bulk material.

The advantage of LIF is that it is a viable measurement for fast wide-area inspection of the surface of composite parts for ITD as shown by the detection setup in Figure 1.5. However, like FTIR it suffers from the same problem of relating surface characterization to bulk properties. In addition, the correlation between the fluorescence behavior and the cure and degradation products is not well understood. Thus it is difficult to know how applicable LIF is to different resin systems.[35]

1.2.3 Thermo-elastic Characterization

Thermo-elastic characterization of ITD is performed using horn to generate acoustic waves that propagate through the material. As the acoustic waves propagate through the sample, some of the energy of the waves is converted into heat due to thermo-elastic effects. This generated heat causes a small increase in the temperature of the sample, which is detected by a sensitive IR camera placed at the backside of the sample. From this measurement the slope of the change in temperature over change in amplitude ($\Delta T/\Delta A$) can be plotted. As the thermal damage to the composite increases the slope of ($\Delta T/\Delta A$) begins to decrease due to the change the thermo-elastic properties of the composite. The setup for thermo-elastic characterization of heat damage in CFRP composites can be seen in Figure 1.6.

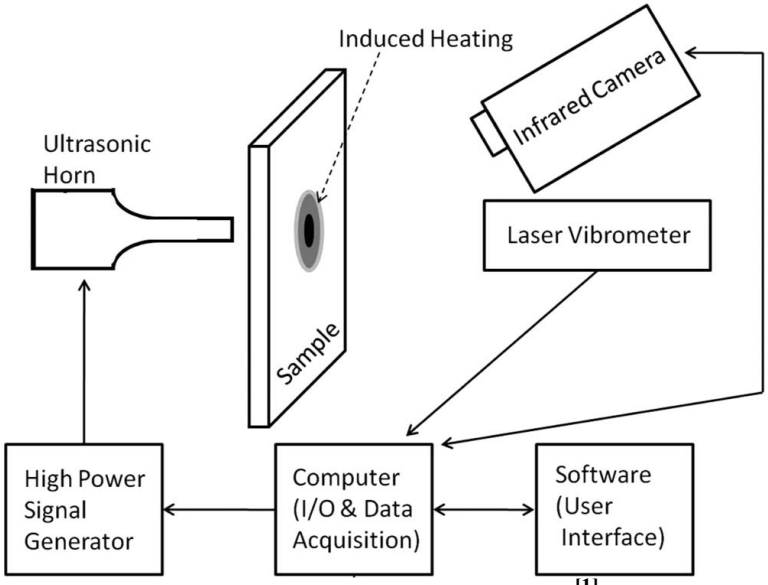

Figure 1.6 Setup for thermo-elastic characterization of ITD [1]

Thermo-elastic characterization is different from the other measurements described above in that it is a volumetric measurement instead of a surface measurement. However, it still does not provide information as to the depth of the damage since it only measures the change in temperature through the whole part. How sensitive this technique is to early signs of ITD is not yet established either.

1.3 Project Motivation

This research is part of a project funded by the Boeing Company #BL8DL and it is a collaborative effort between the Boeing Company, the Flinn research group, and the Jen research group in the Materials Science & Engineering department at the University of Washington. The overall project goals are to develop a system of aerospace resins and coatings suitable for detecting mechanical and thermal damage to aerospace composite parts. The Jen group is responsible for design, synthesis, and characterization of probe molecules. The Flinn group is responsible for incorporation of probe molecules into aerospace polymers, fabrication and testing

of test specimens, and characterization of probe responses in various matrices and external conditions.

The motivation for this project is to establish a NDI technique that can efficiently detect areas of CFRP that have been subjected to localized thermal exposures sufficient enough to cause ITD in the composite. To accomplish this task, matrix and coatings epoxies are functionalized by doping them with a fluorescent thermal damage probe. These thermal damage probes are sensitive to temperatures in the range of ITD and exhibit irreversible changes to their fluorescence properties upon sufficient exposure to these temperatures. The measurement concept is similar to that of LIF; however, it relies on extrinsically doped fluorescent probes for the fluorescence response. This has advantages in that the response of the probes to thermal exposures is known and the probes can be used in many different epoxy systems for consistent fluorescence responses. The probes also have the advantage that it is possible to tailor the wavelength, and the time and temperature response to fit the needs of the application. In addition, the probes have a significantly higher quantum yield than the autofluorescence of the matrix epoxies so it easier to observe and measure changes to the fluorescence in resin poor environments such as those obtained from sanding during composite repair.

This method of inspection has the potential to be a standalone inspection method or as an efficient way to locate localized thermal damage for further measurements with techniques such as DRIFT spectroscopy. There is also a potential to be developed as a tool for not just locating damaging, but also providing an estimation of the thermal exposure history to help guide repairs.

The focus of this doctoral dissertation is to develop the use of the thermal damage probes as an inspection method for ITD detection and to determine what factors affect the probe response.

1.4 Document Organization

In this first chapter, a brief background on ITD in CFRP composites was presented along with an description of the NDI techniques used for detecting ITD. The second chapter contains a literature review of temperature sensors that utilize fluorescence probes and details the proposed mechanism for the fluorescence thermal damage probes used in this research. The third chapter describes the materials and experimental methods used in this research. In the fourth chapter, the fluorescence responses of the thermal damage probes are characterized in structural epoxies. In chapter 5 the probe-doped epoxies are tested as a composite matrix and as a coating material for CFRP panels. In addition, factors that affect the measurement and applications of the probes are discussed. The sixth chapter contains the work done to characterize the kinetics of both thermal damage probes and the model developed from the kinetics measurements. The seventh chapter describes the development of multiplexed probe coatings and their potential use as time-temperature indicators (TTI) for detecting ITD in CFRP. In the last chapter the conclusions and future work for this research are presented.

2. TEMPERATURE SENSING USING FLUORESCENT PROBES

As stated in the previous chapter, the focus of this research is detecting ITD using fluorescent probes extrinsically doped into an epoxy matrix. In this chapter a brief background on fluorescence will be given followed by a review of the use fluorescent probes for temperature sensing. The concept of a time temperature indicator is also introduced. The mechanism for the fluorescent thermal damage probes to detecting ITD in composites is presented, followed by an introduction to the concept of ratiometric fluorescence.

2.1 Fluorescence

Fluorescence is an energy transfer process in which a photon of light is absorbed by a molecule and emitted as a longer wavelength. Fluorescence is one of the de-excitation paths that can occur when a molecule absorbs a photon. A Jablonski diagram is generally used to envision the different de-excitation pathways of the electron excited by a photon. An example of a Jablonski diagram can be seen in Figure 2.1.

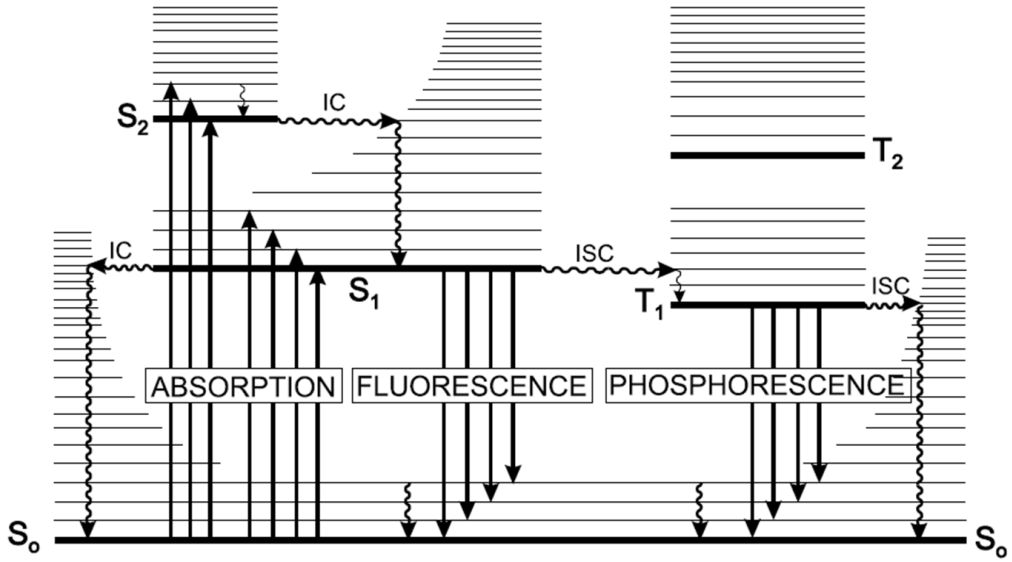

Figure 2.1 Jablonski diagram[36]

In the Jablonski diagram, the electronic states (e.g S_0, S_1) are represented by thick horizontal lines and the lines in between the electronic states represent vibrational energy levels within those states. Straight arrows represent transitions due to the absorption or emission of a photon, while the squiggly arrows represent non-radiative transitions. As shown in the Jablonski diagram, a molecule starts in the ground state S_0. Upon absorption of a photon of sufficient energy an electron is promoted to an excited state that has energy greater than S_1. Once the electron is in the excited state it usually loses some energy to vibrations and relaxations and thus drops to a lower energy level in the excited state. This process is known as internal conversion

(IC). The molecule can then either return to the ground state by continued IC (a non-radiative process) or by emitting a photon (fluorescence). Since the electron loses energy during the process, the photon emitted due to fluorescence is always of a longer wavelength than it absorbed. It should be noted that other potential pathways for de-excitation exist such as phosphorescence and delayed fluorescence through a process known as intersystem crossing (ISC). ISC reduces the number of electrons that de-excite through fluorescence and thus decreases the fluorescence quantum yield.[36]

Fluorescent molecules have characteristic absorption and emission spectra that are defined by the energy levels and the vibrational states within those levels. By changing the molecular structure of the molecules, the absorption, emission spectra, and the quantum yield of the molecules can be significantly altered.[36] Increasing the conjugation length (alternating single and double bonds) leads to a lowering of the energy gap between the ground and excited states and as a result a bathochromic shift is observed in the absorption and emission spectra of the molecule. This is easily seen in the series of linear aromatic hydrocarbons naphthalene, anthracene, napthacene, and pentacene where the addition of a phenyl ring causes these molecules to emit fluorescence in UV, blue, green, and red respectively.[36] Other changes to molecular structure are difficult to generalize because substituents on the aromatic ring can affect the energy levels of a molecule, but such changes are highly dependent on the nature, position, and geometry of the substituent on the ring. It is known that adding atoms with high atomic numbers generally decreases the fluorescence quantum yield of the molecule, but increases the phosphorescence quantum yield due to increased intersystem crossing through spin-orbit coupling. Incorporating electron donating groups (donors) such as –OH, -OR, $-NH_2$, $-NR_2$ often results in increased absorption and broad, structureless peaks compared to the parent aromatic

molecule.[36] The effects of electron withdrawing groups (acceptors) such as carbonyl and nitro compounds are more difficult to predict. The fluorescence of molecules containing carbonyl groups such as ketones is often strongly dependent on the polarity of the environment. Nitro groups often introduce efficient ISC and IC and as result the fluorescence is often almost undetectable.[36]

The above paragraph lists just a few general examples of how changing the molecular structure can change its fluorescence behavior. This illustrates that there are many possible ways to alter the fluorescence properties of a molecule which can be used to tailor a fluorescent probe to specific applications.

2.2 Temperature Sensing Using Fluorescent Probes and Polymers

Fluorescence molecules have a wide range of sensor applications because they are highly sensitive to their local environment such as pH, temperature, polarity, and viscosity.[36-38] Since this research is on thermal damage, the focus of this section will be on temperature sensitive probes.

There are two types of fluorescence based temperature sensors seen in the literature, reversible and irreversible. Reversible fluorescence temperature sensors have many applications for in-situ measurements of temperatures, but they are not suited for ITD detection because the measurements would not be taken during the thermal exposure, but likely sometime afterwards. To learn more about reversible fluorescent temperature probes, readers are referred to the review articles by Pucci and Hu.[39, 40] Irreversible temperature sensors where developed by Weder et al. using cyanooligo (p-phenylene vinylene) (cyano OPVs).[41-43] The cyano OPVs are mixed into a polymer melt and then the melt is rapidly quenched to kinetically trap the dispersed molecules in

a monomer state. When the host polymer is heated above its T_g, the molecules form aggregates, which leads to the formation of excimers that cause an irreversible change in fluorescence. Fluorescence changes due to monomer/excimer aggregate emissions are common mechanisms in mechanochromic based fluorescence applications.[43-45] In fact, these types cyano OPVs have the potential to be used as time-temperature indicators and mechanochromic probes in the same system.[43] The kinetics of the color change can be tuned by manipulating the probe concentration, solubility, or structure and/or altering T_g of the host matrix. The kinetics of a given blend were found to follow an Arrhenius behavior making these probe-doped polymers potentially useful as a time-temperature indicator (see section 2.3) since the kinetic behavior can be easily monitored. An example of how changing T_g of the host polymer affects the kinetics of the fluorescence can be seen in Figure 2.2.

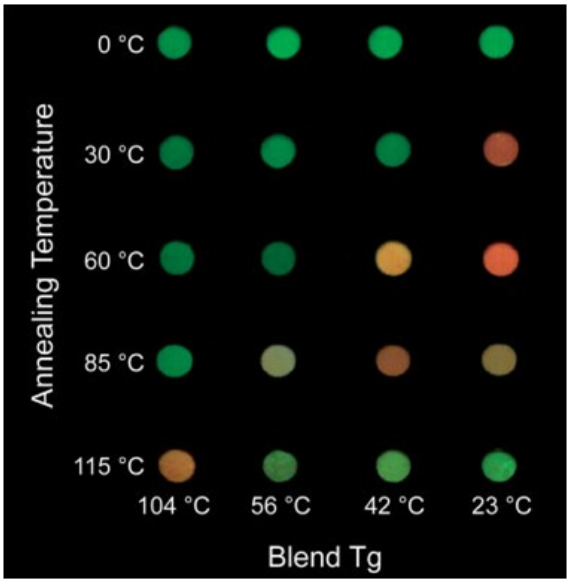

Figure 2.2 Effect of blend T_g on and annealing temperature on fluorescence color in cyano OPV-doped poly(alkyl methacrylate) blends [42]

As seen in Figure 2.2 when the initially quenched samples are heated there is a significant difference in the fluorescence behavior observed depending on the T_g of the poly(alkyl

methacrylate) blends. When T_g is low raising the annealing temperature causes a change from the green monomer fluorescence to that of the orange excimer fluorescence. At higher T_g, the change in fluorescence does not occur until the annealing temperature is above T_g. At temperatures well above T_g a return to the green monomer fluorescence is observed. This return to monomer fluorescence is believed to be caused by a decrease in the aggregation extent due to increased solubility and mobility of the probe and/or the development of large probe aggregates that self-quench excimer emission.[42] Even though the fluorescent probes are often mixed into the polymer at temperatures exceeding 300 ºC, the highest reported use temperature for these temperature sensors is 200 ºC.[41] Although most of the work on TTI has been done in thermoplastic polymer matrices, the same quenching mechanism was also shown to work in an epoxy coating as well.[46]

Since the mechanism for the TTI systems was driven by T_g of the host polymer, the authors also investigated the effects of solvent absorption on the monomer to excimer transition. As expected, solvent absorption was found to also cause the monomer to excimer transition similar to that caused by heating the samples above T_g.[46] While this result could be useful for applications for detecting solvent absorption, it may be detrimental to applications where only thermal exposure of interest because it is possible for the probes to transition between the monomer and excimer states such that the thermal exposure indicated by the fluorescence would be significantly longer than it actually was.

2.3 Time Temperature Indicators

A TTI is different from a temperature sensor in the sense that it gives a record of the cumulative time-temperature history of the object of interest and not just the current temperature.

The vast majority of TTI literature is focused on the food packaging industry and as a way to monitor the shelf life of packaged food subjected to temperature abuse, although TTI have potential in many other industries where products are subject to degradation by temperature abuse.[47-53] This includes products such as pharmaceuticals, medical devices, chemical reagents, cosmetics, paints and coatings, photographic materials, avionics, and plastics.[52] In the TTI literature two-types of TTI are indentified. The first type of TTI is active at all temperatures in the range of interest and provides a measure of the cumulative history of the thermal exposure. These are known as all-temperature TTI, full-history TTI, or time-temperature integrators. The second type of TTI activates only after a threshold temperature has been reached. This type is called partial history or threshold TTI.[51, 53] For ITD, the threshold temperature TTI is of more interest because ITD is limited below certain temperatures as described in section 1.1.

In order to select or design a TTI for an application the kinetics of the reaction of interest and its dependence on temperature should be well characterized such that a TTI with similar kinetics and temperature dependence can be applied. For a degradation process this means that at a given temperature the TTI should activate and reach its end point on the same time scale as the degradation process it is monitoring. In many cases in the literature, the rate constant or activation energy of the food degradation and the TTI are compared as the means of selecting an appropriate TTI.[51-53] Where the rate constant is temperature dependent and it is found to follow the Arrhenius relation in equation 1.1.[52]

$$k = Ze^{\left(-\frac{E_a}{RT}\right)} \qquad \text{equation 1.1}$$

Where k is the rate constant whose units are dependent on the order of the reaction, Z is preexponential factor with the same units as the rate constant, E_a is the activation energy, R is the universal gas constant, and T is the temperature in Kelvin. It should be noted that finding a TTI

with a similar rate constant or activation energy is only effective when the degradation process and the TTI response are fit by similar kinetic models.

The TTI response has been achieved through many different mechanisms such as a biochemical reaction between an enzyme and a substrate, a redox reaction, polymerization, diffusion-based processes, as well as phase changes in the material upon heating that causes a fluorescence change.[50, 53, 54] In most cases the amount of degradation or spoilage is displayed as an easily observable color change so the consumer/supplier can easily determine visually that the product has expired; however, for detecting ITD on aircraft it is preferred that the ITD indicator not be readily visible to the passengers. Thus this research is focused on fluorescence where color changes can only be seen under the proper excitation light. An example of an enzyme-based TTI can be seen in Figure 2.3.

Figure 2.3 Color response of Urease-based TTI at 20 °C[47]

2.4 Fluorescent Thermal Damage Probe Mechanism for Detecting ITD

In this section the proposed mechanism for the novel fluorescent thermal damage probe known as AJNDE16 is presented. In order for the thermal damage probe to be an efficient and reliable tool to detect the ITD of CFRP, the probing molecule is required to respond to the proper temperature window. From the molecular level point of view, dynamic covalent chemistry and non-covalent intermolecular interactions, triggered at elevated temperatures, generally offer intriguing opportunities in inducing fluorescence change. Typically, non-covalent interactions

are generally more susceptible to the external environmental factors, and thus kinetically labile. In this sense, thermally induced covalent chemistry is the more suitable and reliable approach to design efficient fluorescent molecular probes for detection and evaluation of the thermal damage in CFRP samples.

As defined by the temperature range for ITD, the thermal damage probes are expected to operate in temperatures in excess of 200 ºC. Development of thermochromic molecular probes operating at this temperature range is a major challenge since most fluorescent molecules are not thermochemically stable at such temperatures. There was no relevant literature on fluorescent probe molecules used in these temperature ranges to the best of the author's knowledge. On the other hand, there are few chemical reactions that can be applied to induce fluorescence changes before and after the reactions as long as molecular structures of derivatives of the probes after the high temperature exposure can be stabilized. The proposed mechanism for the thermal damage probes AJNDE16 and AJNDE35 is illustrated in Figure 2.4. Specific details of the chemical structure of the probes AJNDE16 and AJNDE35 cannot be presented for intellectual property reasons.

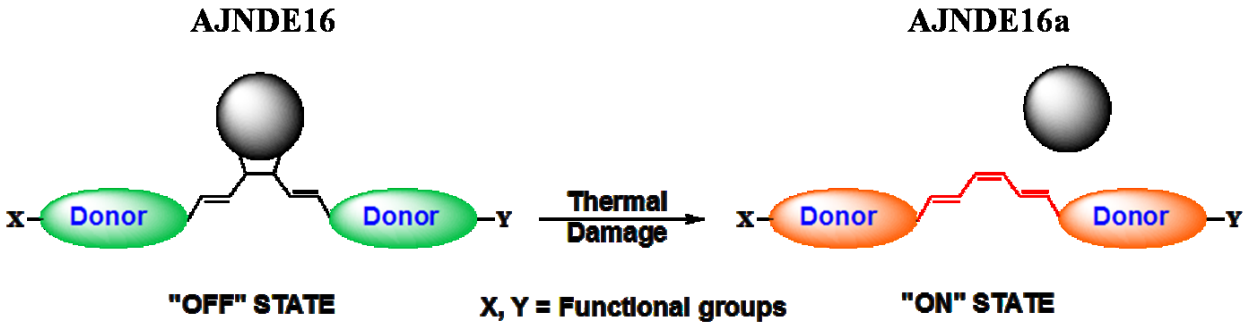

Figure 2.4 Mechanism of thermal damage probe AJNDE16

From Figure 2.4, the probe starts in the off state which is the AJNDE16 molecule. In this state the probe exhibits a blue-green fluorescence under a UV excitation source, but at longer

excitation wavelengths no fluorescence is observed. The conjugation bridge of AJNDE16 is broken by the presence of another molecule that has bonded to the molecule indicated by the gray sphere. When sufficient thermal energy is applied, the molecule interrupting the conjugation bridge is released and subsequently the conjugation bridge is restored. Restoring the conjugation bridge lowers the energy gap E_g between the ground and excited states causing a bathochromic shift of the fluorescence emission of the probe to an orange fluorescence, which signals the on state. The on state molecule will be referred to as the AJNDE16a molecule. This sort of thermochromic behavior caused by changes in the conjugation length has been shown in the literature.[55-58] This change in fluorescence is permanent because the released molecule degrades in the temperature range needed to convert the probe to the on state. Thus once the probe is on, it is expected to stay on. This irreversibility of the fluorescence is key to the design as the measurements for ITD would not be made in-situ, thus the fluorescence of the molecule needs to be stable between inspections. AJNDE35 operates with a mechanism similar to that of AJNDE16, but AJNDE35 exhibits a blue fluorescence in the off state and AJNDE35a (on state) has a green fluorescence. Characterization of the fluorescence response of probes AJNDE16 and AJNDE35 to thermal exposure is described in detail in chapter 4.

An illustration of the concept of using the thermal damage probe for detection of ITD in composites is shown in Figure 2.5. As shown, when the probe-doped composite is subjected to sufficient thermal exposure in a localized area, the probe is turned to its on state and by using an excitation light the area that has been thermally exposed will exhibit a strong fluorescence emission.

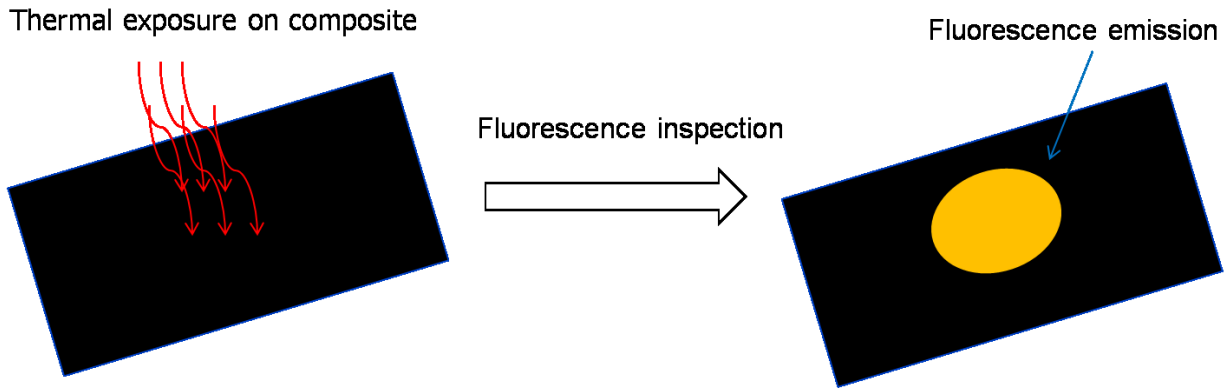

Figure 2.5 Detection of ITD in Composite doped with thermal damage probe

Design and synthesis of thermal damage probes AJNDE16 and AJNDE35 was carried out by our collaborators in Prof. Jen's group. The AJNDE16a and AJNDE35a molecules were also synthesized independently for verification that probes AJNDE16 and AJNDE35a were converting to AJNDE16a and AJNDE35a respectively upon heat-treatment as expected.

2.5 Ratiometric Fluorescence

The design of the thermal damage probe described in the previous section is based on a probe with a single fluorescence emission. Since the peak wavelength of the activated probe does not change with exposure time or temperature this means that only a change in intensity will be measured as more probe molecules turn to the on state as is shown in chapters 6. Fluorescence intensity measurements are difficult to reproduce even on the same sample unless strict experimental controls are utilized due to factors such as variations in excitation source intensity, optical alignment, probe location, and excitation area.[38, 59] To complicate the matter further, oxidation of the epoxy that occurs for longer exposure times can decrease the measured fluorescence intensity even though it is possible more probe molecules are activated.[2, 30] Thus with only a single probe it is difficult to provide quantitative information about the thermal exposure and activation of the probe fluorescence mainly provides the qualitative information

that a thermal exposure significant to active the probe occurred.[59] However, by combining the probe response with another fluorescence signal, a method known as ratiometric fluorescence may be used which may be able to yield more quantitative information about the thermal exposure.[38, 59, 60]

Ratiometric fluorescence is a sensing technique that monitors the ratio of intensity between two fluorescence wavelengths. Compared to a single emission system, ratiometric fluorescence provides additional channels of information and is independent of such issues as photobleaching, excitation source fluctuations, and differences in detector sensitivity.[36, 59] The simplest case of ratiometric fluorescence is where a second fluorescent probe is introduced into the system. The second probe can either act with the existing probe or be a reference dye to account for environmental changes to the material.[59] A diagram illustrating the difference between using a single emissive probe and ratiometric fluorescence with a reference probe can be seen in Figure 2.6.

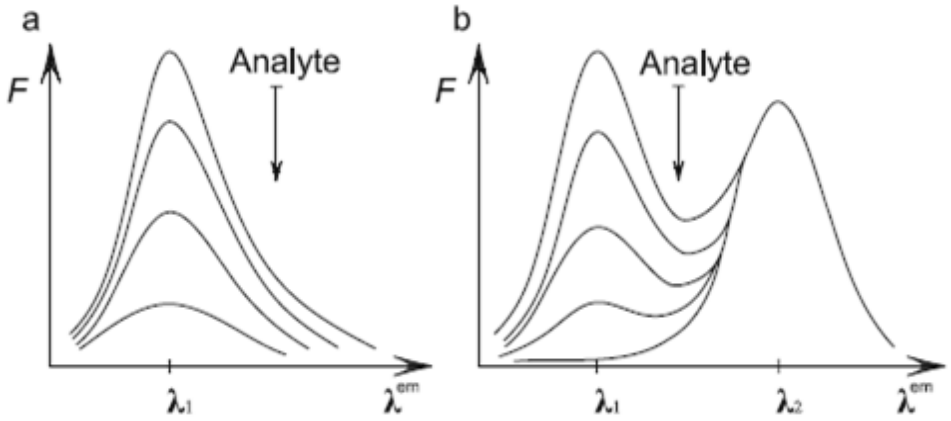

Figure 2.6 Effect of quenching by analyte in (a) single emission (b) ratiometric emission with reference probe[59]

In Figure 2.6, all that can be observed for the single emission is a decrease in the fluorescence intensity in the presence of the analyte. Due to the difficult of making reliably

repeatable measurements of the fluorescence intensity, it could be very difficult to obtain quantitative information about the analyte.[59] In the case of the ratiometric fluorescence, a distinct red shift the fluorescence would be observed due to the unchanging fluorescence emission of the reference probe. By comparing the relative intensity ratio of these two peaks and the subsequent change in emission color, even small changes to the analyte concentration could be detected and quantified.[59]

The aggregation based monomer/excimer emissions described in section 2.2 is one example of a ratiometric fluorescence measurement. Ratiometric fluorescence has also been successfully applied to thermometry of microfluidics systems, polymer processing, and phosphorescent high temperature thermometers.[61-65] Ratiometry is also commonly used in biological applications to obtain quantitative measures of the presence of specific analytes such as ionic species.[66, 67]

3. EXPERIMENTAL METHODS

3.1 Epoxy Matrices

Epoxy resins are a set of thermosetting polymers that have many good material properties such as relatively low viscosity, good mechanical properties, chemical and thermal resistance, strong adhesion, and relatively low shrinkage.[68] As a result epoxies are used in a variety of applications such as adhesives, coatings, and as matrices for composite materials.[69] Epoxies form 3-D polymer networks by the reactions known as “curing” between polyfunctional epoxy monomers and a curing agent (a.k.a. hardener). The main feature of an epoxy monomer is the oxirane groups (a.k.a. epoxides), which is a three member ring formed between two carbon atoms and an oxygen atom. The structure of an epoxide group can be seen in Figure 3.1 below.

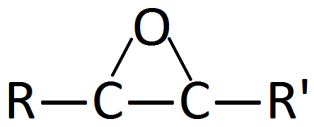

Figure 3.1 Epoxide ring

Due to the high strain of this configuration, the epoxide is more reactive than other ethers and can readily undergo ring opening reactions in the presence of nucelophiles (curing agent). Amines are a common curing agent for epoxies and epoxy-amine systems are utilized in this research.[68, 69] In epoxy-amine polymerization there are four main reactions that can occur. The first is a ring opening reaction where the epoxide group reacts with a primary amine. The product of this reaction is a partially cross-linked site with a secondary amine and a hydroxyl group. The secondary amine can then react with another epoxide group to form a fully cross-linked site (tertiary amine) with two hydroxyl groups remaining. The third potential reaction is an etherification reaction where an epoxide reacts with a hydroxyl group. The last reaction is homopolymerization of the epoxide groups. The etherification and homopolymerization of the epoxide groups are both undesirable reactions, but they can often be neglected when the amine to epoxide ratio is stoichiometric and there is no catalyst present.[69] A summary of these 4 reactions can be seen in Figure 3.2.

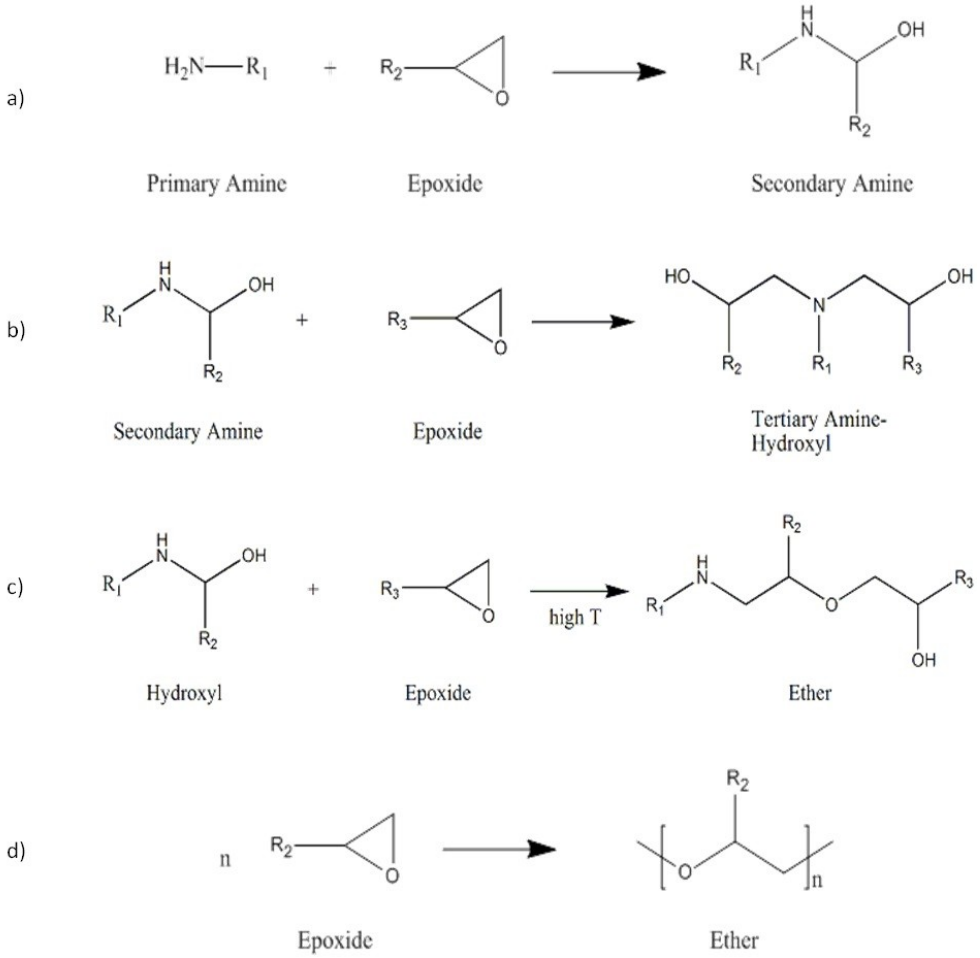

Figure 3.2 Epoxide-amine reactions (a) primary amine with an epoxide (b) secondary amine with an epoxide (c) etherification (d) homopolymerization[70]

This paper will feature three different epoxy resins commonly used for different applications in the aerospace industry. Details of these epoxy resins are given in the following sections.

3.1.1 Toray 3900

Toray 3900 is an epoxy resin that is used as the matrix in composite due to its good mechanical properties and thermal stability.[9] The base monomers for the Toray 3900 resin system are the epoxy tetraglycidal-4-4'-diaminophenylmethane (TGDDM) and the curing agent 4,4'-diaminodiphenylsulfone (DDS). The chemical structures for these two molecules can be

seen in Figure 3.3. Since it is a commercial resin the Toray 3900 resin contains additives whose chemical natures are proprietary and are unknown for this work.

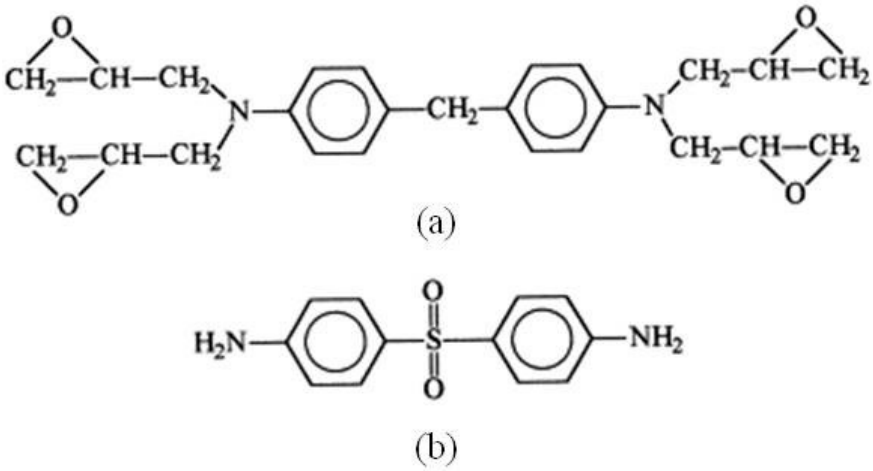

Figure 3.3 Chemical structure of (a) TGDDM (b) DDS

From Figure 3.3 it can be seen that TGDDM is tetrafunctional (contains four epoxide groups) meaning that it has excellent network forming capabilities. TGDDM comes in the form of a viscous liquid while DDS has the form of a white powder. Due to the high melting point of DDS (177 ºC), this resin is usually cured at 177 ºC (350 ºF).

3.1.2 Hysol EA 9390/TGDDM-MMCA

Hysol EA 9390 is a structural adhesive epoxy that is often used as the matrix epoxy in composite repairs. Hysol EA 9390 is another TGDDM based epoxy, but it uses 2,2'-Dimethyl-4,4'-methylenebis(cyclohexylamine) as the curing agent. In this paper 2,2'-Dimethyl-4,4'-methylenebis(cyclohexylamine) will be referred to as MMCA. Like Toray 3900 this is a commercial resin and contains proprietary additives. It should be noted that one of these additives in the curing agent gives the curing agent and subsequently the cured epoxy a strong purple color. The curing agent with no additives has a transparent yellowish color. Both versions of this epoxy system were used in this research at various times. The purple Hysol EA

9390 samples will be referred to as 9390 samples and samples made with the pure MMCA will be referred to as TGDDM-MMCA samples. The structure for MMCA is shown in Figure 3.4.

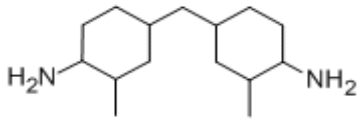

Figure 3.4 Structure of 2,2'-Dimethyl-4,4'-methylenebis(cyclohexylamine)

Since the epoxy monomer is the same as the Toray 3900 system the network forming capabilities are the same; however, MMCA is stronger nucleophile than DDS and can be cured at lower temperatures. Hysol EA 9390 is usually cured at 121 ºC (250 ºF).

3.1.3 DGEBA-DETA

Diglycidylether of bisphenol A (DGEBA) is one of the most commonly used epoxy monomers. In the commercially available resins DGEBA is often an oligomer, where changing the repeat unit 'n' changes the viscosity of the liquid. DGEBA is a bifunctional monomer and it is only capable of forming cross-linking networks if the curing agent has functionality greater than two. For this work, diethylene triamine (DETA), a trifunctional amine, is used as the curing agent. The DGEBA-DETA system has been well studied and is often used as a model epoxy system. For this work DGEBA-DETA is used as a simple room-temperature curing coating for carbon fiber composites panels. The structures for DGEBA and DETA can be seen in Figure 3.5.

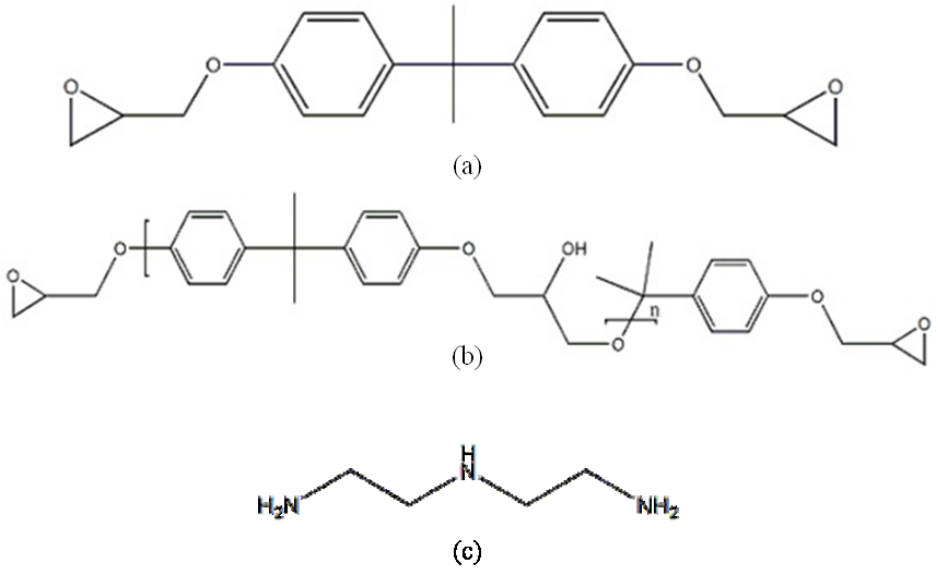

Figure 3.5 (a) DGEBA monomer (b) DGEBA oligomer (c) DETA monomer

3.2 Sample Preparation

For this research thermal damage probes AJNDE16 and AJNDE35 were doped in the epoxy matrices detailed in the previous section. The processing and quantity of the probe-doped samples was the same for both probes in a given epoxy matrix unless otherwise noted.

3.2.1 Toray 3900 Samples

To understand the fluorescence behavior of the probe AJNDE16 it was necessary to test both the neat matrix and the AJNDE16 doped matrix during the same tests. The 3900 resin (Toray Composites Inc.) was received in a partially cured (b-staged) block that was stored in a freezer to dramatically slow the cross-linking reaction in between uses. To obtain samples for curing, pieces of the 3900 resin had to first be chipped off the block. Samples of neat 3900 were processed by first heating pieces of the 3900 in an aluminum pan to 125 ºC on a hot plate lower the viscosity so that the pieces flowed to fill the pan. The sample was then cured in a Thermo Scientific Heratherm Advanced Protocol mechanical convection oven from room temperature to

177 ºC at a rate of 5 ºC/min, followed by a dwell at 177 ºC for 2 hours. After the dwell, the sample was cooled naturally back to room temperature. The cured epoxy was obtained by removing the aluminum pan from the sample. The cured epoxy was then cut into the approximately 0.5 cm by 0.5 cm squares using a low speed saw (PICO 150, Pace Technologies) with a diamond coated wafering blade. Cooling during cutting was provided by a water bath. To dope the 3900 resin with one of the probes, the b-staged resin was heated in an aluminum pan on the hot plate to 125 ºC to reduce the viscosity and then 0.05-0.1 wt% of probe was mixed into the resin by stirring while keeping the pan on the hot plate. The rest of the processing was the same as the neat resin. In this paper the resin with no probe added will be referred to as neat 3900, resin with probe AJNDE16 doped in will be referred to as AJNDE16-doped 3900, and resin with probe AJNDE35 doped in be referred to as AJNDE35-doped 3900. It should be noted occasionally aggregates of the AJNDE16 or AJNDE35 powder could not be broken up by mixing and would remain as an aggregate after curing.

3.2.2 Hysol EA 9390 /TGDDM-MMCA Samples

Hysol EA 9390 Part A (epoxy resin) and part B (curing agent) were obtained from Henkel Corporation and used as-received. For the Hysol EA 9390 two types of samples were made, bulk and thin-film. The bulk samples were used for the experiments involving sanding and the thin film samples were used for UV-Vis measurements. For both types of samples, Part A and Part B were mixed in a ratio of 100:56 parts by weight. The mixture was then degassed in vacuum for 15-20 min. For bulk samples, the mixture was then poured into an aluminum pan and heated in the convection oven from room temperature to 121 ºC at a rate of 3 ºC/min, followed by a dwell at 121 ºC for 150 min. The sample was allowed to cool to room temperature

naturally. The samples were then sectioned using the low speed saw to be approximately 0.5 cm by 0.5 cm squares. 0.05 wt% of the probe AJNDE16 was added to another batch of 9390 during the initial mixing using the same mixing ratio of resin to curing agent as the 9390 resin with no probe. All other processing steps were the same. The batch containing the probe will be referred to as AJNDE16-doped 9390 and the batch containing no probe will be called neat 9390 in this paper.

To form the thin films, small drops of the neat 9390 or the AJNDE16-doped 9390 were spin coated onto glass substrates at speeds between 3,500 and 4,000 rpm. The thin films were then cured using the same cure cycle as the bulk 9390 samples.

The processing procedures for AJNDE16-doped TGDDM-MMCA samples were exactly the same as Hysol EA 9390 samples with the exception that the curing agent was replaced with MMCA received from Sigma Aldrich. AJNDE35 was used only in TGDDM-MMCA and not in the Hysol 9390 in these studies. The processing of AJNDE35 was similar to that of AJNDE16-doped TGDDM-MMCA, but one additional step was needed before mixing the epoxy components. AJNDE35 had a tendency to form aggregates that were difficult to disperse just by mixing the powder into the epoxy so first AJNDE35 was dissolved into methyl ethyl ketone (MEK) in a ratio of 10 mg AJNDE35: 1 g MEK. This solution was then mixed into the TGDDM component and placed in a fume hood at room temperature to allow the MEK to evaporate out of the mixture. Depending on how much of the MEK solution was added it usually took 1-3 days for most of the MEK to evaporate. Evaporation of the MEK out of the mixture was monitored by periodically measuring the mass of the container. The end point of the evaporation was determined to be when there ceased to be significant change in the mass between measurements and the mass loss from the mixture was approximately equal the mass of the MEK solution

added. After the evaporation was complete, the AJNDE35-doped TGDDM component was used as the TGDDM component for processing. No aggregates were visually observed when processing the AJNDE35-doped TGDDM-MMCA using this procedure. Unless otherwise noted, AJNDE16 and AJNDE35-doped TGDDM-MMCA samples contained 0.05 wt % of the probe.

3.2.3 AJNDE16-doped Epoxy/ Carbon Fiber Composite

To fabricate composite panels, the same AJNDE16-doped 9390 mixture from section 3.2.2 was used except the AJNDE16-doped solution contained 0.1 wt% AJNDE16 instead of 0.05 wt%. The amount of probe used was increased to account for the reduced volume fraction of resin in the composite sample. After mixing and degassing, the AJNDE16-doped mixture was used to wet-layup 3 plies of T-800 plain weave carbon fiber fabric (Toray Composites Inc). The wet lay-up the composite panels were then processed by conventional vacuum bag process and cured in an autoclave at 121 ºC (250 ºF) for 2.5 hours. The cured composite panels were 5.08 cm x 5.08 cm. The composites were then cut into 0.5 cm by 0.5 cm squares using the low speed saw.

3.2.4 DGEBA-DETA Coating Samples

DGEBA-DETA samples for the composite coating were made by mixing DGEBA (Der 330 from Dow Chemical Co.) with DETA (Epikure 3223 from Shell Chemical Co.) in a weight ratio of 1:0.111 which corresponds to a 1:1 epoxide to amine ratio. The two components were mixed together for several minutes and then placed under vacuum for 15 min to remove bubbles introduced during the mixing. The mixture without the thermal damage probe was used to make

the neat coating. For the AJNDE16-doped coating, the thermal damage probe AJNDE16 was initially mixed with DETA to form a solution. The probe solution was then mixed with DGEBA in a weight ratio of 1:0.111 of DGEBA to DETA solution. The amount of AJNDE16 in the total mixture was approximately 0.05 wt%. After mixing, the resin was degassed under vacuum for 15 min to remove bubbles from the coating mixture. The degassed mixture was then used to make the AJNDE16-doped coating.

The substrates for the coatings were made by laying up a 30.5 cm x 30.5 cm 8 ply $[0/90/0/90]_s$ panel from uni-directional aerospace grade carbon fiber/epoxy prepreg. The panels were processed by a conventional vacuum bagging procedure with polyester peel-ply (Precision Fabrics 60001) on both sides of the panel. The panel was then placed in an autoclave and cured at 177 ºC for 2 hours under 586 kPa (85 psi) of pressure. After curing the panel was cut into 7.62 cm x 7.62 cm specimen.

The coatings of the neat and AJNDE16-doped mixtures were applied to the composites using a brush. Just prior to coating the sample, the peel-ply was removed from the composite panel to provide a good surface adhesion of the coating. The coating was allowed to cure for at least 18 hours at room temperature, followed by a post-cure for 2 hours at 70 ºC.

3.2.5 Thin-films Samples for Kinetic Measurements

The kinetic measurements required that the samples not become oxidized during thermal exposure in order to obtain reliable measurements. In order to fabricate samples that wouldn't oxidize small drops of the AJNDE16-doped and AJNDE35-doped TGDDM-MMCA samples were placed on a glass slide and then covered with a cover slip. Cover slips were also placed at the ends of the glass slide to act as a spacer between the glass slide and the cover slip covering

the sample. The epoxy was heated on a hot plate at approximately 55 °C for 5 min before applying to the slide to lower the viscosity and remove some bubbles from the mixture. A cross-sectional view of the kinetics sample setup can be seen in Figure 3.6.

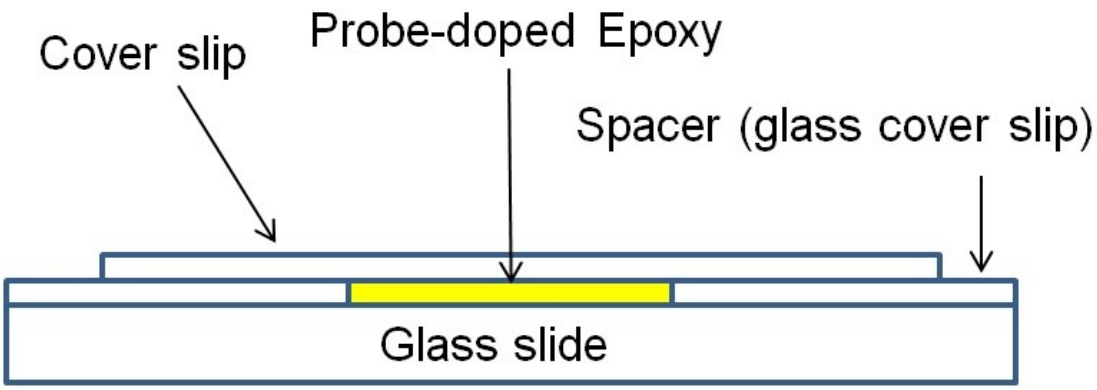

Figure 3.6 Schematic of kinetics measurement sample (cross-sectional view)

The samples were then processed using a conventional vacuum bagging process. Samples were placed with the cover slip side in facing down against the tool to limit the bending of the cover slip when vacuum was applied so that the most of the epoxy was not squeezed out the sides. The samples were put through the standard TGDDM-MMCA cure cycle while the system was under vacuum. Performing the cure without vacuum was found to limit oxidation compared to samples not sandwiched between the glass slide and cover slip, but some oxidation still occurred likely due to oxygen trapped inside the sample during the cure. Thus it was necessary to perform this sample preparation under vacuum.

3.2.6 Multiplexed Thermal Damage Probes in TGDDM-MMCA

The multiplexed samples contained both probes AJNDE16 and AJNDE35 in an approximately 1:1 molar ratio. The molecular weight of AJNDE16 was 642 g/mol and the molecular weight of AJNDE35 was 698 g/mol. Due to the small difference in molecular weight

the weight percent of each probe added to achieve a 1:1 molar ratio was slightly different for AJNDE16 and AJNDE35. By weight the samples contained approximately 0.05 wt% AJNDE16 and approximately 0.054 wt% AJNDE35. Prior to mixing with the epoxy both probes AJNDE16 and AJNDE35 were dissolved in a solution on MEK in the same ratio 10 mg probe: 1 g of MEK. The MEK solution was then mixed into the TGDDM component and allowed to evaporate similar to processing used for AJNDE35-doped TGDDM-MMCA. After evaporation of MEK was complete, the multiplexed probe-doped TGDDM was used as the TGDDM component for processing the epoxy. The rest of the sample preparation was performed using the standard TGDDM-MMCA processing procedures for bulk samples. Multiplexing of probes AJNDE16 and AJNDE35 was only done in TGDDM-MMCA in this study so to simplify naming these samples are referred to as multiplexed samples in this paper.

Multiplexed samples sandwiched between two glass slides to prevent oxidation were used in some of the measurements presented in this paper. The processing of these samples was similar to that of the kinetic measurement samples described in section 3.2.5 with the exception that the AJNDE16 or AJNDE35-doped TGDDM-MMCA was replaced with the multiplexed epoxy. Coatings on composite panels using the multiplexed epoxy were also prepared using a procedure similar to that in section 3.2.4, except that the multiplexed epoxy was used in place of the AJNDE16-doped DGEBA-DETA coating and the curing was carried out using the standard TDGGM-MMCA curing procedure.

3.3 Heat-treatment of Samples

3.3.1 Bulk Sample Heat-Treatment

The samples of neat epoxy and the AJNDE16-doped epoxy were subjected to heat-treatments at temperatures of 204 ºC (400 ºF), 232 ºC (450 ºF), and 260 ºC (500 ºF) in the convection oven. The samples were removed from the oven at set intervals ranging from 5 min to 480 min to measure the fluorescence and/or UV-Vis absorption spectra. Two different sampling methods for the heat-treatment were tried. In the first case, multiple samples of the same batch were placed in the oven at the same time and one sample was removed at every interval for measurement. In the second case, individual samples were placed in the oven and removed for measurements. After the measurements the same samples were placed back in the oven and heated again until the next time increment. There was not much difference found between the two methods so for the most part the second method was used to save materials.

The kinetic measurement and also multiplex thin-film samples were also heat-treated in the convection oven. For the kinetic measurements it was very important that the same sample be used from start to finish for a given measurement to achieve good results. Kinetic measurements were made in temperatures ranging from 191 °C (375 °F) to 232 °C depending on the probe.

3.3.2 Localized Heat-Treatments

3.3.2.1 Localized Heat-Treatment of AJNDE16-doped DGEBA-DETA coating

The localized heating experiments on the composite panels with AJNDE16-doped coatings were performed using an in-house setup. An 18.4 mm diameter aluminum rod was

placed in a Brookfield Thermosel furnace such that the top of the rod was about 15 mm outside the furnace. Aluminum foil was wrapped around the outside of the rod in order to make it fit tightly in the furnace chamber and minimize air gaps; thus improving heat transfer from the furnace to the rod. 2 mm holes were drilled at the top of the rod and also through the coated composite samples. K-type thermocouples were placed at the top of the rod, and at three areas on the composite in the area of interest. A pin inserted in the hole in the rod was used to align the composite samples on the rod and achieve reliable placement of the thermocouples. The thermocouple measurements were recorded using a National Instruments NI USB 9211A data acquisition system (DAQ) and an in-house LABView program for reading thermocouples. The aluminum rod was preheated to the desired temperature as measured by the thermocouple in contact with the rod. The panels were then placed with the coating in contact with the preheated rod. After steady state temperature had been reached, the panels were left in contact with the rod for set increments of time: 5 min, 15 min, 30 min, and 60 min. Insulation blankets were placed around the exposed area of the rod and on the backside of the composite panel to reduce heat loss. A ceramic weight was placed on top of the blanket to ensure good contact between the sample and the rod. A diagram of the setup can be seen in Figure 3.7 below.

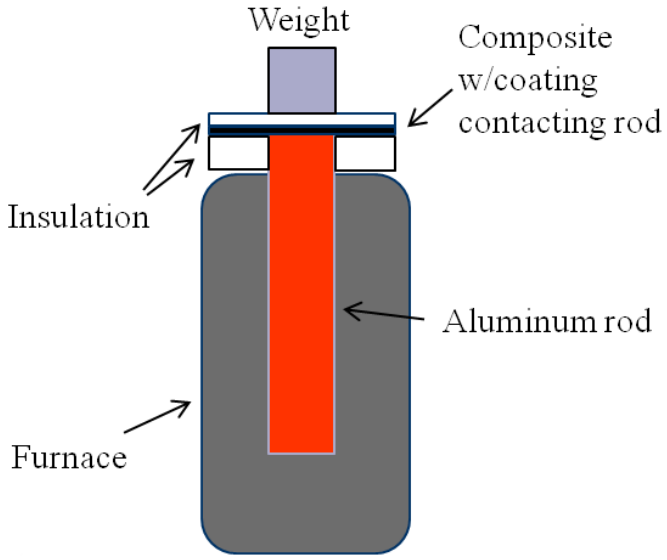

Figure 3.7 Diagram of localized heating setup for composite panel with AJNDE16-doped DGEBA-DETA coating

3.3.2.2 Localized Heating of Panels with Multiplexed Coatings

A set of localized heating experiments were also performed on the composite panels with the multiplexed coating; however, a different set up was used with those samples. In this setup, two silicone heat blankets (Omega Engineering Inc.) were placed on separate sides of the panel. A 3" circular heat blanket was placed on the uncoated side of the panel and a 1" square heat blanket was placed on the side with the multiplexed coating. The 3" blanket was used to warm the whole panel up to reduce the heat flow through the composite panel from the locally heated area and increase the size of the thermal gradient outside of the area locally heated by the 1" square blanket on the coating side. 6 thermocouples aligned in a line were used to monitor the temperature in and just outside of the locally heated area on the coating side of the panel. 2 more thermocouples were placed on the backside of the panel to monitor the temperature during heating using the 3" blanket. The entire setup was then sandwich between two insulating blocks and wrapped in an insulating cloth to reduce heat loss. Images of this setup can be seen in Figure

3.8. This set up was used over the one in Figure 3.7 primarily because it allowed for the thermal gradient away from the localized heat source to spread out over a larger area so that it was easier to take fluorescence measurements in the area where the gradient occurred.

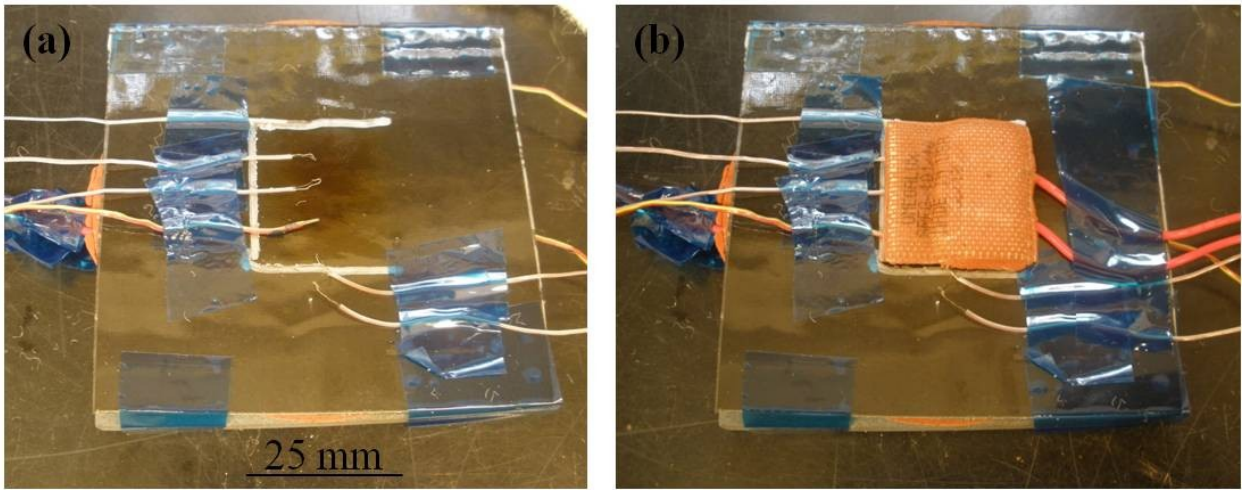

Figure 3.8 Images of local heating setup for composite panel with multiplexed coating (a) thermocouple placement (b) heating blanket placement

3.3.3 Inert Atmosphere

To test the effects of oxidation of the epoxy matrix on the fluorescence behavior a set of samples from both the neat 9390 and the AJNDE16-doped 9390 thin-films were heated in an inert atmosphere. For the inert atmosphere heat-treatment, the samples were placed on an alumina boat and set in the center of a tube furnace. The ends of the tube were capped and then a vacuum was applied to remove air from the tube. Once the vacuum was low enough, the tube was filled with argon gas that had been purified using a titanium getter furnace. The process of evacuation and filling was repeated 2 more times, with the Ar gas left flowing through the tube in the last step. The flow rate of the argon gas was 40 ml/min. The samples were then heated at a rate of 10 ºC/min to 204 ºC and held for 1 hr. For comparison to the samples heat-treated in the

inert atmosphere, a set of samples were heat-treated in the tube furnace in air under the same heating conditions.

3.4 Optical Characterization

3.4.1 Fluorescence Measurements

Fluorescence measurements were made on a Stellarnet BlueWave UVN spectrometer with a R600-8-UVVIS SR reflectance probe. The probe contains a 600 μm read fiber (detector) at the core and is surrounded by 7 fibers that focus the excitation source onto the sample. Depending on the measurement, either a 390 nm, 430 nm, or 470 nm LED were used as the excitation source for the fluorescence measurements. The use of the different excitation wavelengths will be discussed further in chapters 4 and was dependent on the probe and resin system combination. For the 390 nm LED, a bandpass filter centered at 390 nm with a 40 nm bandwidth (Edmund Optics) was used to remove reflections of the excitation light from interfering with the detection of the fluorescence spectrum. For the 430 nm led, a 435 nm bandpass with a 40 nm bandwidth (Edmund Optics) was used. In the case of the 470 nm LED, a 472 nm bandpass filter with a 50 nm bandwidth (Edmund Optics) was used. The filters were placed in the optical path using a BFH105 in-line filter holder (B&W Tek Inc.) that was connected by fiber optic cables between the excitation source and the probe. The reflectance probe was set at a 45º angle to the surface of the sample and the probe rested on the surface of the sample to try to reduce the effects of variations in the thickness of the samples on the distance to probe. The spot size of the excitation light was approximately 2-3 mm. To block out ambient light, the measurements were performed under a double layer of thick black cloth. Baselines for the measurement were taken with no illumination from the excitation source. Due

to differing intensities of the LED sources different detection settings were used to obtain relatively noise free spectra and/or avoid saturation of the detector. For the 390 nm and 435 nm LED, the integration time for the detector was generally set to 10,000 ms and 3 scans of each spectrum were averaged. The detector was generally set to 1,000 ms and an average of 9 scans for the 470 nm LED. For some measurements the integration time was adjusted to either increase a weak signal or reduce a signal that saturated the detector. For the composite panels with localized heating of the coating, the panels were constrained such that they could only translate in one dimension and fluorescence measurements were taken approximately every 5 mm across the panel near the center of the heated zone. A diagram and image of fluorescence measurement setup can be seen in Figure 3.9.

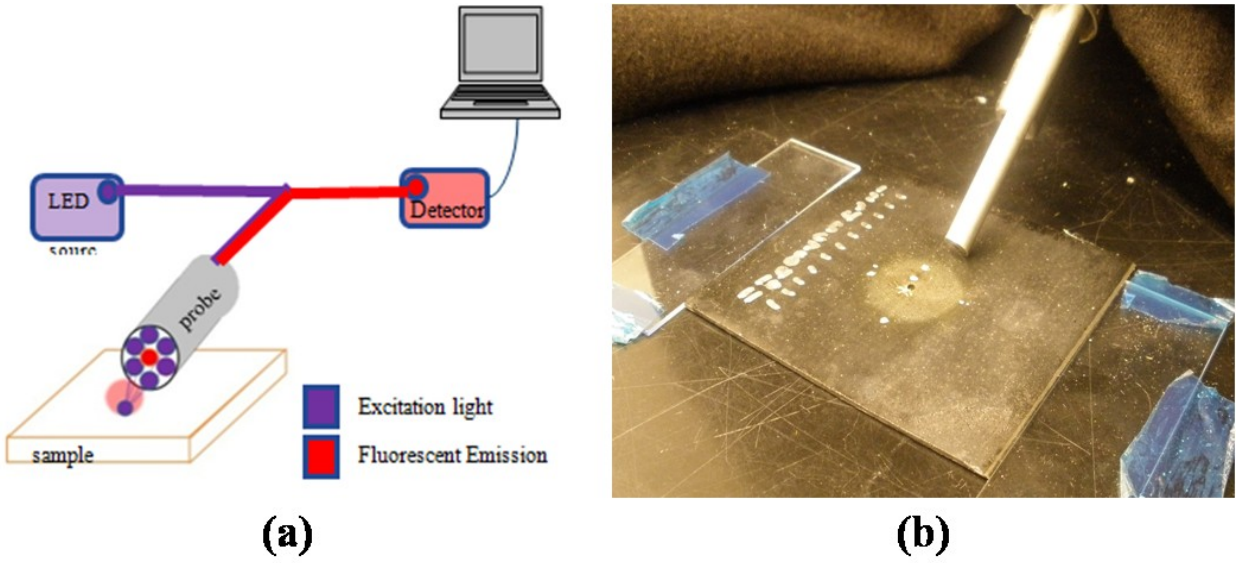

Figure 3.9(a) Fluorescence measurement setup (b) image of fluorescence probe and sample

3.4.2 Kinetic Measurement of Probes AJNDE16 and AJNDE35

The kinetic of probes AJNDE16 and AJNDE35 were measured using fluorescence intensity. As mentioned in section 2.5, fluorescence intensity measurements are difficult to reproduce unless done under strict experimental conditions so a specialized testing procedure was developed in order to obtain acceptable results for the kinetics measurements. In order to achieve reproducible results the exact same location on the sample had to be excited and measured every time. In order to make this sort of measurement accuracy possible, a fixture was prepared using three glass slides were fixed to the countertop and arranged such that they left a cavity almost the exact size of the sample. The sample did have a small amount of maneuverability after insertion into the fixture so to improve accuracy of the placement alignment markings were made on the sample and the fixture. The position of the spectrometer was held constant throughout the measurement. An image of this measurement setup can be seen in Figure 3.10.

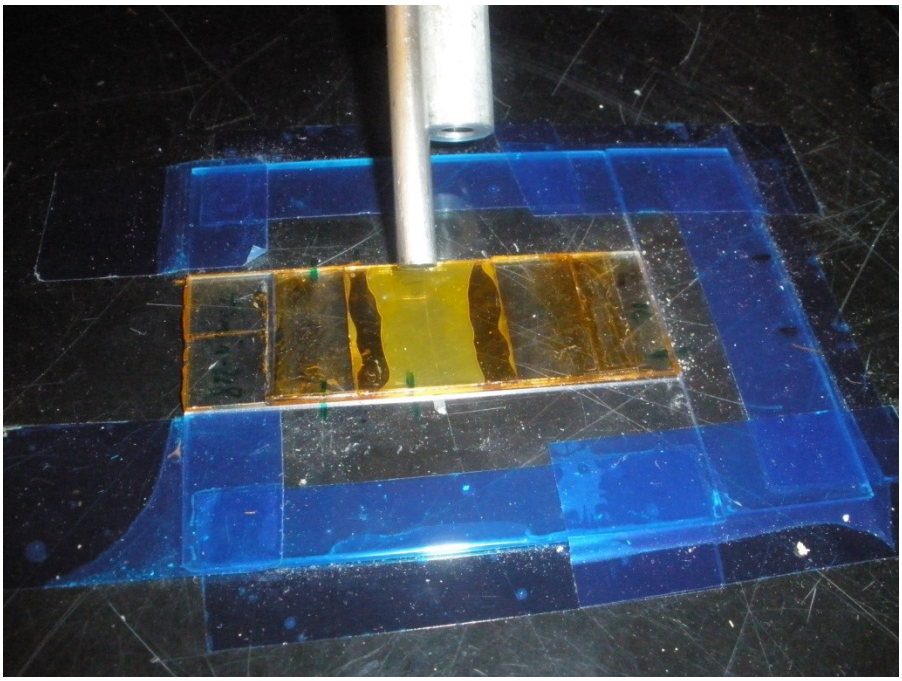

Figure 3.10 Kinetic measurement setup

Using this method the sample could be remove from the fixture and replaced with the difference in the intensity measurements being on the order of noise in the measurements. If the sample was even 1-2 mm off of the desired location changes in measured fluorescence intensity were found to be as high as 20 %. In addition to measuring the same position on the sample every time, after the heat-treatment the sample had to be completely cooled to room temperature before the measurement was recorded. If the sample was not at room temperature the measured fluorescence intensity was affected by thermal quenching caused by the increase in efficiency of non-radiative decay processes at higher temperature.[36] To ensure that the measurement was cooled to room temperature, the sample was placed in the fixture immediately after removing it from the oven. The fluorescence spectrum was then monitored as the sample cooled down and once the change in intensity between measurements was on the order of the noise of the measurements the spectra was recorded. To verify the measurement was reproducible the removed from fixture and replaced and another spectrum was recorded. This process was

repeated at least 3 times. If the difference in the intensities was on the order of the noise in the measurements, the measurements were considered satisfactory and the average of the measurements was taken.

3.4.3 UV-Vis Measurements

To measure the absorbance of the samples, UV-Vis spectra of the thin films of both the neat and probed-doped samples were measured from 250 to 900 nm at a scan rate of 240 nm/min using a Thermo Scientific Evolution 300. An uncoated glass substrate was used as the reference. Samples had been cooled to room temperature after heat-treatments before the spectra were measured. When possible, spectra were normalized by the maximum absorbance in the UV-region to account for variations in thickness of the samples.

4. CHARACTERIZATION OF THERMAL DAMAGE PROBES AJNDE16 AND AJNDE35 IN EPOXY

In this chapter the fluorescent properties of the materials are characterized. It starts with characterizing the autofluorescence of the epoxy matrices. The fluorescence behavior of thermal damage probes AJNDE16 and AJNDE35 and their response to heat-treatment is also detailed. Lastly the fluorescence response of the thermal damage probes doped into the epoxy matrices is presented.

4.1 Autofluorescence of Epoxy Matrices

During the course of the preliminary experiments it was found that all the epoxy matrices studied samples possessed autofluorescence of their own that had to be accounted for when taking fluorescence measurements. Details of the autofluorescence are provided in this section.

4.1.1 Toray 3900

The autofluorescence spectra of as-cured neat 3900 samples were measured using both the 390 nm and 470 nm excitation sources. The results can be seen in Figure 4.1.

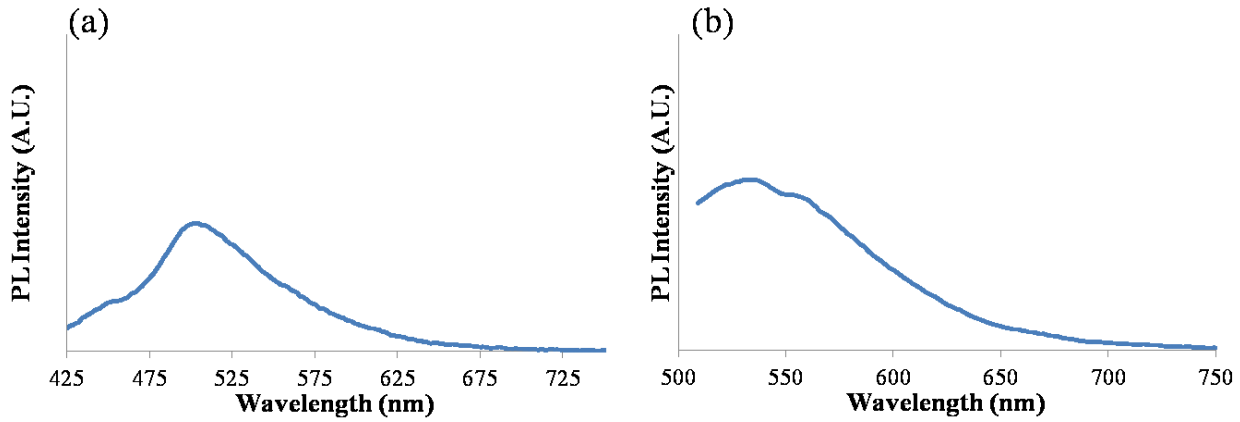

Figure 4.1 Autofluorescence measurements of as-cured 3900 under (a) 390 nm excitation (b) 470 nm excitation

From Figure 4.1 it can be seen that at 390 nm excitation the 3900 resin exhibits an autofluorescence peak with a maximum around 505 nm. Under the 470 nm excitation a broad peak at 535 nm with a shoulder at 557 nm is present. This peak overlaps the wavelength region where the fluorescence of the activated probe molecule AJNDE16a is expected and thus could affect the fluorescence measurements. Knowing how these autofluorescence peaks behave during heat-treatments was also necessary to understanding the response of the thermal damage probe. The neat 3900 samples were heat-treated at 204 ºC, 232 ºC, and 260 ºC and their

fluorescence responses were measured. It was found that the fluorescence response was similar during heat-treatment at all the temperatures except for the difference in the kinetics of the changes observed. The fluorescence of the neat 3900 heat-treated at 232 ºC is shown in Figure 4.2 as a representative of this behavior.

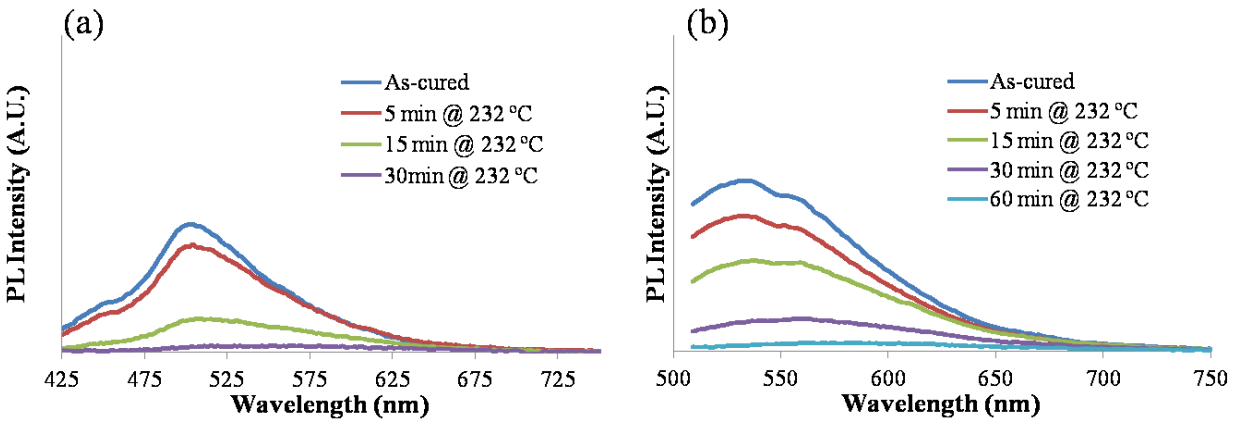

Figure 4.2 Autofluorescence of neat 3900 heat-treated at 232 ºC (a) 390 excitation (b) 470 nm excitation

Figure 4.2 shows that as the heat-treatment progresses autofluorescence peaks under both excitations exhibit bathochromic shifts and broadening of the peak, as well as eventual quenching of the fluorescence. For the three heat-treatment temperatures applied to the resin, it was found that the autofluorescence peak from the 390 nm excitation quenched faster than the peaks from the 470 nm excitation. This quenching behavior will be discussed more in section 5.1.

4.1.2 Hysol EA 9390/TGDDM-MMCA

The autofluorescence spectra of as-cured neat 9390 samples were measured using both the 390 nm and 470 nm excitation sources. The spectra can be seen in Figure 4.3.

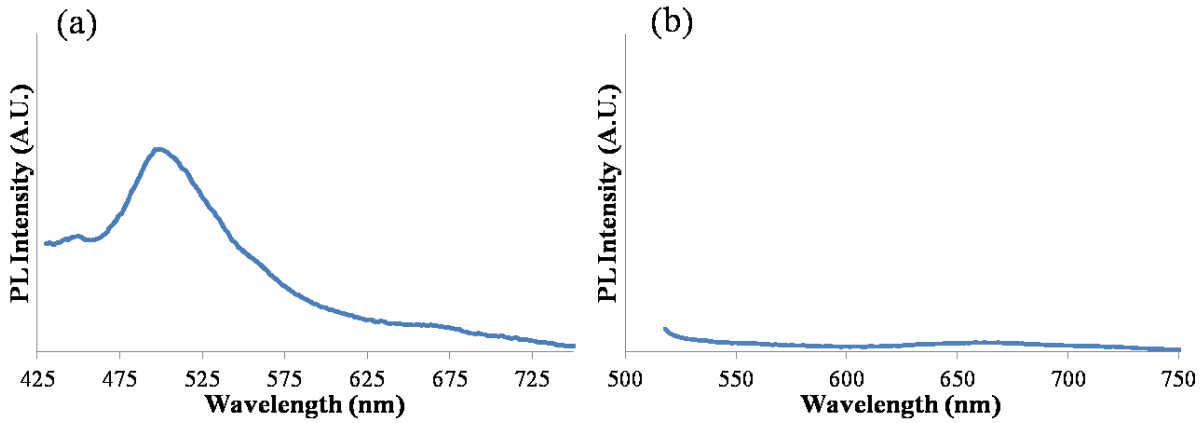

Figure 4.3 Autofluorescence measurements of as-cured 9390 under (a) 390 nm excitation (b) 470 nm excitation

From Figure 4.3, it can be seen that the neat 9390 emits a fluorescence peak at 505 nm under 390 nm excitation. This appears to be the same peak observed in the 3900 samples under the same excitation. Using the 470 nm excitation source, no fluorescence peak is observed. Similar to the 3900 system, heat-treatments were performed on the neat 9390 samples to determine the effects on the autofluorescence. The results of the heat-treatment at 232 ºC can be seen in Figure 4.4.

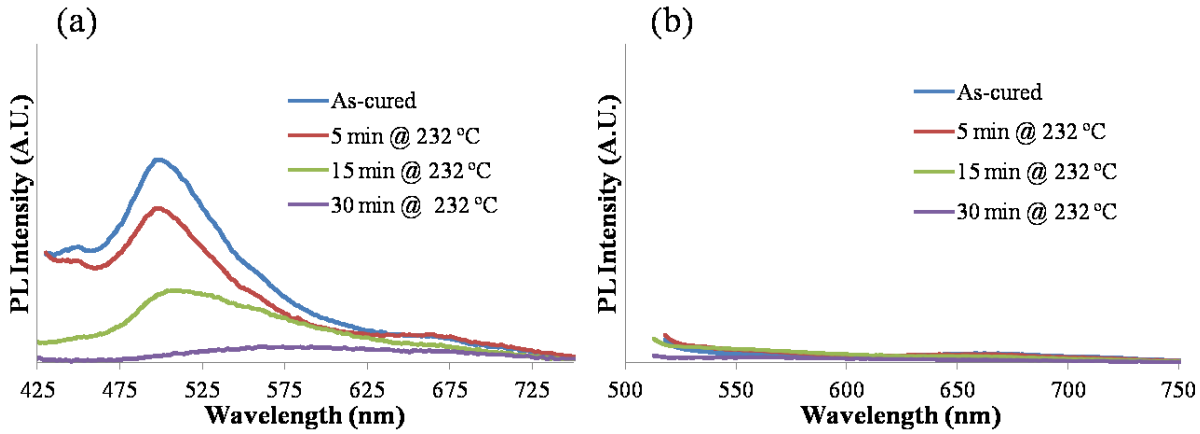

Figure 4.4 Autofluorescence of neat 9390 heat-treated at 232 ºC (a) 390 excitation (b) 470 nm excitation

In Figure 4.4, it can be seen that the autofluorescence peak using the 390 nm excitation is quenched just like in the 3900 resin. Under the 470 nm excitation no fluorescence peak is observed during the heat-treatment making this a good excitation source to use for monitoring the response of the probe AJNDE16 to heat-treatment in the 9390 system. The TGDDM-MMCA system (the base components of Hysol EA9390) was also tested and no differences were found in the autofluorescence measurements.

4.1.3 DGEBA-DETA Fluorescence Behavior

The autofluorescence of as-cured DGEBA-DETA is displayed in Figure 4.5.

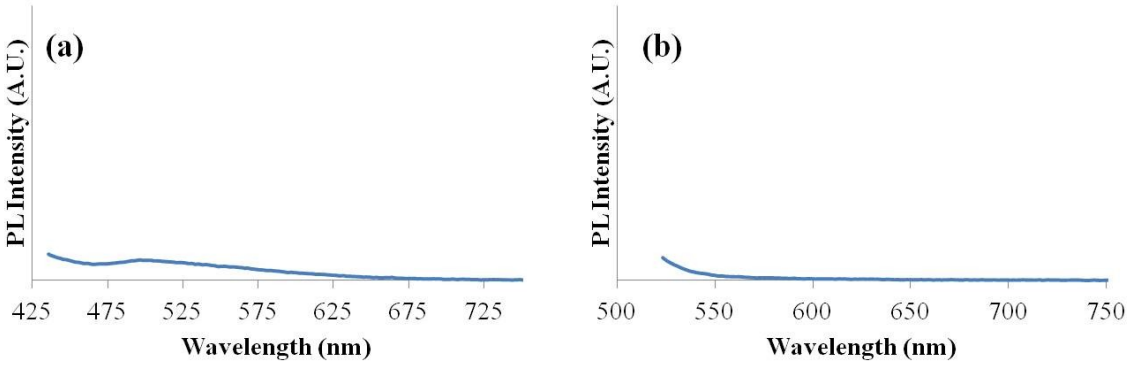

Figure 4.5 Autofluorescence measurements of as-cured DGEBA-DETA epoxy under (a) 390 nm excitation (b) 470 nm excitation

From Figure 4.5 it is seen that as-cured DGEBA-DETA exhibits a weak autofluorescence under the 390 nm excitation source and no autofluorescence under the 470 nm excitation source. Initially this may seem like a good matrix to test the fluorescence of the probes without interference; however, an interesting phenomenon was observed upon the heat-treatment of the DGEBA-DETA. This is shown in Figure 4.6.

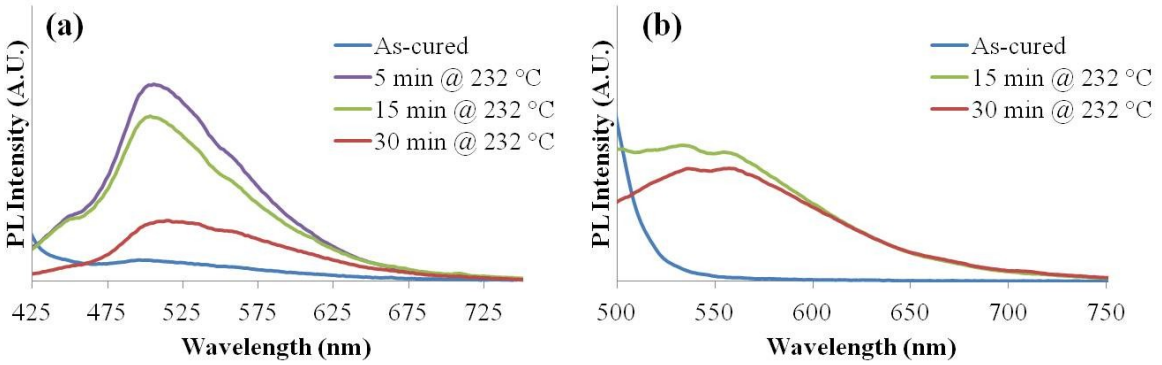

Figure 4.6 Autofluorescence of neat DGEBA-DETA heat-treated at 232 ºC (a) 390 excitation (b) 470 nm excitation

From Figure 4.6 it can be seen that after 5 minutes at 232 °C DGEBA-DETA autofluorescence develops under both excitation sources DGEBA-DETA exhibits. In essence, this behavior is very similar to that of a thermal damage probe in that the fluorescence is activated by thermal exposure although it would not be useful for detecting ITD since the autofluorescence has been found to grow at temperatures below 100 ºC. Figure 4.6a it can be seen that after heat-treatment DGEBA-DETA exhibits the same autofluorescence peak at 505 nm under the 390 nm excitation as was observed in both the Toray 3900 and the Hysol EA 9390 systems. Under the 470 nm excitation source, the DGEBA-DETA autofluorescence resembles that of the fluorescence of the Toray 3900 system under the same excitation source. Like in the 3900 system this autofluorescence covers the spectral range where the activated probe AJNDE16a fluoresces so this excitation was avoided when using this AJNDE16 in this matrix.

It is interesting that the same fluorescence peak is found in all three epoxy matrices given the different structures of the epoxies. There is literature on the intrinsic autofluorescence of epoxies, but the observed peak at 505 nm was not mentioned in any of the studies found even when the studies were based one of the above epoxy systems.[2, 30, 37, 71-74] The fact that this same autofluorescence peak is seen in epoxies with 3 different resin and curing agent systems indicates

this peak may be occurring due to a common additive or impurity in the epoxy systems.[73] There is literature on using fluorescent additives to monitor the degree of cure in the epoxy.[38, 60, 75, 76] The nature of this fluorescent species is not known with any certainty at this time, but the origin of the autofluorescence is not necessary for use with the thermal damage probes as long as its presence is known.

4.2 Characterization of Thermal Damage Probes

Two fluorescent thermal damage probes AJNDE16 and AJNDE35 were synthesized by our collaborators in the Jen group. AJNDE16 was the first generation probe that was extensively tested and it is the probe that was used for most of the research presented in this dissertation. AJNDE35 was a second generation probe that was developed from the knowledge gained from the testing on AJNDE16. It should be noted that the kinetics of the probe activation is not covered in this chapter. That topic is covered in detail in chapter 6.

4.2.1 AJNDE16

The absorbance and fluorescence emission spectra of the powder form of thermal damage probe AJNDE16 (the off state) and AJNDE16a (the on state molecule) can be seen in Figure 4.7a and Figure 4.7b respectively. The AJNDE16a in the figure was synthesized as a reference and was not made through heat-treatment of AJNDE16. The fluorescence spectrum was collected using a 370 nm excitation source. A fluorescence image of the two powders using a 365 nm excitation source is shown in Figure 4.7c. The data and image shown in Figure 4.7 was provided by our collaborator Dr. Zhengwei Shi, who synthesized the probe.

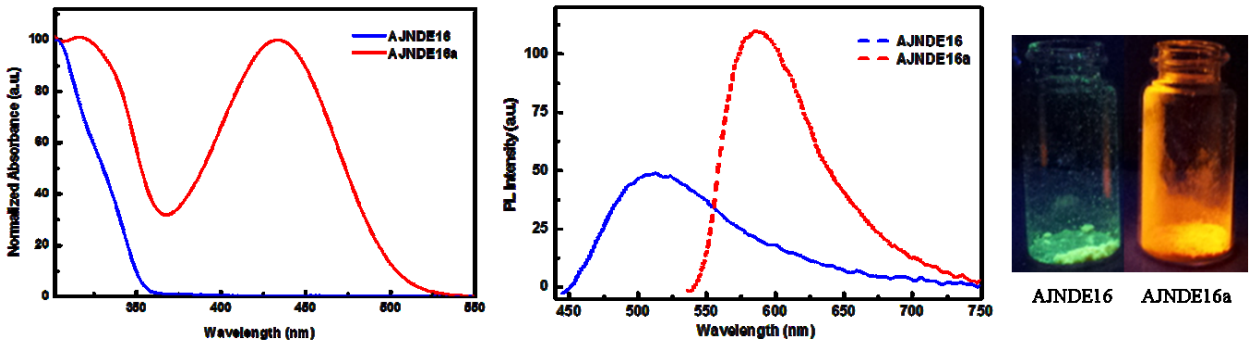

(a) (b) (c)

Figure 4.7 Properties of probe AJNDE16 and AJNDE16a (a) absorbance (b) fluorescence emission (c) fluorescence image (data and image provided by Dr. Zhengwei Shi)

It can be seen that AJNDE16 emits a green fluorescence (λ_{max} = 510 nm) even though it was represented in section 2.3 as being in an off state with no fluorescence. However, as shown in the absorbance spectra AJNDE16 does not absorb above the UV range so by using an excitation source above the UV range the probe does indeed work as a turn-on type sensor. AJNDE16a exhibits two absorbance peaks at 325 nm and 430 nm and thus its fluorescence can be excited using UV light or blue visible light. The orange fluorescence of AJNDE16a powder was found to have λ_{max} = 596 nm.

To verify that AJNDE16 converts to AJNDE16a upon sufficient thermal exposure as described in section 2.4, a small sample of the AJNDE16 powder was heat-treated in an oven at 232 °C for 5 min. The fluorescence spectrum of the powder before and after heat-treatment was measured and the heat-treated spectrum was compared to that of the synthesized AJNDE16a powder. The results of this measurement can be seen in Figure 4.8. All spectra were normalized by the maximum intensity of the respective spectra. The excitation source was the 390 nm LED.

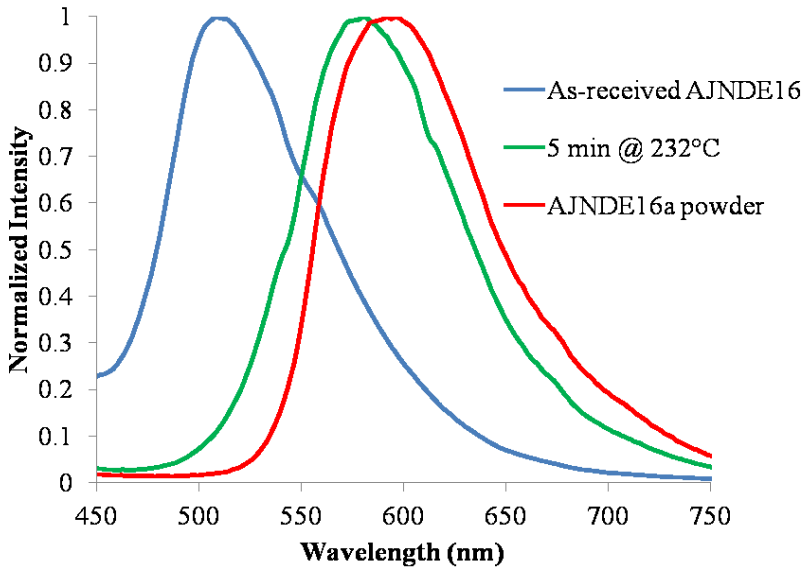

Figure 4.8 Fluorescence spectra of AJNDE16 before and after heat-treatment at 232 °C for 5 min

As it can be seen in Figure 4.8, the fluorescence of AJNDE16 heat-treated for 5 min at 232 ºC exhibits a fluorescence peak close to that of powder that of the synthesized AJNDE16a. There is a small difference between the heat-treated powder and the synthesized AJNDE16a as it can be seen that the heat-treated powder has peak that is slightly blue-shifted compared to the synthesized AJNDE16a peak. In addition, the heat-treated powder also exhibits a small shoulder around 540 nm that is not observed in the synthesized AJNDE16a. This may be because for this heat-treatment not all of the AJNDE16 molecules were converted into AJNDE16a during the heat-treatment and thus the spectrum for the heat-treated powder is actually a combination of the AJNDE16 and AJNDE16a fluorescence.

4.2.2 AJNDE35

AJNDE35 was the second generation of thermal damage probe. AJNDE35 was designed to be more thermally stable than AJNDE16 which had some compatibility issues with the cure of 3900 as described in section 4.3.1. The mechanism of activation for AJNDE35 is similar to that

of AJNDE16; however, the molecular structure is different and it has a different fluorescence emission than AJNDE16 as shown in Figure 4.9. The fluorescence spectra and images were provided Dr. Zhengwei Shi, who synthesized the probe.

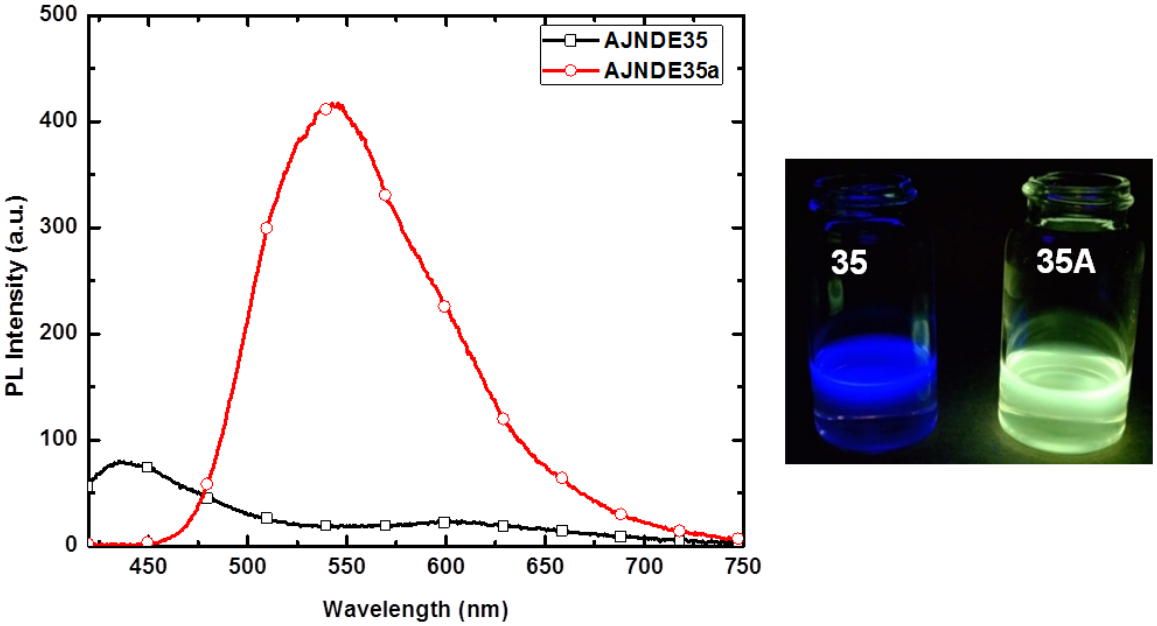

Figure 4.9 Fluorescence spectra of AJNDE35 and AJNDE35a powder (left) fluorescence image of probes in THF (right) (spectra and image provided by Dr. Zhengwei Shi)

As shown in Figure 4.9, AJNDE35 emits at 440 nm (blue) and AJNDE35a emits at 542 nm (green). Heat-treatment of the powder for 10 min at 232 °C confirmed that the fluorescence of the treated powder matched that of the synthesized AJNDE35a.

4.3 Fluorescence Behavior of Thermal Damage Probes in Epoxy Matrices

For the thermal damage probe to be useful for detecting ITD in composites it must be compatible with the epoxy matrices into which it is doped. This means that it must be able to withstand the cure cycle without activating and also not have its signal significantly drowned out by the autofluorescence of the matrix. The fluorescence behavior of probes AJNDE16 and AJNDE35 doped into Toray 3900 and Hysol EA9390/TGDDM-MMCA matrices is presented in

this section. Also AJNDE16-doped DGEBA-DETA is shown. Unless otherwise noted the amount of thermal damage probe doped into the matrix was 0.05 wt%.

4.3.1 AJNDE16-doped Toray 3900

As shown in section 4.1.1, the neat 3900 resin exhibits a broad fluorescence peak around 535 nm when exposed to the 470 nm excitation source. This is near the wavelength of the fluorescence of molecule AJNDE16a that is activated after heat-treatment in order to avoid the significant overlap between the peaks, the fluorescence measurements were performed using the 390 nm excitation source. For comparison, a synthesized AJNDE16a molecule was doped into another 3900 resin sample in order to simulate the spectra of the activated molecule. The fluorescence of the as-cured 3900 samples doped with AJNDE16 and AJNDE16a can be seen in Figure 4.10. The intensity of the fluorescence was normalized by the maximum intensity of the spectra in order to obtain a good comparison of the position of the fluorescence peaks.

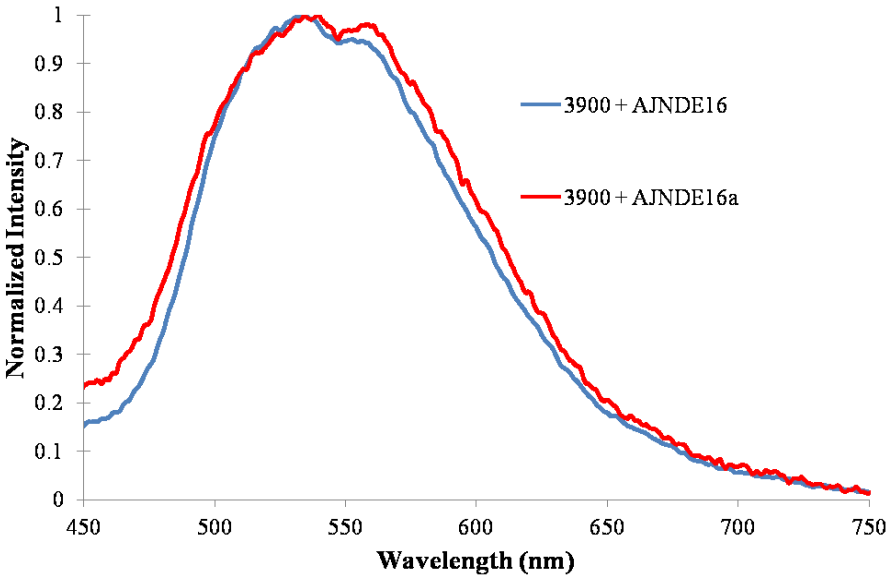

Figure 4.10 Fluorescence of as-cured 3900 doped with AJNDE16 and AJNDE16a

From Figure 4.10, it appears that the fluorescence peaks of the AJNDE16 and AJNDE16a doped samples are similar. Since AJNDE16a is the fluorescent molecule released during the activation of the probe during heat-treatment the sample doped with it the spectra represents what the spectra would look like if the probe had activated. In addition, the spectra appears to have two peaks at 534 nm and 558 nm, which is most likely a result of the superposition of the matrix autofluorescence (505 nm) and the fluorescence of AJNDE16a. It should be noted that when AJNDE16a is an epoxy it was found that its λ_{max} is shifted from 595 nm to 565 nm. This blue shift was found with AJNDE16a in all the epoxy matrices in this study. Since the spectra from the AJNDE16 probe is so similar to the AJNDE16a spectra this would infer that the enough of the AJNDE16 molecule was converted to the AJNDE16a molecule during cure for it to be considered in the activated state. If this was the case then it would be expected that little to no change in the fluorescence would be observed upon heat-treatment. To test this, the AJNDE16-doped 3900 sample was heat-treated at 232 ºC. The results are shown in Figure 4.11.

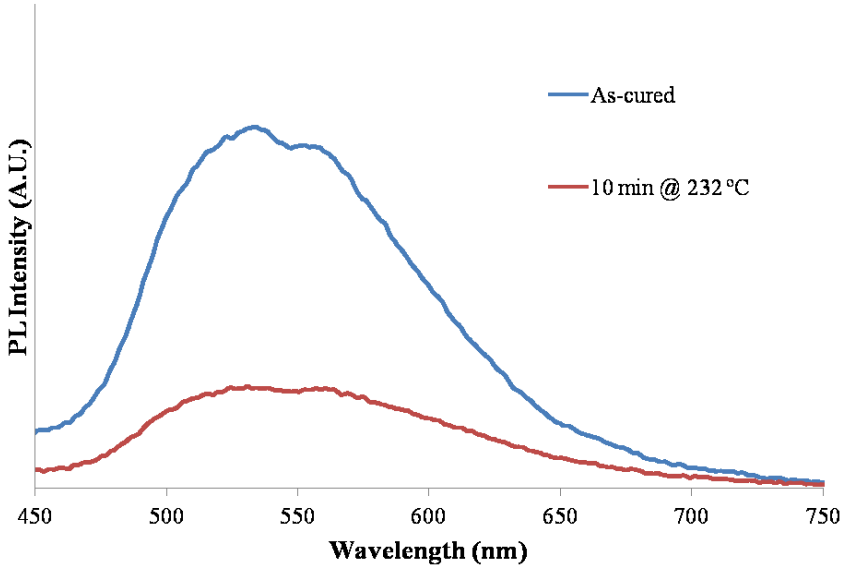

Figure 4.11 Fluorescence of AJNDE16-doped 3900 heat-treated at 232 ºC

From Figure 4.11, it can be seen that the AJNDE16-doped 3900 fluorescence spectrum did not show any significant change in response to heat-treatment besides a decrease in intensity which was similar to decrease in intensity observed for neat 3900. This indicates that probe AJNDE16 was activated during the cure. One more measurement was performed to verify this was the case. Fluorescence measurements of the AJNDE16-doped 3900 were taken prior to curing at 177 ºC and in the as-cured state. The results are presented in Figure 4.12. The fluorescence intensities in the figure were normalized.

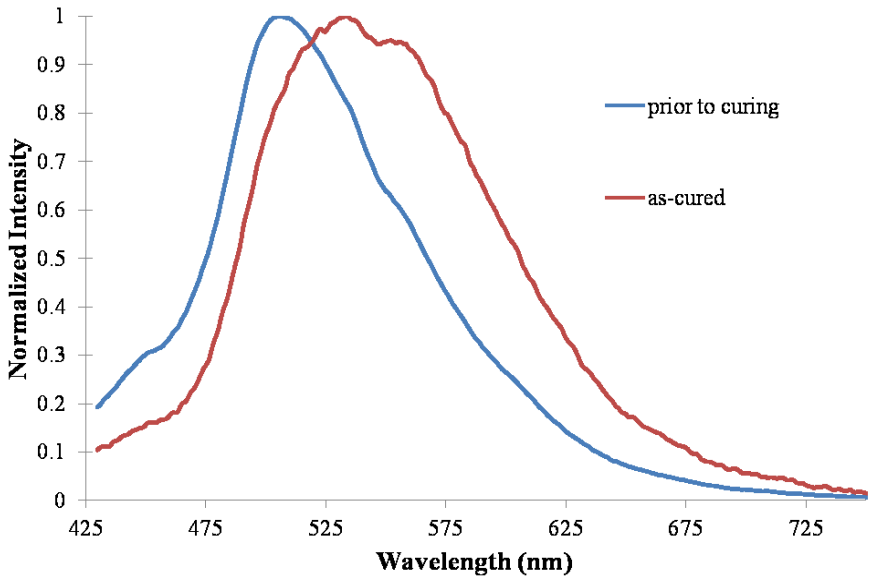

Figure 4.12 Fluorescence measurements of AJNDE16-doped 3900 prior to curing and as-cured

Prior to curing the AJNDE16-doped epoxy exhibits a fluorescence peak around 505 nm (autofluorescence of 3900) and as seen before the as-cured state has two peaks at 534 nm and 558 nm. So clearly a change in the fluorescence occurs during the curing. The as-cured state fluorescence appears similar to the 3900 doped with AJNDE16a in Figure 4.10, it is reasonable to conclude that probe AJNDE16 was activated during the cure of 3900 and was not useful as a probe in this system.

4.3.2 AJNDE16-doped Hysol EA 9390

The fluorescence response of AJNDE16-doped 9390 to heat-treatment was measured in bulk and thin films. There was no significant difference found between the bulk and thin film fluorescence response. Both types of samples were used for different measurements. The thin film samples were necessary for making UV-Vis absorbance measurements, while the bulk samples were used in the experiments involving sanding where thicker samples were needed. In this section only the results from the thin films of the AJNDE16-doped 9390 will be presented. The fluorescence measurements of the thin films subjected to heat-treatments at 204 ºC, 232 ºC, and 260 ºC are shown in Figure 4.13. For these measurements the 470 nm excitation source was used since the host matrix exhibits no fluorescence under this excitation wavelength. The as-cured samples of the AJNDE16-doped 9390 displayed no fluorescence under this excitation as well and it was not included the figure.

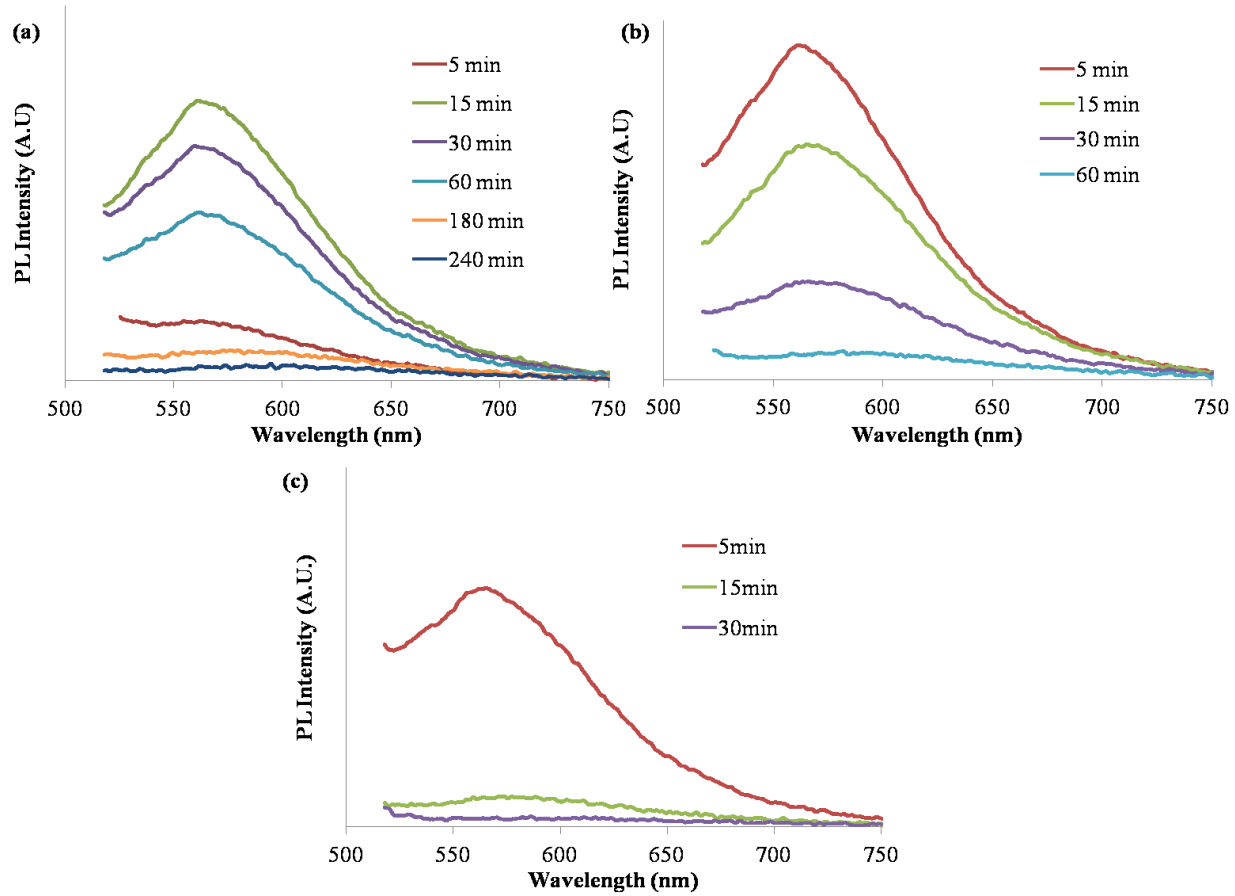

Figure 4.13 Fluorescence spectra of AJNDE16-doped 9390 samples heat-treated at (a) 204 ºC (b) 232 ºC (c) 260 ºC

The fluorescence of the probe can be seen to initially exhibit a fluorescence peak with λ_{max} around 565 nm. With increasing exposure time λ_{max} also exhibits a bathochromic shift and broadening. These phenomena have also been observed using LIF spectra.[2, 30] The samples treated at 232 ºC and 260 ºC exhibited maximum fluorescence intensity after 5 minutes of exposure time. However, in the case of thermal treatment at 204 ºC, it can be seen that the maximum recorded intensity occurred at 15 min, indicating that the kinetics of fluorescence activation were slower at the lower temperature as would be expected. It can also be seen that after prolonged exposure to all of the heat-treatment temperatures, the intensity of the fluorescence emission is quenched to where it could no longer be observed. This was similar to

the quenching seen in the neat epoxy systems. The rate at which the fluorescence was quenched was strongly dependent on the heat-treatment temperature. At 260 ºC the fluorescence was no longer observed after 30 minutes, while it took 240 min for complete quenching to occur at 204 ºC. Even though the fluorescence emission becomes harder to see with long exposure times to the point where it cannot be observed visually, this result may not be detrimental to this inspection method. Most thermally damaged parts have a thermal damage gradient surrounding the damage site where the fluorescence is still visible as will be shown in section 5.5. In that case, the quenched fluorescence emission can actually be useful because it indicates an area where significant thermal damage has occurred.[2, 30] In section 5.1, the origin of this quenching and how the fluorescence can be restored is discussed.

Bright field and fluorescence emission images showing the effects of exposure time on the fluorescence and the darkening of the matrix for several exposure times at 232 ºC are shown in Figure 4.14. A 590 nm long-pass colored glass filter was used to remove most of the reflected blue light from the excitation source in order to obtain a clearer picture of the fluorescence (note the true color of the probe fluorescence is more yellow-orange).

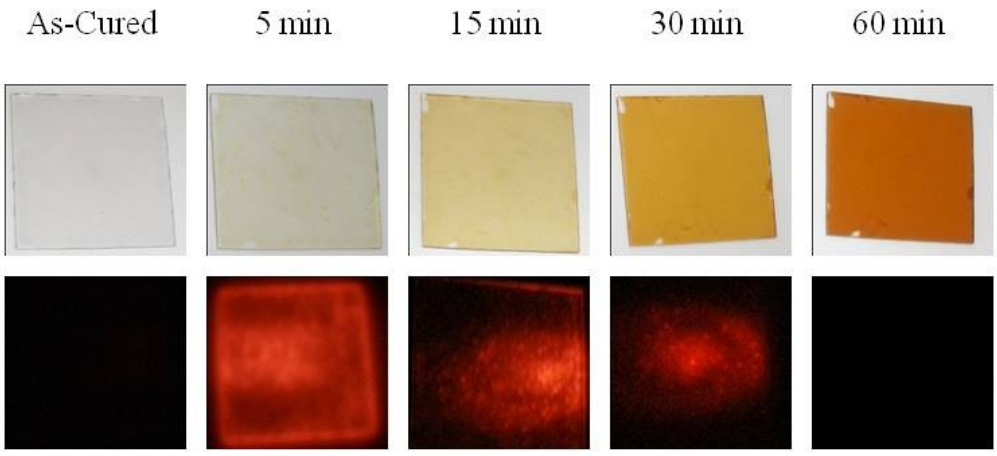

Figure 4.14 Bright field (top) and fluorescence (bottom) images of AJNDE16-doped 9390 thin-films heat-treated at 232 ºC for several exposure times

As in the fluorescence spectra, the images show the fluorescence of the sample becomes progressively weaker with exposure time. In addition, the bright field images show that the matrix darkens considerably during this thermal exposure. Whether the darkening had an impact on the fluorescence properties of the AJNDE16-doped 9390 will be explored in section 5.1.

4.3.3 AJNDE16-doped DGEBA-DETA

The fluorescence response AJNDE16-doped DGEBA-DETA to heat-treatment at 232 °C is shown Figure 4.15. The spectra were taken using the 390 nm LED excitation source.

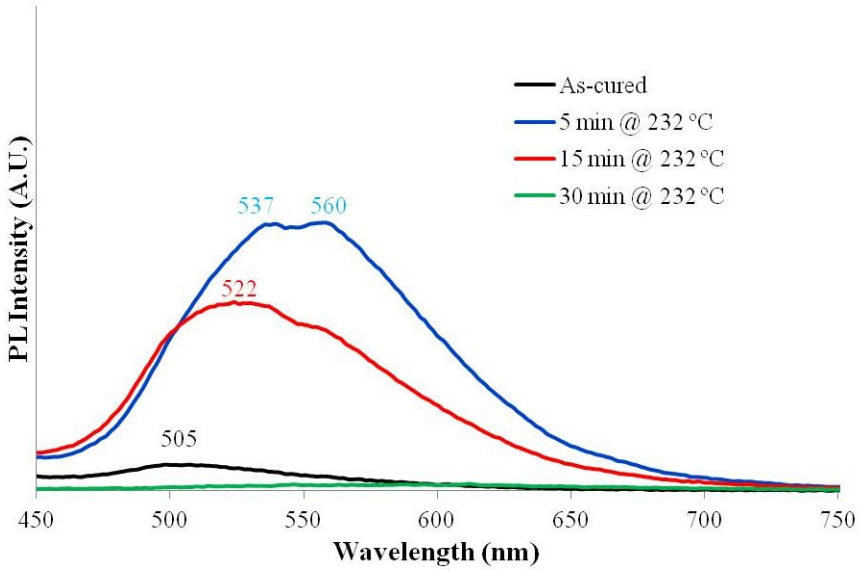

Figure 4.15 AJNDE16-doped DGEBA-DETA heat-treated at 232 °C for several exposure times

From Figure 4.15 it can be seen that AJNDE16-doped DGEBA-DETA exhibits some interesting behavior. After 5 minutes there appears to be two peaks at 537 nm and 560 nm. It can be recalled from the previous sections that activated AJNDE16a exhibits fluorescence around 565 nm in epoxy and DGEBA-DETA has a fluorescence emission at 505 nm under the 390 nm excitation. From this it can be ascertained that the spectra seen for 5 min @ 232 °C is a

combination of the fluorescence of AJNDE16a and the autofluorescence. As the exposure time increases the fluorescence appears to blue shift to a λ_{max} of 522 nm, which has not been seen before in response to the heat-treatment. As mentioned in section 3.1.3, the autofluorescence of DGEBA-DETA was found to increase with thermal exposure much like a thermal damage probe. It is believed that this blue shift is caused by an increase in the amount of autofluorescence relative to that of the AJNDE16a fluorescence. So essentially this is acting like a system with two thermal damage probes in it which is known as a multiplexed system. This multiplexing of thermal damage probes has some interesting properties that can be used for a TTI detecting ITD in CFRP as discussed in chapter 7. It should be noted that even though this AJNDE16-doped DGEBA-DETA exhibits multiplexed behavior, it is not a good TTI candidate for detecting ITD because the activation kinetics of both probes are much faster than that of the matrix degradation. After 30 min the fluorescence was quenched as has been in observed in all the other systems.

4.3.4 AJNDE35 –doped Toray 3900

The fluorescence spectra for the as-cured AJNDE35-doped Toray 3900 and a sample heat-treated at 232 °C for 30 minutes can be seen in Figure 4.16. The excitation source was the 390 nm LED. It should be noted that the heat-treated sample was sanded for reasons discussed in section 5.2.

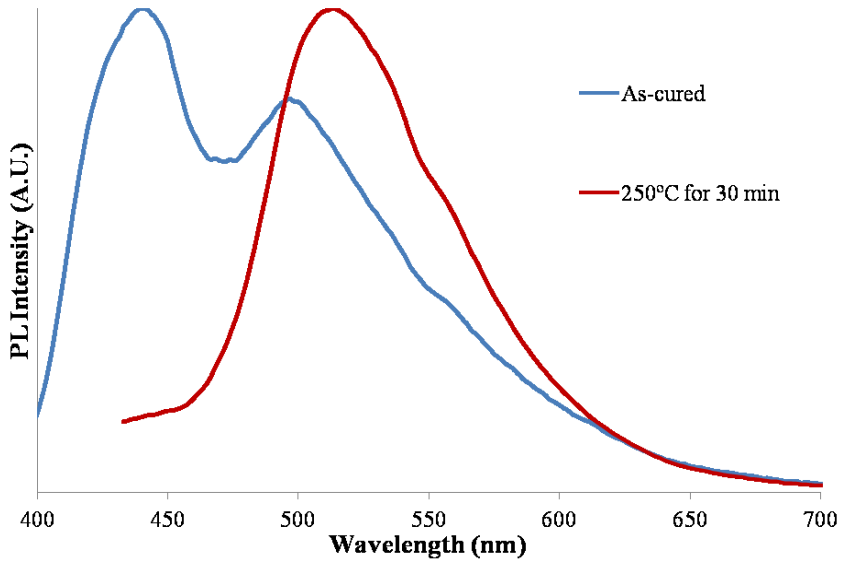

Figure 4.16 Fluorescence spectra of as-cured and heat-treated samples with AJNDE35-doped 3900 samples

In the as-cured spectrum two peaks are found. The first peak is at 440 nm which is the fluorescence of the AJNDE35 molecule and the second is at 500 nm which is the autofluorescence of 3900 blue-shifted about 5 nm, likely due to superposition with the AJNDE35 fluorescence. The heat-treated spectrum only exhibits one peak at 514 nm, which is the fluorescence of AJNDE35a blue-shifted like in the case of AJNDE16a in the epoxy. Since a clear change can be seen in the spectra after heat-treatment it was concluded that AJNDE35 was compatible with the Toray 3900 system unlike AJNDE16.

4.3.5 AJNDE35-doped TGDDM-MMCA

The fluorescence spectra of AJNDE35-doped TGDDM-MMCA can be seen in Figure 4.17. The spectra were measured using a 430 nm LED. The 430 nm LED was preferred for working with AJNDE35-doped TGDDM-MMCA because the spectra 470 nm LED partially overlapped the fluorescence of AJNDE35a. The surface of the heat-treated sample was sanded.

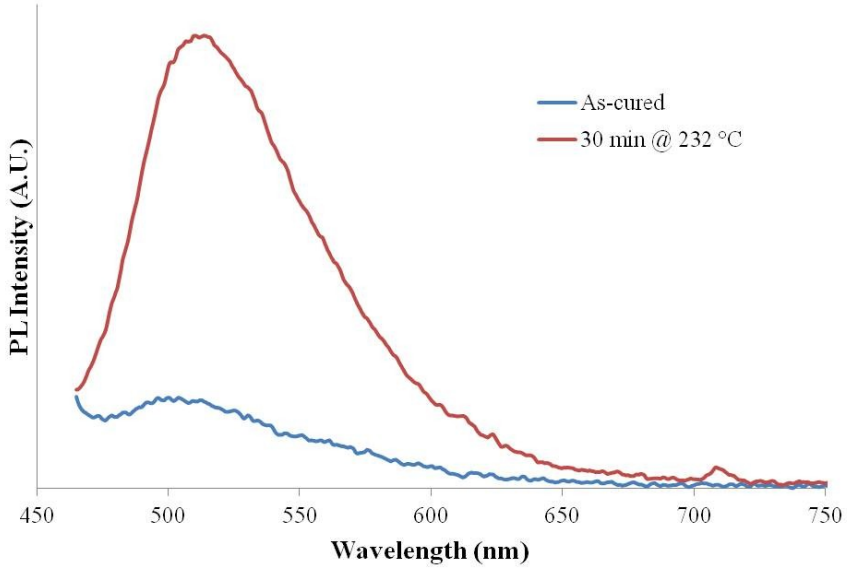

Figure 4.17 Fluorescence spectra of as-cured and heat-treated AJNDE35-doped TGDDM-MMCA samples

A small peak is seen in the as-cured AJNDE35-doped TGDDM-MMCA samples, which is likely the epoxy autofluorescence of the tail end of the AJNDE35 "off" state fluorescence. After heat-treatment the same peak at 514 nm as the heat-treated AJNDE35-doped 3900 sample was observed. This is indicative of the "on" state AJNDE35a. Thus AJNDE35 is also compatible with the TGDDM-MMCA epoxy system.

4.4 Summary

The autofluorescence of the Toray 3900, Hysol EA9390/TGDDM-MMCA, and DGEBA-DETA matrices was characterized so it could be accounted for the probe-doped samples. All of the epoxies had a fluorescence emission peak at 505 nm under a 390 nm excitation and Toray 3900 and DGEBA-DETA exhibited fluorescence emission peaks at 535 nm and 557 nm using a 470 nm excitation source. The response of the autofluorescence to heat-treatment was also studied. In general, it was found that the autofluorescence was quenched with prolonged thermal

exposures. DGEBA-DETA exhibited an interesting behavior where initially the intensity of the fluorescence increased during heat-treatment similar to a thermal damage probe.

The behavior of the fluorescent thermal damage probes AJNDE16 and AJNDE35 in response to heat-treatments in the temperature range for ITD was also presented. As expected both thermal damage probes exhibited a change in fluorescence emission upon thermal exposure. The activated probes (AJNDE16a and AJNDE35a) were found to emit at 595 nm and 542 nm respectively. The fluorescence emission of the probes doped in the various epoxy matrices was also characterized. The AJNDE16-doped 3900 resin cured at 177 ºC, the sample did not show any observable fluorescence response that could be attributed to the probe because it had activated to the cure. Thus AJNDE16 was found to not be compatible with the 3900 epoxy system. In the AJNDE16-doped 9390 cured at 121 ºC, the fluorescence was found to not be activated by the cure, but the fluorescence of AJNDE16a could be observed after heat-treatment. The AJNDE16-doped DGEBA-DETA fluorescence emission blue-shifted with increasing thermal exposure time. It was found that this occurred because the DGEBA-DETA autofluorescence acted like a thermal damage probe as well creating a multiplexed system when combined with AJNDE16. This multiplexed behavior is the foundation of developing a TTI for detecting ITD of CFRP, but the kinetics of activation of this system was too fast to be useful for this application. The fluorescence emission of AJNDE35a was shown to be detectable in the Toray 3900 and TGDDM-MMCA matrices after heat-treatment. For both probes the fluorescence emission was found to blue-shift when doped into the matrix.

5. CONSIDERATIONS FOR THE APPLICATION OF FLUORESCENT THERMAL DAMAGE PROBES

In this chapter, factors pertinent to the application of the fluorescence thermal damage probes are explored. In the first part of the chapter the cause of the fluorescence quenching observed with prolonged thermal exposures is investigated. In the next part the temporal stability of the probes in both the on and off state is discussed. This is followed by a study of the effect of carbon fibers on the fluorescence emission of the probes to determine if they were feasible to use in a composite matrix. Finally the ability of the thermal damage probe to detect localized heat damage is demonstrated on an AJNDE16-doped DGEBA-DETA coating.

5.1 Effect of Optical Properties of Matrix on Fluorescence

As seen in the previous chapter, as exposure time increases at a given temperature the intensity of the fluorescence emission begins to decrease until almost no emission is observed. In addition, the peak wavelength is also found undergo a bathochromic shift for prolonged exposures. There are two possible causes for the observed changes to the fluorescence to occur. One is that the fluorescent probe molecule is degrading or reacting at these temperatures and thus the fluorescence emission is changing. Due to small concentration of probe in the samples it is difficult to determine if the probe has degraded by techniques such as FTIR or NMR. The other possible scenario is that changes to the optical properties of the matrix, namely, the darkening of the resin may have influenced the observed fluorescence. This can be examined by measuring the UV-Vis absorbance of the samples.

5.1.1 UV-Vis Absorbance Spectra of Thermally Exposed 9390 samples

The UV-Vis absorbance spectra as a function of time and temperature for the both the neat and AJNDE16-doped 9390 thin films were measured to determine the effect of the heat-treatment on the absorbance of the film. The absorbance of each spectrum was normalized relative to its maximum absorbance A_{max} to account for small variations in the thickness of the films. The absorbance of some of the thin-films of the AJNDE16-doped 9390 was too high for the detector to record reliable values at wavelengths in the UV-range so those spectra could not be normalized. At a certain point in the spectra, which was dependent on the heat-treatment conditions, the absorbance began to take on the form of an exponential decay. After the decay began the UV-Vis spectra of the AJNDE16-doped 9390 thin films were almost identical to that of the neat 9390 exposed to the same heat-treatment. Since the decay always started at wavelengths shorter than the range of interest (450 nm to 650 nm) it was possible to analyze the behavior of the AJNDE16-doped epoxy using the UV-Vis spectra from the neat 9390 samples. The normalized absorbance spectra of the neat 9390 samples can be seen in Figure 5.1.

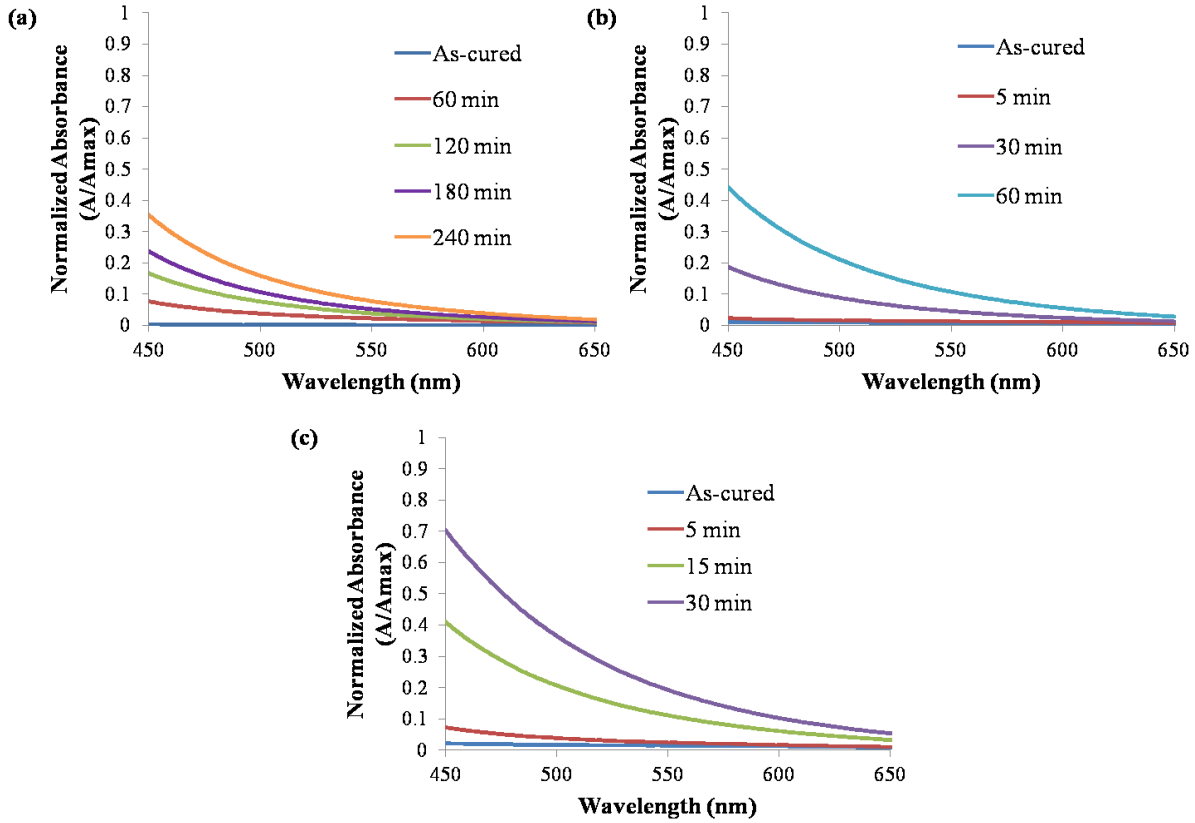

Figure 5.1 UV-Vis absorbance spectra of neat 9390 thin-films as a function of exposure time for heat-treatments at (a) 204 ºC (b) 232 ºC (c) 260 ºC

From Figure 5.1 it can be seen that for all three of the heat-treatment temperatures that the absorption between 450 to 650 nm increased as exposure time increased. Looking at the absorption values at 470 nm (excitation source peak) the absorbance increases strongly with increasing exposure time. For example at 260 ºC the absorption increases after 15 and 30 min to more than 5 and 10 times respectively the absorbance after 5 min exposure. This means that a significantly less amount of the excitation light is able to penetrate through the epoxy matrix and excite the dye. In addition, the absorbance at 560 nm (the fluorescence peak) also increases, which means that the fluorescence is likely being absorbed by the matrix as well. The increase in absorbance of the matrix can be attributed to the formation of chromophores during the degradation process. In similar epoxy-amine cured systems this darkening has been attributed to

the formation of highly conjugated structures as products of the thermal oxidation of the epoxy.[7, 15]

5.1.2 Effect of Heat-Treatment in Inert Atmosphere on Absorbance

If thermo-oxidation of the matrix affected the fluorescence of the samples then it would be expected that if the oxidation could be prevented that the fluorescence of the samples would not be quenched during heat-treatment. To test this theory, samples of the neat 9390 and AJNDE16-doped 9390 thin films were heat-treated in a tube furnace in an inert argon gas atmosphere at 204 ºC for 1 hour. For comparison a set of neat and AJNDE16-doped samples were also heat-treated under the same temperature cycle in air. UV-Vis measurements were taken of the samples heat-treated in argon and air and the results of those measurements and bright-field images of the heat-treated films can be seen in Figure 5.2. The neat 9390 samples are represented by the dashed lines and the AJNDE16-doped 9390 samples are displayed as solid lines. It should be noted that these spectra have not been normalized because as mentioned previously it was not possible to normalize all the spectra due to the limitations of the detector.

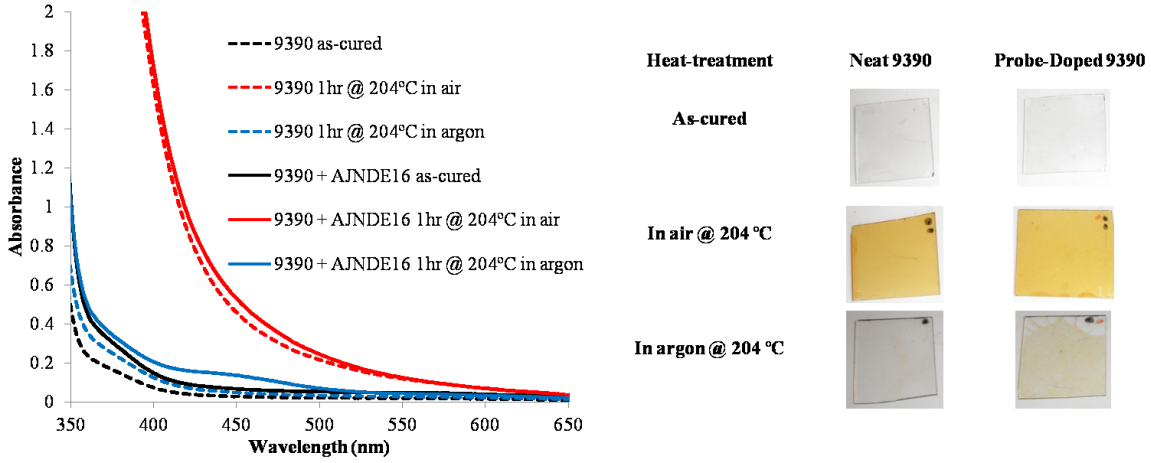

Figure 5.2 (a) UV-Vis spectra of neat and AJNDE16-doped 9390 heat-treated in air and argon atmospheres (b) bright field images of heat-treated thin films

As previously seen, the samples heat-treated in air showed a significant increase in absorbance over the as-cured films. However, the samples heat-treated in inert atmosphere showed very little increase in absorbance compared to the as-cured samples indicating that the darkening of the matrix is a result of thermo-oxidation. It should be noted from the images that the AJNDE16-doped 9390 did darken some compared to the as-cured sample. In the UV-Vis spectra this darkening shows up as a small broad peak with a maximum around 430 nm, which is similar to the peak seen in the UV-Vis measurements in Figure 4.7 for AJNDE16a. This peak is not observed in the AJNDE16-doped sample heat-treated in air due to the significantly higher absorbance of the sample in this region.

As stated earlier, it was believed this darkening of the matrix was responsible for the quenching of the fluorescence observed. To determine if there was a correlation between the matrix darkening and the quenching, the fluorescence of the AJNDE16-doped 9390 samples heat-treated in air and argon were measured. The results are presented in Figure 5.3. The fluorescence spectra were recorded using the 470 nm excitation source.

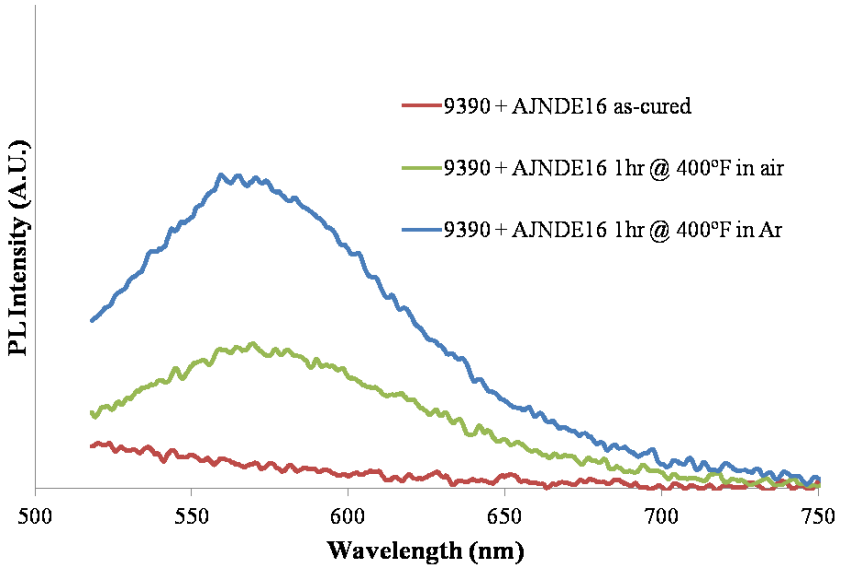

Figure 5.3 Fluorescence spectra of AJNDE16-doped 9390 samples heated in air and argon gas at 204 ºC for 1hr

As the results show, the sample heat-treated in argon exhibited a stronger fluorescence than the sample heat-treated in air indicating oxidation plays a role in the quenching of the fluorescence, which is a possible reason why quenching is observed in the neat epoxy systems. From these measurements it is inconclusive if the probe has been damaged by the combination of high temperature and oxygen.

5.2 Sanding of AJNDE16-doped Epoxy

The repair of damaged composites uses a sanding technique known as scarfing to remove the damaged layers of the composite. A possible issue with the probe during the repair process is that sanding often generates a considerable amount of heat. If enough heat was built up it could potentially activate the probe, which would be detrimental to using the probe in a repair process. Another interesting effect of sanding is that can remove the oxidation layer of the epoxy. The results from section 5.1.2 suggest that if the oxidation layer is removed the fluorescence in areas that were quenched would be restored. These issues are examined in the following sections.

5.2.1 Effect of Sanding on Fluorescence of AJNDE16-doped Epoxy

The effects of different types of sanding methods (hand, orbital, and belt) were investigated to determine if the probe would activate during the sanding. The method that builds up the most heat is belt sanding. This will be the only method of sanding discussed in this paper. To test if the heat generated during sanding would activate the probe, bulk AJNDE16-doped 9390 samples approximately 5 mm thick were held on a belt sanded for 45 seconds using 120 grit sand paper. No cooling liquid was used during the sanding and an insulating ceramic block was used to apply pressure on the sample. The sanding removed between 2~2.5 mm of the epoxy. In addition to the potential activation of the probe from the heat built up during sanding, another potential issue with sanding is that it could potentially remove the probe from the matrix if the probe had segregated near the surface. To verify the probe was still present, the samples were heat-treated at 232 ºC for 5 min to see if fluorescence of the probe could still be activated. The fluorescence measurement of the samples can be seen in Figure 5.4.

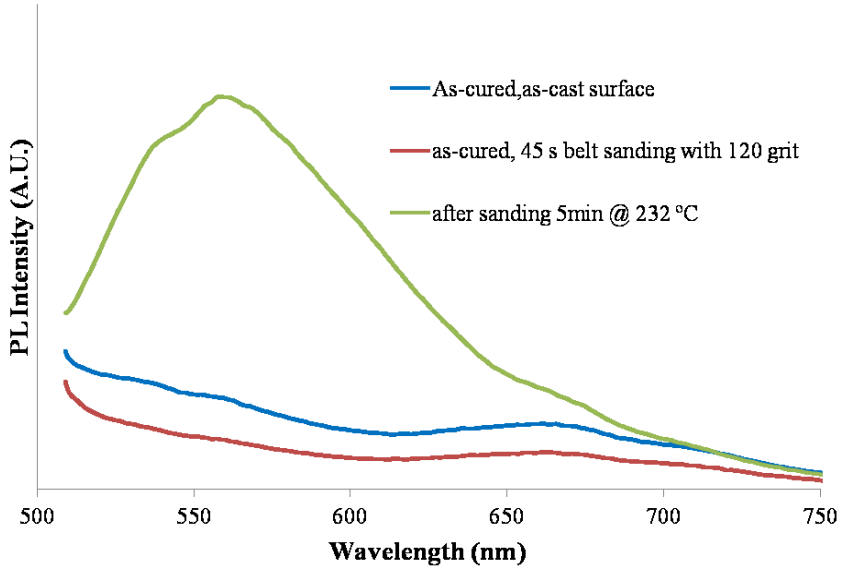

Figure 5.4 Fluorescence measurements of belt sanded AJNDE16-doped 9390 samples

Figure 5.4 shows that the probe was not activated during the sanding process even during a fairly aggressive sanding procedure. There is a small difference in the intensity of spectra of the as-cured and sanded samples, but this is most likely due to differences in the surface roughness and the difficulty to reproduce fluorescence intensity measurements. Since this is an epoxy sample the thermal conductivity is much lower than in a composite sample so more heat would build up during the sanding of the pure epoxy specimen. This means that the above experiment was essentially a worst case scenario for sanding and the probe was not activated. In addition, it can also be seen that besides almost half of the thickness of the sample being sanded away, the probe is still present and can be activated by the usual heat exposure. This indicates that the probe is relatively well distributed throughout the sample. Although no testing was performed on AJNDE35-doped epoxy, it is presumed that there would be no issue with AJNDE35 since it thermally more stable than AJNDE16.

5.2.2 Removal of Oxidation Layer by Sanding

As discussed in section 5.1.2, oxidation of the matrix that occurs at long exposure times appears to quench the fluorescence of the probe. Thus it is expected that if the oxidation is removed, that the fluorescence of the probe would no longer be quenched. The oxidation layer in a similar epoxy heat-treated at 250 ºC for over 700 hours was found to reach only 50 μm.[6, 11] Thus it should be possible to remove the oxidation layer and determine if the fluorescence is restored. To test this theory bulk AJNDE16-doped 9390 samples were heat-treated at 232 ºC for 60 min, a heat-treatment known to cause quenching of the probe fluorescence, and then hand sanded with 240 grit sandpaper to remove the oxidation layer. The results of the fluorescence measurements can be seen in Figure 5.5.

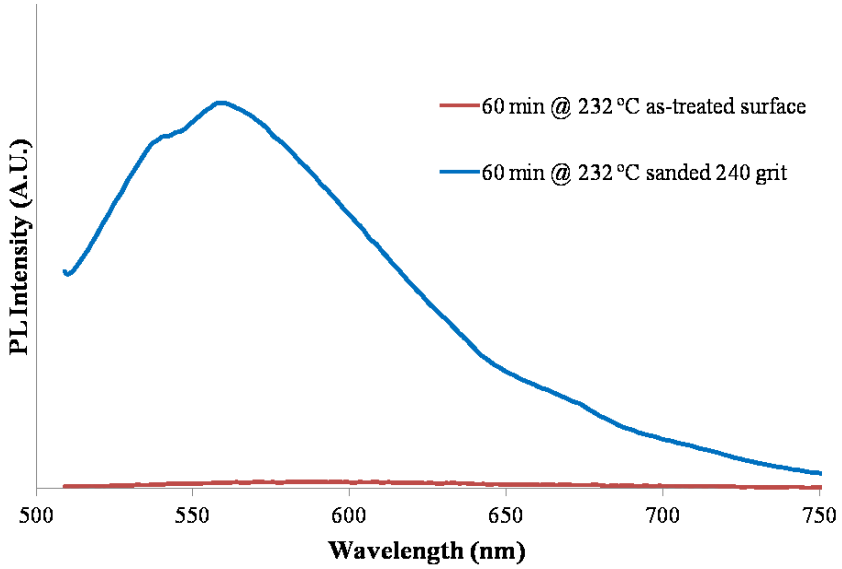

Figure 5.5 Fluorescence after heat-treatment at 232 ºC for 60min for as-treated and sanded surfaces

As Figure 5.5 shows, the sample with the as-treated surface that was heat-treated exhibits no fluorescence, while after sanding a very strong fluorescence peak is present. This result is consistent with the result under inert atmosphere in that preventing or removing the oxidation layer shows the AJNDE16a molecule is stable under the given heat-treatment conditions. This result also shows the viability of the probe for inspection during repairs since even when the fluorescence is quenched by oxidation at the surface the fluorescence can still be observed during the sanding process to access potential damage to plies.

5.3 Temporal Stability of AJNDE16-doped 9390

For the probe to be useful for in field inspections, the temporal stability of the probe in both the off and on states must also be considered.

5.3.1 Temporal Stability of Off State

If the probe is not stable in the off state, two possibilities can happen. The first case is that the probe activates without significant thermal exposure which would yield a false positive on inspection. The second case is that the probe degrades and does not change into the on state even when sufficient thermal exposure occurs thus causing a false negative during the inspection. To test the temporal stability of the off state samples of the AJNDE16-doped Hysol EA 9390 epoxy that had not been heat-treated were left in ambient laboratory conditions. After 3 months, the fluorescence spectrum of one of the samples was taken to test the first case. The sample was then heat-treated at 232 ºC for 5 min to see if the probe would turn to the on state to test case 2. The measurements were made using the 470 nm excitation source. The results of the temporal stability measurements can be seen in Figure 5.6.

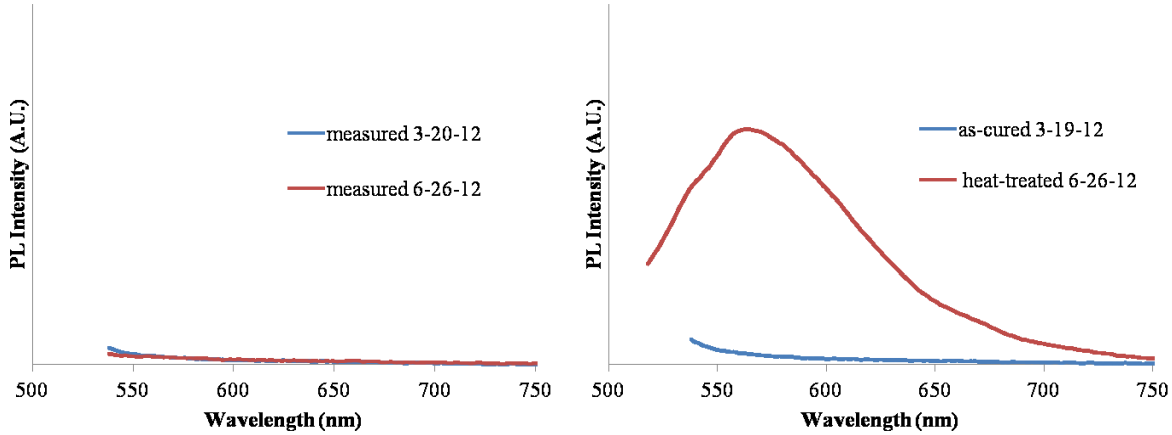

Figure 5.6 Temporal stability of off state of probe (a) first case (b) second case

As it can be seen from Figure 5.6a, at ambient laboratory conditions the fluorescence of the probe does not activate even over the span of months. In addition, if the sample was thermally exposed after long periods of time with no exposure it also activates in a similar manner as that seen when fresh samples were heat-treated. The results of these measurements

were expected because the amount of thermal energy available at room temperature should not be enough to activate or degrade the probe which is designed to be thermally stable for temperatures well over 100 °C.

5.3.2 Temporal Stability of On State

Similar to the off state, it is important that once the probe has been turned on that the fluorescence stays on for the extended period of time that could happen between inspections. To test the temporal stability of the on state, a set of samples were heat-treated after curing to activate the fluorescence and then left in ambient conditions. The fluorescence of the samples was measured periodically to determine if any changes in the spectra could be observed. The results of the temporal stability measurements for the on state can be seen in Figure 5.7.

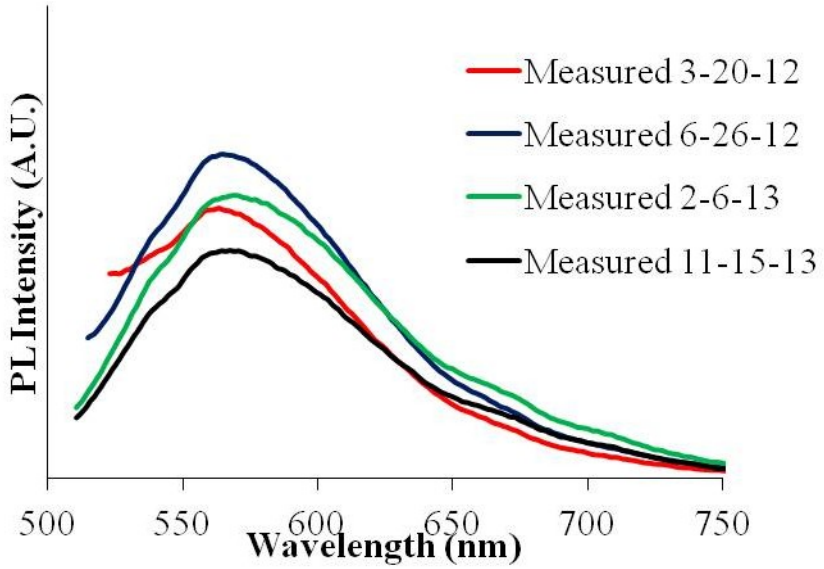

Figure 5.7 Temporal stability of on state of probe

From Figure 5.7, it would appear that changes in the intensity of the fluorescence can be observed after measuring the fluorescence several months apart. However, these changes in fluorescence intensity are within experimental error. Fluorescence intensity is a highly sensitive

measurement that can vary due to a number of factors including intensity of the light source, sensitivity of the detector, the illuminated volume, the optical path of the fluorescence emission to the detector, and many other factors. Unless measured under the exact same experimental conditions, fluorescence intensity measurements are very difficult to reproduce and thus are not quantified on an absolute scale.[59] Given the long time scale between measurements and the frequent use of the spectrometer it was very difficult to reproduce the exact conditions. Even removing the sample from under the reflectance probe and immediately placing it back was found to change the measured intensity by up to ~15%. In addition, it should also be noted that the LED source had to be replaced between the measurements in June and February and the intensity of the new LED is slightly greater than the old one and could contribute to the differences as well. Although it is difficult to determine if there is any change in the fluorescence, it can be seen that the on state is still strong even after 20 months in ambient conditions. Again this result is expected based on the design of the probe since the quenching molecule volatizes upon the decomposition of AJNDE16 leaving it no way to recombine with the fluorescent molecule AJNDE16a.

5.4 AJNDE16 doped into Hysol 9390/ T-800 Carbon Fiber Composite

As shown in the previous sections, probe AJNDE16 was shown to work to detect thermal exposure capable of causing ITD in the Hysol EA 9390 epoxy. However, even though the probe was shown to work in the epoxy, there were some potential complications with introducing the carbon fibers that could affect the performance of the probe. One of the potential issues associated with introducing the carbon fibers was that the carbon fibers could potentially absorb or scatter the excitation source and/or fluorescence emission. Another issue is that the amount of

probe in the optical cross-section is much less than in an epoxy sample since only ~40-50 % of the volume in the composite is the epoxy. This would most likely lead to a decrease in signal since there are less fluorophores available to emit.

5.4.1 Effect of Fiber Orientation on Fluorescence Measurements

The orientation of the fibers in carbon fiber composites is known to affect the signal received from light-based measurements such as FTIR because the scattering behavior of the light is dependent on how the light source and/or detector is positioned relative to the fibers.[33] The effects of the fiber orientation relative to the reflectance probe that is the light emission source and detector for the fluorescence measurements was tested by rotating unidirectional composite samples with a tool surface finish under the probe and observing the change in the fluorescence spectra.

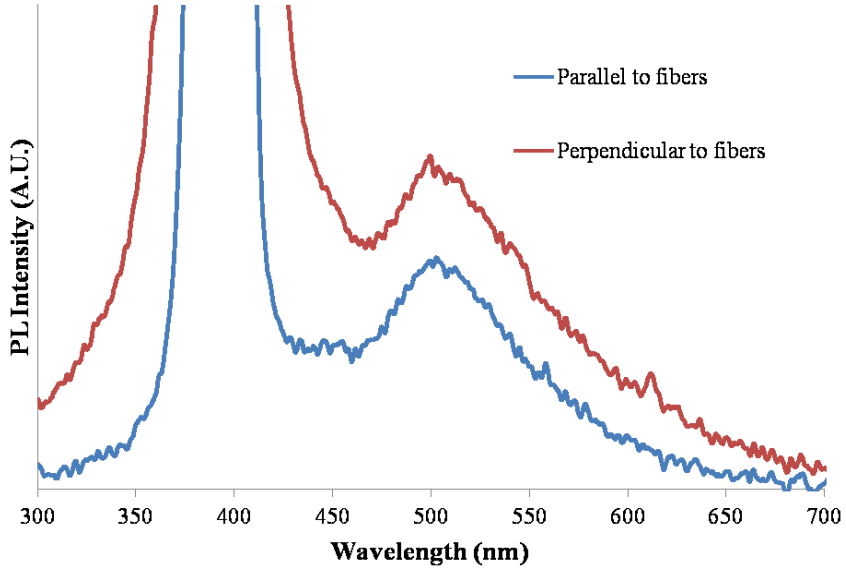

Figure 5.8 Effect of orientation of excitation source with respect to fiber direction on fluorescence measurements

In Figure 5.8, the broad peak on the left is from the excitation source, which is usually excluded from the plots of the fluorescence emission. However, in this case it is useful to be

able to see this peak as it provides information about how the fibers reflect the excitation source. As it can be seen the excitation peak for when the spectrometer probe was oriented perpendicular to fibers is much broader than one where it is orientated parallel to the fiber direction. This is indicative that more excitation light was reflected back from the surface of the composite to the detector when the probe was oriented perpendicular to the fibers. In Figure 5.8, this reflected light does not significantly change the fluorescence spectrum, but it is possible for the peak to broaden to the point where it could obscure weak fluorescence emission. From these results aligning the source parallel to the fibers would appear to be the best orientation due to the lower amount of scattering of the incident light. However, using a proper set of bandpass and longpass filters should be able to reduce much of this effect. In the current measurement system, it was not possible to utilize the filters necessary to reduce this effect since only one in-line filter holder that was compatible with the fiber optic setup was available.

In the 0-90 fabric composite samples the orientation of the excitation source in relation to the fibers is more difficult to control since the spot size covers areas that have both 0º and 90º orientations. So the measurements end up more of average of the two domains. For imaging a fabric sample, an angle of 45º is recommended so that the reflection of the light is relatively equal over the two domains.

5.4.2 Effect of Carbon Fibers on Excitation and Emission of AJNDE16-doped Epoxy

0-90 fabric composites samples with the AJNDE16-doped 9390 as the matrix were subjected to the same heat-treatments as the resin samples. A plot of the fluorescence response of the composite samples heat-treated at 232 ºC for several time increments is shown in Figure 5.9. A peel-ply surface was used to provide a consistent surface for measurement. The

fluorescence measurements were taken using the 470 nm excitation source and the source was oriented parallel to the weft of the fabric.

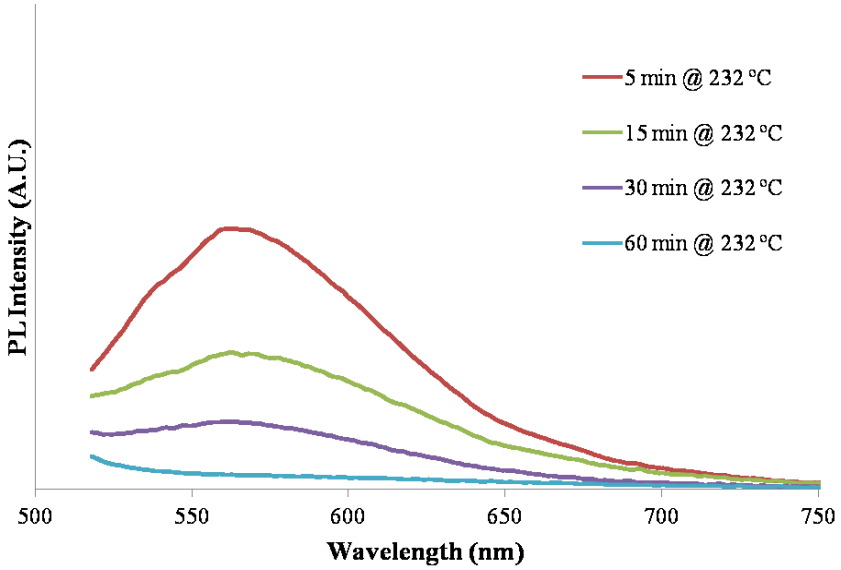

Figure 5.9 Fluorescence spectra of AJNDE16-doped composite heat-treated at 232 ºC

Comparing Figure 5.9 to Figure 4.13b, it can be seen that the fluorescence response is of the AJNDE16-doped composite is very similar to that of AJNDE16-doped 9390 samples. The bright field and fluorescence images of the AJNDE16-doped composite heat-treated at 232 ºC are shown in Figure 5.10. For the fluorescence images, a 590 nm long-pass colored glass filter was placed on the camera lens to prevent the excitation wavelengths reflected off the composite surface from interfering in the image.

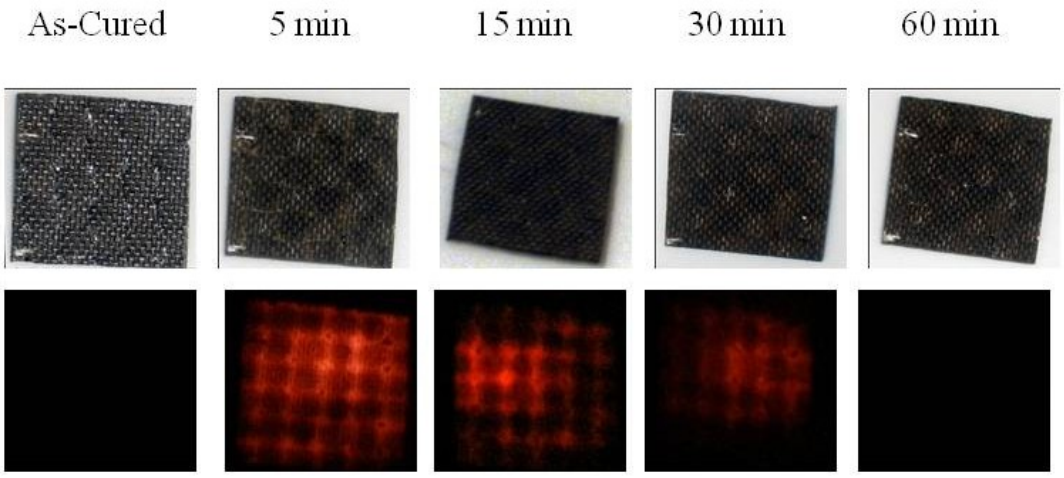

Figure 5.10 Bright field (top) and fluorescence images of composite with the AJNDE16-doped epoxy matrix heat-treated at 232 ºC for different exposure times

Compared to the resin samples in Figure 4.14 where the thermo-oxidation of the matrix was visible due to the darkening of the matrix, the thermal degradation is difficult to observe to in the bright field images due to the presence of the already black carbon fibers. There is some discoloration that can be observed, but against the black carbon fibers the contrast is difficult to observe visually without close inspection. However, the fluorescence behavior of the probe can be clearly seen and behaves similar to that seen in the pure resin samples. This indicates that it is feasible to use the probe for detecting thermal exposure in composite systems. Worth noting in the fluorescence images is that the resin rich areas at the corners of where the warp and the weft intersect are significant brighter than the surrounding areas. This is a result of having more resin in these areas which means that there are more of the probe fluorophores in this area as well; thus a brighter emission is observed. In fact, the surface of composite tends to be more resin-rich than the rest of the composite, however, during the repair process the resin-rich surface is removed and the volume fraction of resin available to fluorescence is significantly lower. This was one of the potential issues with LIF and the thermal damage probe presented in this work. Figure 5.11 shows a comparison of the fluorescence spectra of the composite sample heat-treated

for 5 min at 232 ºC, 60 min at 232 ºC, and the sanded composite. Also shown is the fluorescence image of the sanded composite. It should be noted that this image was taken using a different filter system then the previous composite samples. In this case the image was taken using a 472 nm bandpass filter on the excitation and a 515 nm longpass filter on the camera to remove more of the excitation light reflections. As a result the image below is more representative of the actual color fluorescence of the probe.

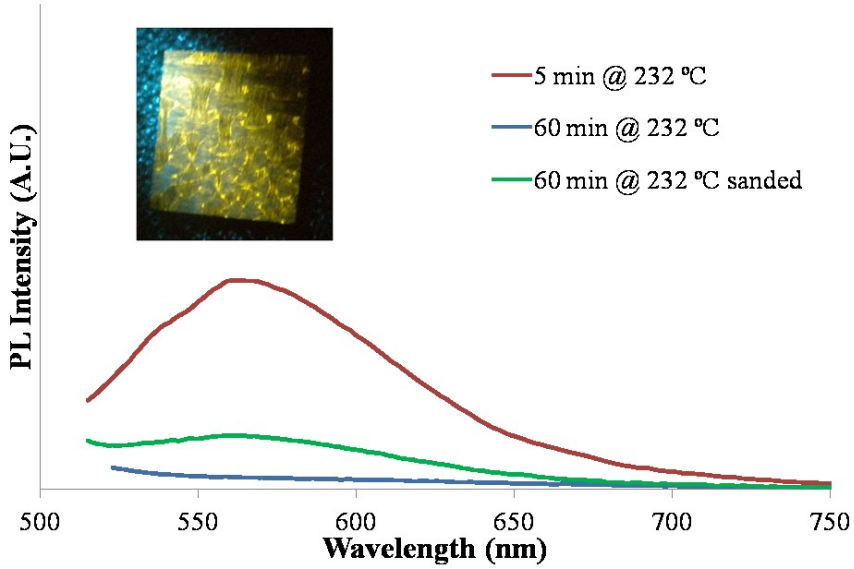

Figure 5.11 Fluorescence spectra of AJNDE16-doped composite samples before and after sanding and the fluorescence image of the sanded composite

As seen in Figure 5.11, the fluorescence can still be observed after sanding the surface of the composite although the fluorescence spectra is much weaker than the maximum intensity measured after 5 min at 232 ºC. In the fluorescence image, this fluorescence can still be easily seen. The difference in the intensity of the spectra between the sample before and after sanding is probably due a less resin rich surface in the sanded sample. This weaker intensity can easily be resolved by increasing the detector integration time.

5.5 AJNDE16-Doped Coating on Composite Panel

It may not always practical to dope the probe into the composite matrix resin. One issue as seen in the case of the Toray 3900 system is that AJNDE16 was incompatible with the cure cycle. Another potential drawback is that the structural parts would require large amounts of the probe and it may not be cost effective to utilize that much probe in the structure. In addition, certification of parts for use on airplanes is very stringent, costly, and time consuming and modifying the matrix resin can result in the need to recertify a part. A potential solution to these issues is to dope the thermal damage probes into a coating that is applied on the outside of the part. While this would limit the ability to detect thermal exposure while scarfing through composite during the repair process a coating still allows for the detecting where a thermal exposure occurred and using another measurement such as FTIR to guide the repairs.

5.6 Fluorescence Behavior of AJNDE16 Doped Coating

The performance of the thermal damage AJNDE16-doped epoxy coating were tested at two different temperatures 204 ºC (~400 ºF) and 232 ºC (~450 ºF). The thermal profile for the two different temperature experiments were measured using 3 K-type thermocouples. The thermocouples were placed relative to the center of the contact area at 7.5 mm (within the diameter of the rod), at 10 mm (~ 0.8 mm outside of rod), and at 12.5 mm (~ 3.3 mm outside of rod). The measured temperature profile for the samples exposed to the aluminum rod heated at 204 ºC is shown in Figure 5.12.

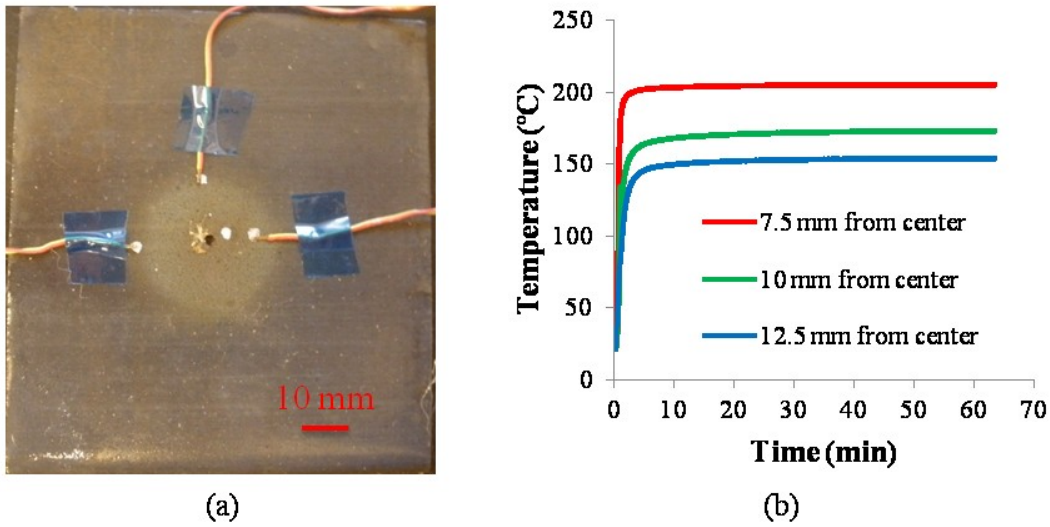

Figure 5.12 (a) Thermocouple placement on coatings (b) Measured temperature profiles from coating exposed to max temperature of 204 ºC

The temperature in the coating reached steady state after about 3-5 min depending on how close the thermocouple was to the sample. For the fluorescence response measurements of the AJNDE16-doped coatings the beginning of the exposure time was taken as the time at which the temperature of the thermocouple in contact with rod reached steady state. As it can be seen in Figure 5.12b, the temperature dropped off significantly outside of the area in contact with the rod. At approximately 0.8 mm outside the contact area the steady state temperature was 173.5 ºC and at about 3.3 mm the temperature was 153.8 ºC. The large temperature drop-off in a short distance from the heat source indicates that highly localized heating was achieved. The fluorescence behavior of the localized thermal exposure of the coating at 204 ºC can be seen in Figure 5.13. For the fluorescence measurements the 390 nm LED was used as the excitation source. The colored ellipses represent the approximate area where the measurements for the fluorescence spectra were taken. The images were taken using a 365 nm excitation source and using a 435 nm longpass colored glass filter to remove reflections of the excitation source from

the image. The approximate temperatures of the fringe of the fluorescent areas were extrapolated from the data in Figure 5.12b.

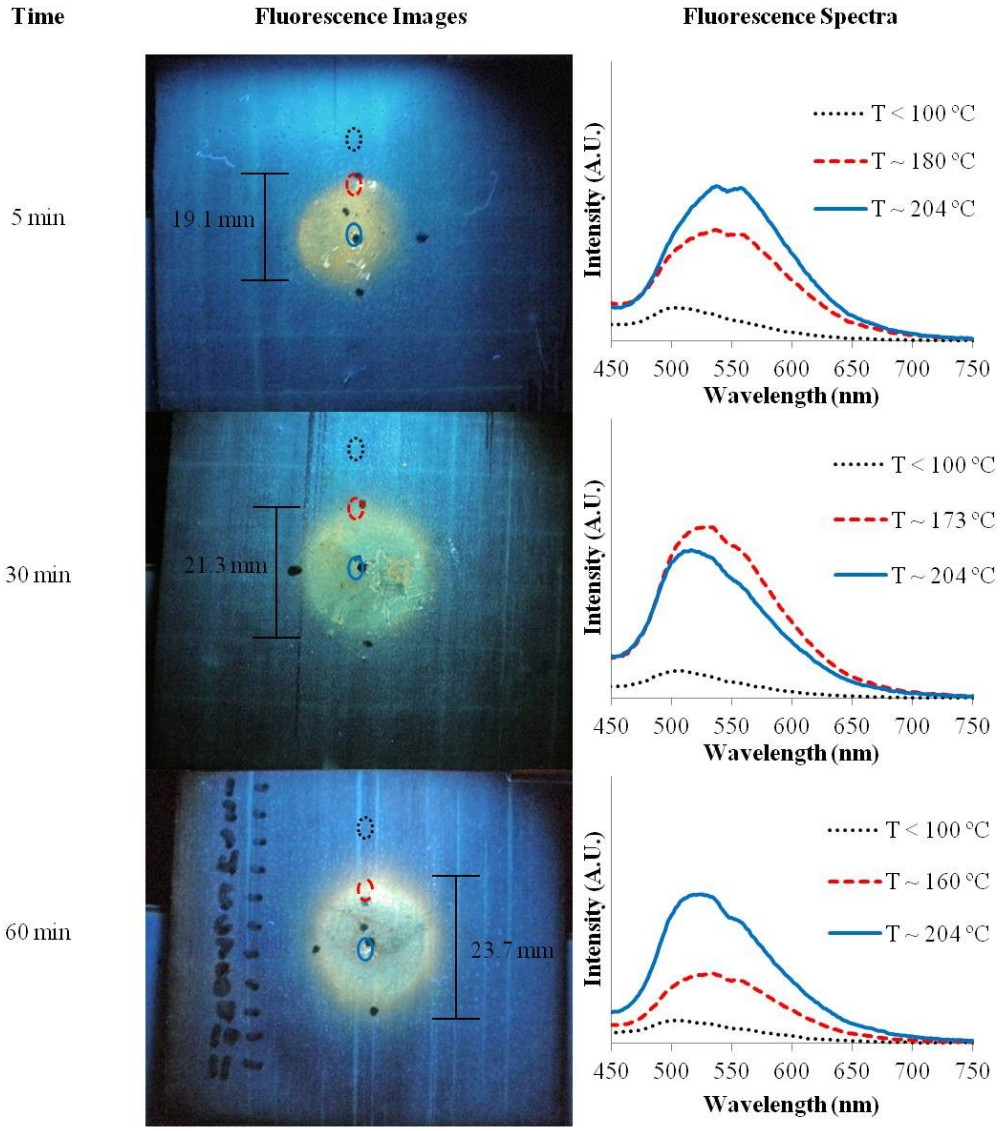

Figure 5.13 Fluorescence images and spectra of localized heating of AJNDE16-doped epoxy coating at 204 ºC for various exposure times

Several features can be noted from the Figure 5.13. In the first few minutes the diameter of the fluorescent area is only about 19.1 mm which is about 0.7 mm larger than that of the aluminum rod. As the exposure time increases, the fluorescent area becomes larger. The ITD damage area would also be expected grow with longer exposure times. However, it should be

noted that the probe can be seen to activate at thermal exposures as low as 160 ºC in a time of about 60 minutes, which is well below the time-temperature range for incipient thermal damage in most composite systems. It also means that this probe is incompatible with 177 ºC curing epoxies such as was seen in the case of the Toray 3900 resin system.

The other feature to note is the development of the color of the fluorescence emission. As it can be seen in Figure 5.13, the probe exhibits a yellow-orange fluorescence (peaks at 534 nm and 560 nm) in the initial heating stages, but as the heating continues the fluorescence begins to turn blue-green (peak at 518-522 nm, shoulder at 556 nm) with the yellow-orange fluorescence on the fringes. In the spectra for 5 min at 204 ºC, the peak at 560 nm can be attributed to probe AJNDE16a and the peak at 534 nm is a combination of AJNDE16a and the autofluorescence of DGEBA-DETA. The yellow-orange fluorescence in this early stage of heating indicates that the intensity of AJNDE16a is initially stronger than that of the autofluorescence of the matrix. However, as the exposure time increases, the intensity of the autofluorescence grows faster than that of AJNDE16 causing the shift towards the blue-green emission. On the fringes though there are still areas where the fluorescence of AJNDE16a is stronger. As mentioned earlier the autofluorescence is essentially another thermal probe, whose kinetics and peak wavelength are different from that of AJNDE16. Since the 2 fluorescent probes emit at different wavelengths (in this case 505 nm and 565 nm) the wavelength shifts as a result of superposition of the fluorescence spectrum of each molecule based on the relative intensity (activation) of the fluorescence at a given time. This is essentially a system with multiplexed thermal damage probes, although in this case it is not much use for a TTI because the activation of both probes occurs at thermal exposures below where ITD occurs in composite panels. However, this does provide a preview of what behavior to expect when thermal damage

probes AJNDE16 and AJNDE35 are multiplexed. The multiplexed AJNDE16 and AJNDE35 and its application as a TTI will be discussed in detail in chapter 7.

The temperature profile for the coatings exposed to 232 ºC is shown in Figure 5.14. Again a considerable drop off in temperature is found away from the center, however, the temperatures at 10 mm and 12.5 mm were 24 ºC and 18 ºC higher respectively than in the case at 204 ºC at those locations, as would be expected since the initial temperature is higher.

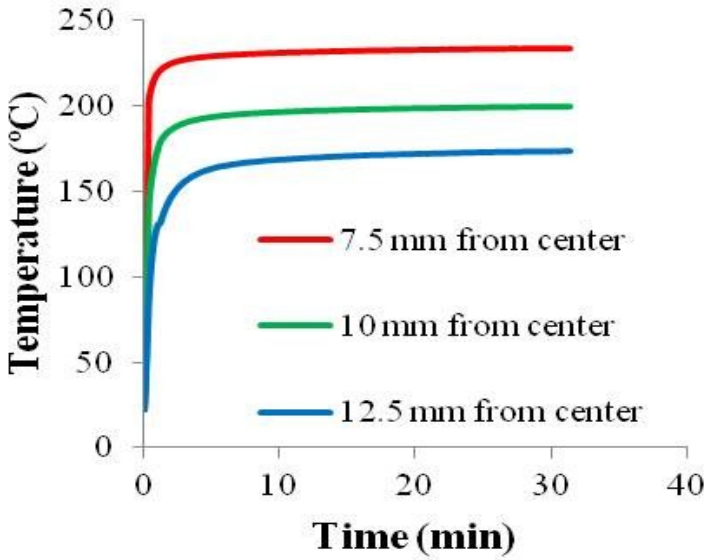

Figure 5.14 Temperature profile for coating exposed to 232 ºC

The fluorescence behavior of the localized thermal exposure of the coating at 232 ºC can be seen in Figure 5.15. The images and spectra were taken using the same methods as the samples heated at 204 ºC. The approximate temperatures of the fringe of the fluorescent areas were extrapolated from the data in Figure 5.14.

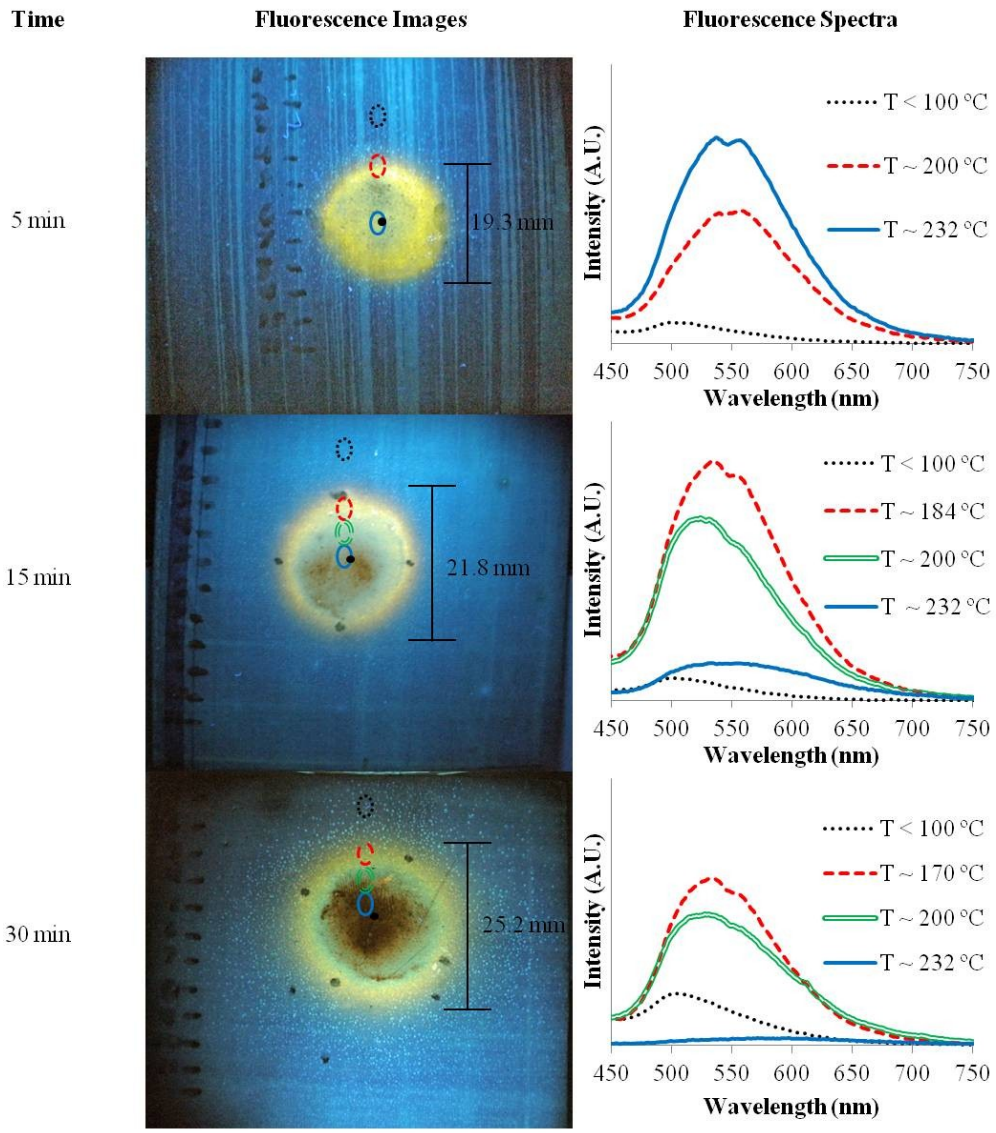

Figure 5.15 Fluorescence images and spectra of localized heating of AJNDE16-doped epoxy coating at 232 ºC for various exposure times

Similar to the samples heated at 204 ºC, the sample heated at 232 ºC for 5 minutes exhibits the yellow-orange fluorescence and the diameter of the fluorescent area was only 19.3 mm. However, at the longer exposure the diameter of the fluorescent area grows significantly larger reaching 25.2 mm after 30 minutes. This is significantly larger than the 21.3 mm observed for 30 minutes at 204 ºC. Similar to the Hysol EA 9390 and Toray 3900 systems, for exposure times longer than 5 minutes at 232 ºC, areas where the fluorescence begins to fade due to

oxidation were observed. After 30 minutes, almost no fluorescence is observed in the area in direct contact with the rod. As mentioned previously, these highly oxidized areas where the fluorescence is quenched are likely indicators of potential areas where significant ITD has occurred.[2, 30] However, the localized heating experiments show an important result that was not seen in the bulk samples that were heat-treated in the convection oven. The difference in the local heating experiments is that the area surrounding the oxidized site still emits fluorescence making it possible to locate the damage site even though the fluorescence of the oxidized area is no longer visible. In fact, unless the whole part is subjected to the thermal exposure that causes enough oxidation to quench the fluorescence of the probe, it is expected that there should always areas of fluorescence surrounding areas where the fluorescence has been quenched. This is due to the temperature gradients that will always develop away from the exposure area during a localized heating event.

In section 5.2.2, it was seen that sanding was able to remove the oxidation layer and thus restore the fluorescence of the sample. Figure 5.16 displays the results of sanding a highly oxidized sample of the AJNDE16-doped coating. Again it can be seen that removing the oxidation layer restores the fluorescence of the sample.

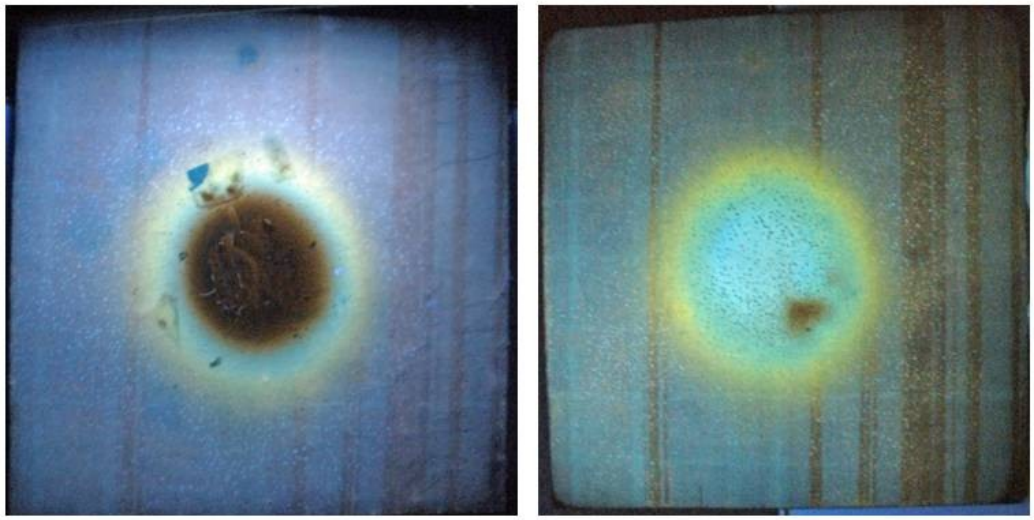

(a) (b)

Figure 5.16 (a) coating with fluorescence quenched by oxidation (b) sample after sanding to remove oxidation

5.7 Summary

Factors that could affect the application of thermal damage probes were investigated. To examine the quenching behavior, UV-Vis absorbance measurements were taken of samples heat-treated in air and in argon and it was found that increasing absorbance caused by thermo-oxidation of the matrix was correlated to the quenching of the fluorescence. By removing the oxidation layer by sanding it was found that the fluorescence could be restored. The probe was designed to work with composite repair processes which involve sanding away the damaged layers; however, there was the potential for heat generated during the sanding to activate the probe. The AJNDE16-doped 9390 samples were aggressively sanded and showed no activation after the sanding process, and the probe could still be activated by heat-treatment. The temporal stability of the probe in both the on an off states was found to excellent as the probe was able to maintain its fluorescence state in ambient conditions with no significant changes observed over the span of months. The fluorescence response of using AJNDE16-doped 9390 as a matrix for a

carbon fiber composite was also examined. The orientation of the excitation source relative the fiber direction has a small effect on the fluorescence measurements. When the excitation source was oriented perpendicular to the fibers more of the excitation light was reflected which broadened the excitation peak, and can lead to a possible overlap into the emission spectra. This effect can be reduced by having a proper set of bandpass and longpass filters. The fluorescence response of the AJNDE16-doped composite was found to be similar to that of the AJNDE16-doped resin samples. However, in the composite the intensity of fluorescence was affected by whether the region was resin rich or resin poor.

Doping the thermal damage probe into a coating was investigated as an alternative to doping the composite matrix with the thermal damage probe. To determine the AJNDE16-doped coating fluorescence response, the coatings were subjected to localized heating experiments. From the localized heating experiments it was found that the diameter of the fluorescence grew as exposure time increased. The farther the area is from the heat source, the lower the temperature is and thus a longer time for the probe fluorescence to become visible is needed. Another interesting result that was observed was that the color of the fluorescence emission was found to shift from yellow-orange to blue-green during the exposure. This shift was attributed to the superposition of the autofluorescence of DGEBA-DETA and the fluorescence of the probe, both of which were activated in response to the thermal exposure. As previously described quenching of the fluorescence was observed in areas of long exposure to high temperature. Even when the fluorescence was quenched in the most heat-damaged regions, the fluorescence could still be observed around the quenched area. It was suggested that in these cases that the quenching is a good indicator of areas that may have significant ITD. As expected, it was found that sanding to remove the oxidized layer from the quenched areas restored the fluorescence.

6. KINETICS AND MODELING OF PROBES AJNDE16 AND AJNDE35

In this chapter the kinetics of the activation of probes AJNDE16 and AJNDE35 are measured and models for the kinetics of the probes are also developed.

6.1 Kinetic Measurements

As described in section 3.4.2 the kinetic measurements of the activation of probes AJNDE16 and AJNDE35 doped in a TGDDM-MMCA matrix were done using fluorescence intensity measurements. As has been previously mentioned fluorescence intensity measurements are difficult to reproduce unless successive measurements are performed under the exact same experimental conditions. UV-Vis absorption would have been the preferred method for measuring the kinetics of activation, but due to the very small amount of probe used (0.05 wt%) in the doped TGDDM-MMCA samples it was difficult to observe and quantify the change in absorbance from the probes. Perhaps this may have been feasible at higher concentrations, but the amount of probe available was limited. Thus fluorescence intensity measurements were chosen as the method to measure kinetics. Section 3.4.2 describes in detail the experimental setup used to obtain repeatable fluorescence intensity measurements. However, the measurement setup was not the only issue that had to be addressed for the fluorescence intensity measurements. As described in section 5.1, oxidation of the epoxy during thermal exposure can also reduce the measured fluorescence intensity. Thus to obtain accurate measurements of the probe activation by fluorescence intensity oxidation of the sample had to also be prevented. To achieve this goal the probe-doped TGDDM-MMCA samples were sandwiched between two glass substrates and cured under vacuum to help remove air trapped in the sample. To verify that this sample preparation was preventing oxidation samples of neat TGDDM-MMCA were

measured using UV-Vis before and after heat-treatment at 232 °C for 60 min; a heat-treatment that was known to cause significant oxidation in the samples. The results of these measurements can be seen in Figure 6.1. The absorbance was normalized by the maximum absorbance which occurred at 310 nm.

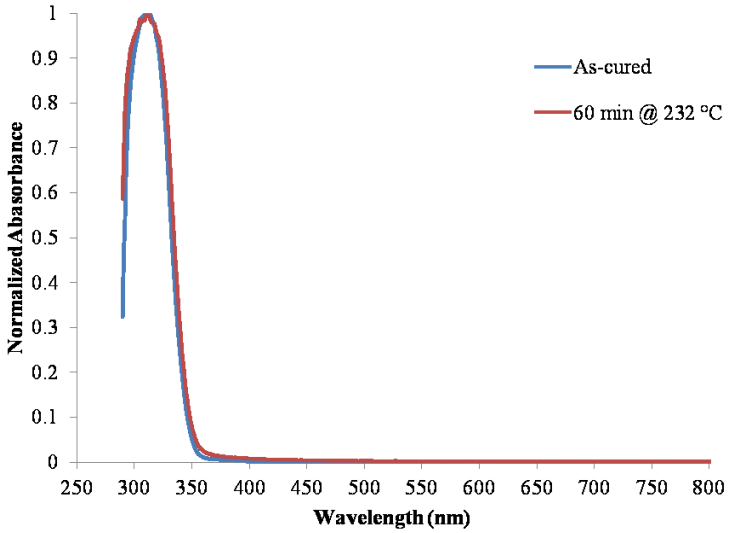

Figure 6.1 UV-Vis spectra of neat TGDDM-MMCA sandwiched between glass substrates before and after heat-treatment at 232 °C for 60 min

As seen in Figure 6.1, almost no change in the UV-Vis spectra of the neat TGDDM-MMCA was observed even after heat-treatment that would usually cause a significant increase in the absorbance of the sample due to oxidation. This indicates that this sample preparation procedure does a satisfactory job of preventing oxidation of the sample at least for the range of thermal exposures used for these measurements and thus was suitable for using to do the kinetic measurements of the probe-doped epoxy.

From section 2.3 activation of the thermal damage probes AJNDE16 and AJNDE35 was expected to be a unimolecular decomposition reaction. In general the unimolecular decomposition reaction described in section 2.3 has a chemical equation [77]

$$aA \rightarrow bB + cC$$

Where A in this case represents the probe molecule before decomposition (AJNDE16), B and C represent the molecular products of the decomposition (the activated probe molecule AJNDE16a and the volatile species), and a,b,c give the stoichiometry the reaction. For an irreversible unimolecular decomposition reaction, the kinetics can be represented by equation 6.1.[77]

$$r = -\frac{1}{a}\frac{d[A]}{dt} = -k[A]^n \qquad \text{equation 6.1}$$

Where r is the reaction rate which equals the instantaneous rate of change of the concentration of molecule A ($\frac{d[A]}{dt}$), k is the rate constant, [A] is the concentration of molecule A, and n is the order of the reaction. The rate constant k is temperature dependent and is assumed to follow an Arrhenius relationship seen in equation 1.1. equation 6.1 cannot be applied in this case because the distribution of the probe inside the matrix and the volume of the sample excited by the excitation source are not known. In addition, the measured intensity may not reflect all of the activated molecules since the matrix may absorb some of the excitation light or the fluorescence emission of some of the probes. So instead a phenomenological analog to the reaction rate equation is needed. If α represents the fraction of measureable probe that has not been activated and β is the fraction of measureable probe that has been activated the relation between α and β is given by equation 6.2.

$$\alpha + \beta = 1 \qquad \text{equation 6.2}$$

In terms of the decomposition reaction α corresponds to the percent of the initial probe molecule (AJNDE16 or AJNDE35) remaining and β corresponds to the percent of probe molecule in the activated state (AJNDE16a or AJNDE35a). Since β represents the relative amount of activated probe it is the quantity that is measured by the fluorescence intensity. Thus β is defined as

$$\beta = \frac{I}{I_\infty} \qquad \text{equation 6.3}$$

Where I is the measured intensity, and I_∞ is the measured intensity at infinity when all the measureable probe has been activated (i.e. the intensity where $\beta = 1$). From these definitions the phenomenological rate equation analog to equation 6.1 can be defined as

$$r = \frac{d\alpha}{dt} = k\alpha^n = k(1-\beta)^n = k(1-\frac{I}{I_\infty})^n \qquad \text{equation 6.4}$$

6.1.1 Kinetic Measurements of AJNDE16

An example of the fluorescence intensity measurements for the AJNDE16-doped TGDDM-MMCA samples heat-treated at 191 °C can be seen in Figure 6.2a. These fluorescence intensity measurements were normalized by I_∞ which was determined to be when the measured change intensity between heat-treatments was on the order of the noise in the measurements. The spectra were taken using the 470 nm LED excitation. A plot of α as a function of time for AJNDE16-doped TGDDM-MMCA samples heat-treated at 191 °C, 204 °C, 218 °C can be seen in Figure 6.2b.

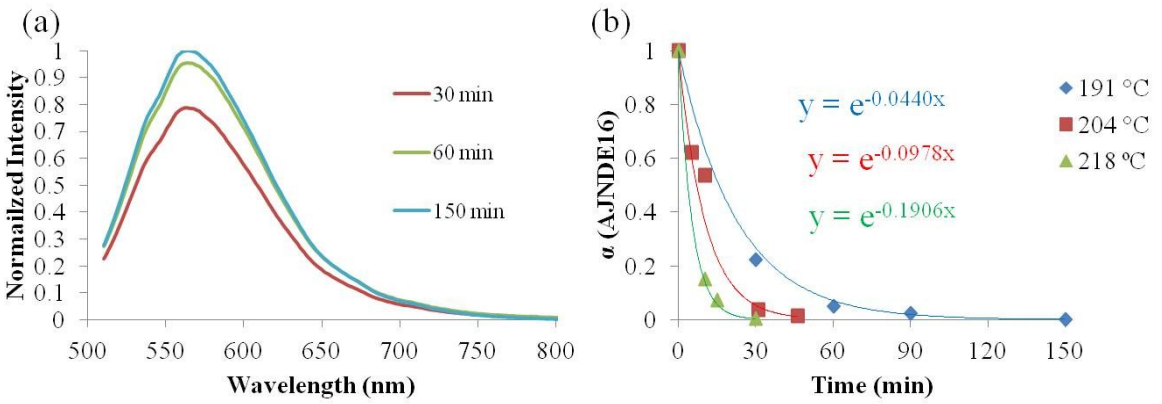

Figure 6.2 AJNDE16-doped TGDDM-MMCA kinetic measurements (a) fluorescence spectra from 191 °C measurements normalized by I_∞ (b) α vs time plots for different temperatures

As it can seen in Figure 6.2b all the plots for α as a function of time are best fit by exponential functions. It was not shown in the plots, but the R^2 values for each of the exponential fits was greater than 0.98. In traditional unimolecular kinetics an exponential function is found when the reaction has first order kinetics. Integrating the rate law in equation 6.4 with order n = 1 the expression for α takes on the form in equation 6.5.[77]

$$\alpha = \alpha_0 \exp(-kt) \qquad \text{equation 6.5}$$

Where α_0 is the initial value of α, k is the rate constant, and t is time. No fluorescence from activated AJNDE16a was observed in as-cured spectra so α_0 was assumed to be equal to 1 at time = 0.

It should be noted that some error in the actual heat-treatment times may exist because the samples went through a transient heating stage each time the sample was replaced in the oven. To try to account for this error another sample of neat TGDDM-MMCA epoxy with a k-type thermocouple embedded in it was prepared using the same glass substrates sample preparation method as the kinetic samples. The sample with the embedded thermocouple was

placed in the oven at the same time as the probe-doped sample and it was used to monitor the temperature during the initial heating stage such that the measurement time could be adjusted to account for time spent in this stage. It is not likely that probe molecules activated during the initial heating stages had a significant effect on the measurements because of the strong temperature dependence of the rate constant. As it can seen in Figure 6.2b, the rate constant essentially doubles for every ~13-14 °C difference in temperature. Thus only when the sample was close to the heat-treatment temperature would the activation rate of the probe be significant enough to potentially affect the results. Typically the sample was only in this transient temperature range for a short time (~5-6 min) before reaching the steady state heat-treatment temperature and this was accounted for in the measurements. An example of the measured temperature profile for one of the heat-treatment can be seen in Figure 6.3.

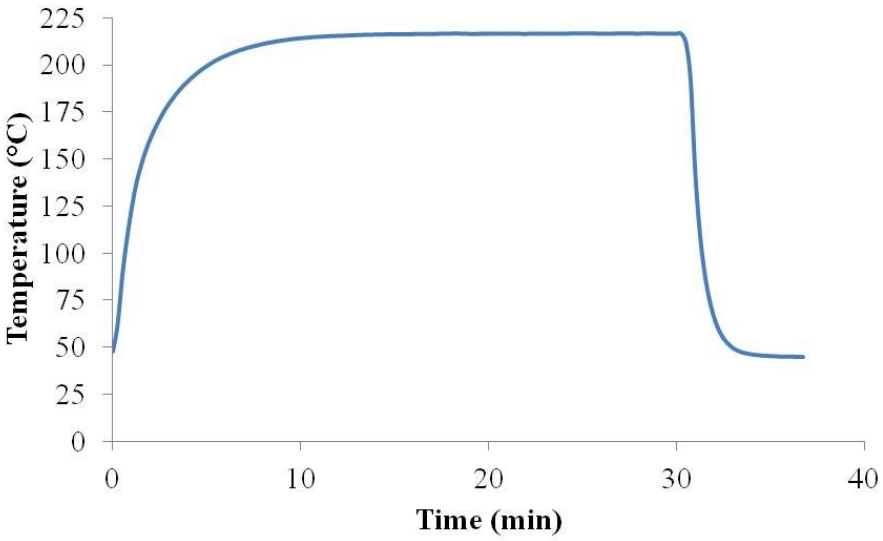

Figure 6.3 Example temperature profile for kinetic measurement sample heat-treated at 218 °C

6.1.2 Kinetic Measurements of AJNDE35

An example of the fluorescence spectra measurements for AJNDE35 heat-treated at 204 °C as a function of time is shown in Figure 6.4a. Not all the spectra measured are shown to make the plot easier to read. These spectra were collected using the 430 nm LED as an excitation source. Again the spectra were all normalized by I_∞. It should be noted that for the AJNDE35 kinetic measurements I_∞ was not measured directly due to the significant amount of time necessary for the process to go to completion. Instead I_∞ was extrapolated by fitting a function to the difference in intensities between each time increments and then using that function to predict when the changes between time increments would be on the order of the noise in the measurements. This extrapolated I_∞ is a possible source of error in the measurements. A plot of α as function of time for AJNDE35 at temperatures of 204 °C, 218 °C, and 232 °C can be seen in Figure 6.4b.

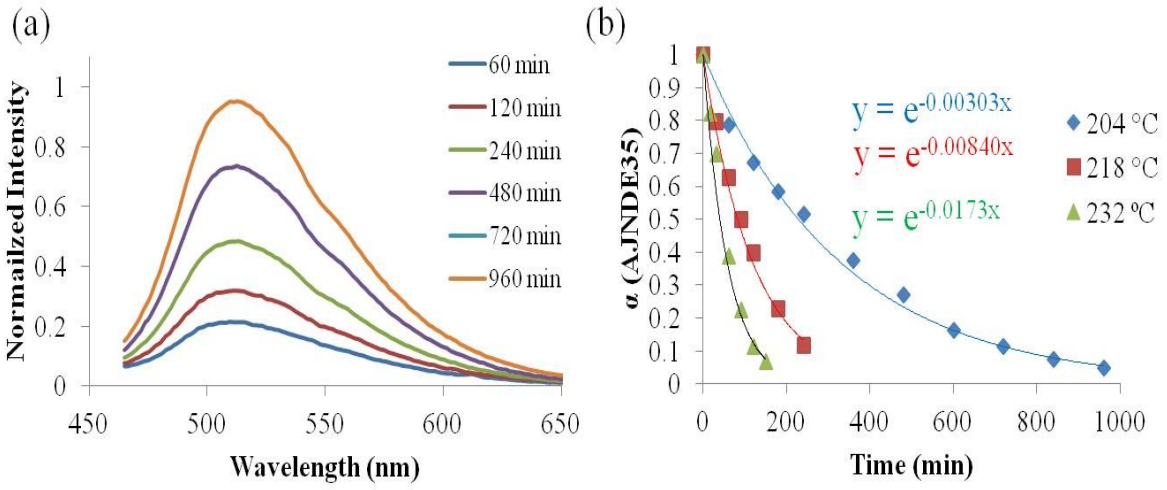

Figure 6.4 AJNDE35-doped TGDDM-MMCA kinetic measurements (a) fluorescence spectra from 204 °C measurements normalized by I_∞ (b) α vs time plots for different temperatures

Like AJNDE16, the decomposition of AJNDE35 is best fit by exponential functions and thus the decomposition of AJNDE35 is considered to be first order reaction as well. Comparing the results in Figure 6.2b and Figure 6.4b it can be seen that the decomposition of AJNDE35 occurs at a much slower rate than AJNDE16 at the same temperature. For example at 204 °C AJNDE16 is almost completely activated after 60 min, but only approximately 95% of AJNDE35 is activated after 960 min. These results seem to match the qualitative results that AJNDE16 activation can be seen at much lower temperatures and times than AJNDE35, which may explain why AJNDE16 was found to activate in Toray 3900 during the cure cycle, but a measurable amount of AJNDE35 did not during the same cure cycle.

6.1.3 Apparent Activation Energies of AJNDE16 and AJNDE35

From the kinetic measurements detailed in the previous sections, the activation energies of the AJNDE16 and AJNDE35 can be found by taking the natural log of equation 1.1. Since the kinetic measurements are based on phenomenological results the activation energy obtained from these results is not necessarily the actual activation energy and it more aptly described as the apparent activation energy.[4]

$$\ln(k) = \ln(Z) - \frac{E_a}{RT} \qquad \text{equation 6.6}$$

By plotting ln (k) versus 1/T from equation 6.6 the apparent activation energy for the probe can be determined from the slope assuming the function is reasonably fit by a linear function. The plot of ln (k) versus 1/T is known as an Arrhenius plot. The Arrhenius plot for AJNDE16 and AJNDE35 is shown in Figure 6.5.

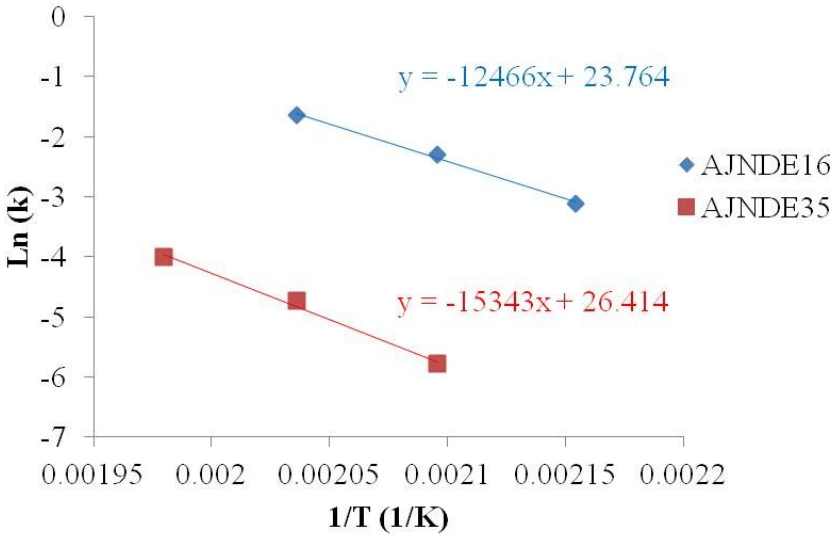

Figure 6.5 Arrhenius plot for AJNDE16 and AJNDE35

From Figure 6.5 it can be seen that the plots for both AJNDE16 and AJNDE35 are fit well by linear equations indicating that they do appear to exhibit an Arrhenius relationship. Using equation 6.6 the apparent activation energy and preexponential factors for both AJNDE16 and AJNDE35 were found and those results are presented in Table 6.1.

Table 6.1 Apparent activation energy and preexponential factor for probes AJNDE16 and AJNDE35

Probe	Apparent E_a (kJ/mol)	Z (s^{-1})
AJNDE16	104	$2.09(10^{10})$
AJNDE35	128	2.96(1011)

As mentioned in section 2.3 if the probe and degradation reaction are fit by similar kinetic models then a comparison of activation energies can give a good measure of the effectiveness of the probe as a TTI for this system. There is limited literature available that reports the activation energies for the first step in TGDDM-DDS degradation and the reported values exhibit a range from 124 – 196 kJ/mol.[4, 26, 27] This wide range is because the activation energy of the degradation is measured using TGA measurements and the calculated activation energy is dependent on the experimental conditions (e.g. heating rate, temperature range) as well

as the method used for calculating the activation energy.[27] As an example for the same TGA measurements Buch and Shanahan calculated the activation of TGDDM-DDS by the Kissenger method, Flinn and Wall or Ozawa method, and the invariant kinetic parameter (IKP) method over a temperature range of 300-450 °C and came up with activation energies of 196 kJ/mol, 191 kJ/mol, and 124 kJ/mol respectively.[27] In two separate papers Rose and Le Bras used the IKP method to calculate the activation energy of TGDDM-DDS over the temperature ranges of 275-425 °C and 200-400 °C and came up with 127.7 kJ/mol and 149 kJ/mol respectively.[4, 26] As it can be seen the activation energies calculated by IKP match well with probe AJNDE35. However, as mentioned to use activation energy as a reliable selection tool for a TTI the probe and the degradation process should fit similar kinetic models. Using the IKP method the authors were able to compare 18 possible kinetics models for the degradation reaction and determine the highest probability degradation model. From the analysis it was found that the most probable kinetic models were either a diffusion limited model or a combination of a potential law and a reaction rate order law model.[4, 26] In either case they did not exhibit the first order kinetic rate law that the probes did. Thus comparing activation energies may not be reliable in this case. However, comparing the activation kinetics of AJNDE35 in Figure 6.4b with the SBS strength retention numbers in Figure 1.1, it can be seen that at similar temperatures that the activation of AJNDE35 occurs on roughly the time scales shown as the loss SBS strength associated with ITD. This indicates that AJNDE35 still has the potential to work for as a probe for a TTI application for composites with TGDDM-DDS as a matrix.

6.2 Modeling of AJNDE16 and AJNDE35 Fluorescence

The main limitations in the ability to conduct this research have been the availability of the probe and the time necessary to characterize the response of the probes to different thermal exposures. These issues were somewhat mitigated by developing a model to predict the fluorescent response of the probes to a given thermal exposure. In addition, having a model of the fluorescent responses of the individual probes will be helpful when trying to understand and predict the multiplexed probe system presented in chapter 7. The model presented is this section is developed from the kinetics measurements in previous section.

6.2.1 Peak Fitting of AJNDE16 and AJNDE35

The first step in establishing a model for AJNDE16 and AJNDE35 was to find functions that could accurately describe the peak shape. Five peak functions were evaluated as potential fits for the fluorescence peaks of AJNDE16 and AJNDE35 using Igor Pro 6 software (Wavemetrics). Those peak functions were Gaussian, Lorentzian, Voigt, lognormal, and exponentially modified Gaussian models. The best peak fit was determined by finding the minimum of the sum of squared residuals (SSR) between the experimental data and the model. Due to the skewed peak shape of the fluorescence peaks of both AJNDE16 and AJNDE35, Gaussian, Lorentzian, and Voigt functions did not fit the peaks very well. Plots showing the lognormal and exponentially modified Gaussian fitting functions with the experimental peaks for AJNDE16 and AJNDE35 are displayed in Figure 6.6.

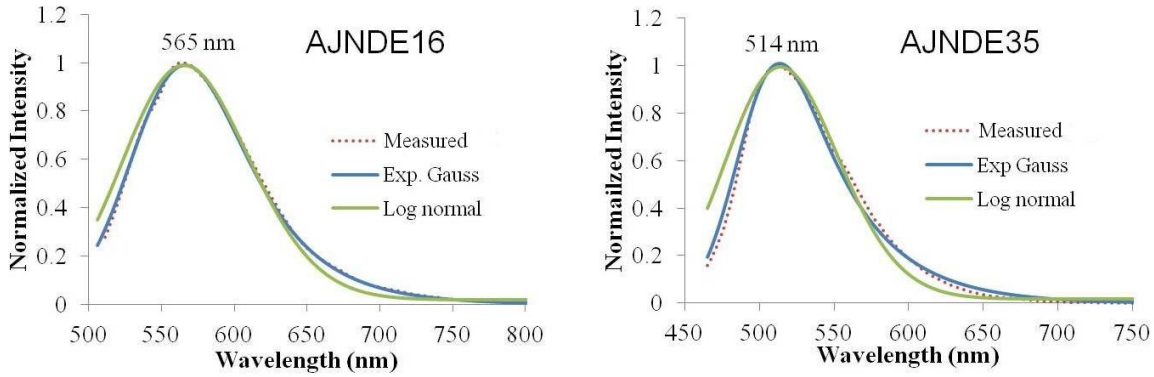

Figure 6.6 Comparison of peak fitting functions to fluorescence peaks for AJNDE16 (left) and AJNDE35 (right)

From Figure 6.6 it can be seen that for both AJNDE16 and AJNDE35 the exponentially modified Gaussian function was the best fit visually of the experimental data. This was confirmed by the fact the exponentially modified Gaussian function also had the smallest SSR of all the functions. To verify that the peak shape was not changing significantly during activation, peak fitting was performed on five peaks from at with different exposure time and/or temperature. It should be noted that all the peaks were normalized by maximum intensity of the spectrum before peak fitting was performed. This was done to avoid large variations in the height parameter of the fitted curves since the fluorescence intensity between spectra varied significantly. Little variation was found in the peak fitting parameters indicating the peak shapes for both probes were constant throughout the activation process. The equation for the exponentially modified Gaussian function is given in equation 6.7 below.[78]

$$Aexp\left(0.5(w/(\tau)^2) - \frac{x - x_c}{\tau}\right)\left(0.5 + 0.5\,\mathrm{erf}\left(z/\sqrt{2}\right)\right) \qquad \text{equation 6.7}$$

Where A is the amplitude, w is the peak width, τ is the skewness factor, x is the variable wavelength, x_c is wavelength of the peak center , erf is the standard error function, and z is a parameter derived from x, x_c, w, and τ whose value is expressed by equation 6.8.[78]

$$z = \frac{x - x_c}{\tau} - w/\tau \qquad \text{equation 6.8}$$

The peak fitting parameters for AJNDE16 and AJNDE35 are given in Table 6.2.

Table 6.2 Exponentially modified Gaussian peak fitting parameters for AJNDE16 and AJNDE35

Probe	A	w	τ	x_c
AJNDE16	2.673	30.96	39.98	541.2
AJNDE35	2.171	21.92	42.09	491.5

6.2.2 Kinetic Modeling of AJNDE16 and AJNDE35

As mentioned in the previous section the shapes of the fluorescence peaks of AJNDE16 and AJNDE35 do not change during the activation so assuming the peak fitting parameters in Table 6.2 represent the spectrum of the probe fluorescence at maximum intensity then

$$P_i = \beta_i P_i^{\infty} \qquad \text{equation 6.9}$$

Where P_i is the peak at a given level of activation (β_i) for probe "i" (i.e. AJNDE16 or AJNDE35), β_i is the fraction of probe "i" that has been activated as described by equation 6.3, and P_i^{∞} is the peak whose height parameter is defined when $\beta_i = 1$ (i.e. peak with maximum height). β_i for the model was found using by first calculating α_i using equation 6.5 for the probe and then using the relation in equation 6.2 to find β_i. The rate constant k was determined using equation 1.1 and the apparent activation energy found in Table 6.1. A comparison of the model predictions and the experimental results for probes AJNDE16 at 191 °C and AJNDE35 at 204 °C is shown in Figure 6.7.

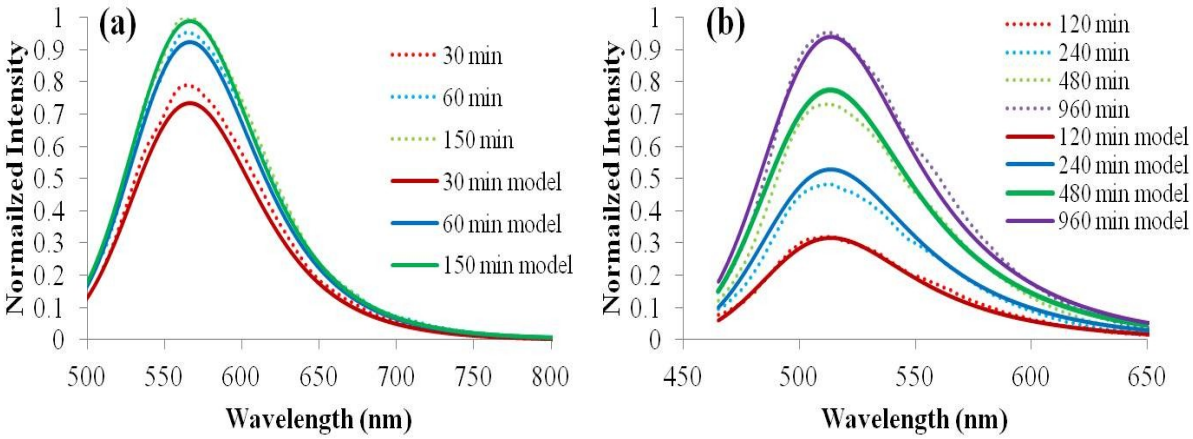

Figure 6.7 Comparison of kinetic model to experimental data for (a) AJNDE16 at 191 °C (b) AJNDE35 at 204 °C

From Figure 6.7 it can be seen that for both AJNDE16 and AJNDE35 the model matches well with the experimental data for the most part. There are a few times where the model does not exactly match the experimentally data, but the relative error was always found to be less than 10 % which is reasonable when taking into account the experimental error in the measurement. These results show that the model in equation 6.9 can be expected to reasonably predict the kinetics of activation for both probes at a desired temperature. In addition, it will be shown in chapter 7 that these models can be used to predict the kinetics of a multiplexed system of AJNDE16 and AJNDE35.

6.3 Summary

The activation kinetics in response to thermal exposure for probes AJNDE16 and AJNDE35 in a TGDDM-MMCA matrix were characterized using a phenomenological rate equation based on fluorescence intensity measurements and the apparent activation energy for both probes was determined. It was found that both AJNDE16 and AJNDE35 exhibited first order kinetics. The activation energies for probe AJNDE16 and AJNDE35 was found to be 104

kJ/mol and 128 kJ/mol respectively. While the kinetic model of probe AJNDE35 is not the same as that as the kinetic models for TGDDM-MMCA in the literature, it was found that the activations kinetics of AJNDE35 were on approximately the same time-scale as the SBS strength loss in the composite. Thus AJNDE35 has the potential to be a good TTI for detecting ITD in CFRP. In addition, kinetic models were developed for both probes. The first step in the modeling process was peak fitting the fluorescence spectra of probes AJNDE16 and AJNDE35 with mathematical functions. The best peak fitting function for both probes AJNDE16 and AJNDE35 was an exponentially modified Gaussian function. The kinetic models for both probes were found to match the experimentally data reasonably well allowing the prediction of the activation kinetics of one of the probes at a given temperature without the need for measurements.

7. MULTIPLEXED PROBES AND THEIR APPLICATION AS TTI

As it has been previously described, a single fluorescent thermal damage probe such as AJNDE16 and AJNDE35 can be used to indicate areas where a significant thermal exposure has occurred. While this is useful for locating potential damage sites, it does not provide any quantitative information about the extent of the thermal exposure which would be useful for determining the level of the damage caused by the exposure event(s). A potential solution to this issue is to utilize a ratiometric fluorescence technique. As was described in section 2.5, a ratiometric fluorescent measurement utilizes two or more fluorescent peaks and measures the relative change in the peaks by taking the ratio of the intensities of the peaks as they change. In this work, ratiometric fluorescence was accomplished by multiplexing the two thermal damage probes AJNDE16 and AJNDE35 in a TGDDM-MMCA epoxy matrix. In the first part of this

chapter the fluorescence response to thermal exposure of the multiplexed system is characterized. A model for the multiplexed system is presented in the second section. Finally how the multiplexed system can be used as a TTI is presented.

7.1 Multiplexed AJNDE16 and AJNDE35 in TGDDM-MMCA

In section 5.6 it was seen that when the fluorescence emission of AJNDE16 was combined with the autofluorescence of the DGEBA-DETA matrix the fluorescence spectra varied significantly depending on the relative strength of each fluorescent species. This was essentially a multiplexed system in that two thermally responsive fluorescent species were present and the observed fluorescence emission was formed by a combination of the emission of the two individual species. Unfortunately since both of the probes could activate at thermal exposures well below those known to cause ITD in composites with Toray 3900 as the matrix, that particular multiplexed system was not useful this application.

As it has been previously detailed AJNDE16 is not compatible with the Toray 3900 resin system because it activates during the cure cycle and is thus not responsive to thermal exposure after curing. Thus it was decided to use the TGDMM-MMCA as the matrix for the multiplexed system. As described in section 3.2.6 a multiplexed system with AJNDE16 and AJNDE35 doped into a TGDDM-MMCA matrix was fabricated with a 1:1 molar ratio of the probes which corresponded to 0.05 wt% AJNDE16 and 0.054 wt% AJNDE35. The multiplex samples were prepared using the same method as the kinetic measurement specimens to eliminate the effects of oxidation on the measurement so only the response of probes would be observed. An example of the response of the multiplexed AJNDE16 and AJNDE35 in TGDDM-MMCA to heat-treatment at 232 °C for several exposure times is shown in Figure 7.1. The spectra were normalized by the

maximum intensity of the individual spectrum to give a better view of the changes in the peak shape. The excitation wavelength used for the multiplex measurements was the 430 nm LED.

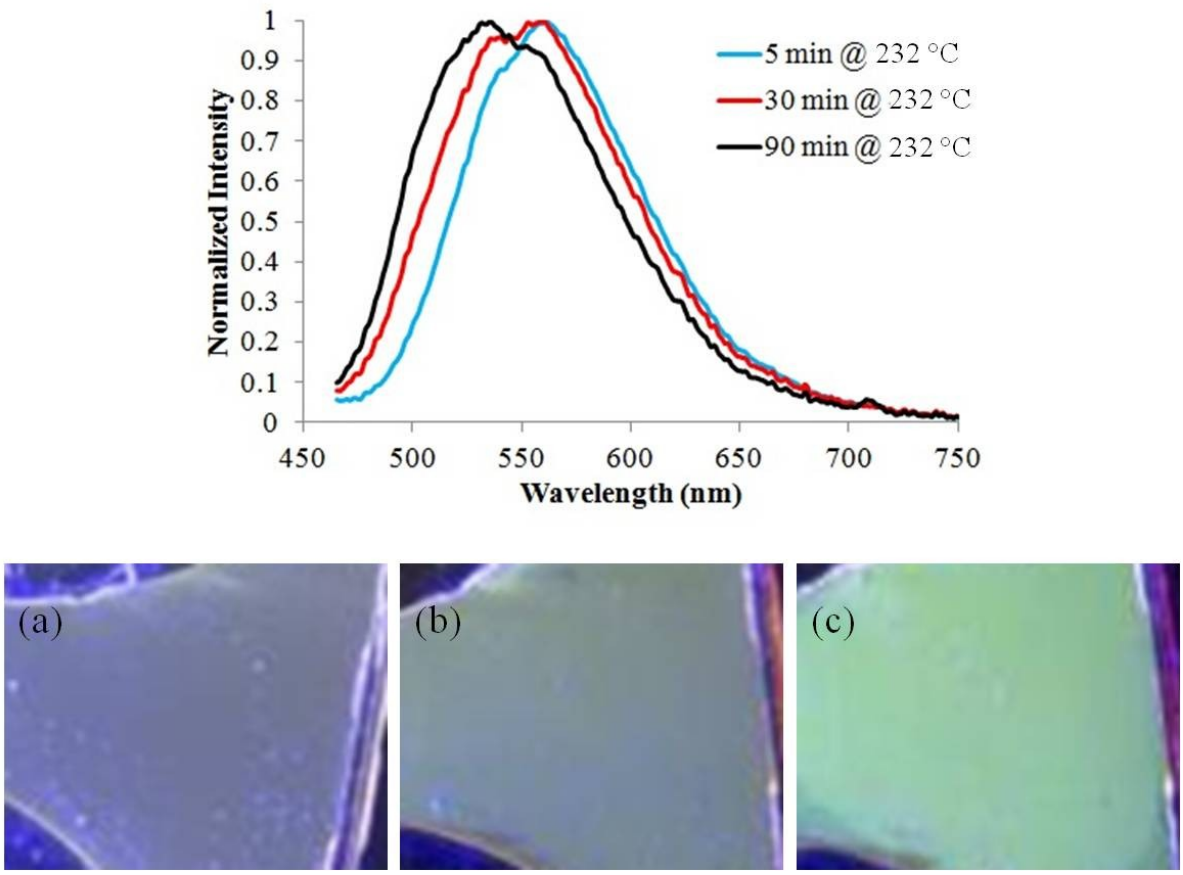

Figure 7.1 Multiplexed sample of AJNDE16 and AJNDE35 in TGDDM-MMCA (Top) Fluorescence spectra of multiplexed system for various times at 232 °C (Bottom) Fluorescence images of heat of multiplexed AJNDE16-AJNDE35 at 232 °C for (a) 5 min (b) 30 min (c) 90 min

From Figure 7.1 it can be seen that after the short 5 minute the peak maximum is found around 563 nm. The peak from the 5 minute exposure is very close to the peak observed from AJNDE16 by itself. From the kinetics measurements it is known that AJNDE16 will activate much quicker than AJNDE35 so it is expected that for a short exposure the AJNDE16 peak would be dominate. As the exposure time increases a shoulder around 535-540 nm starts to grow and eventually becomes the peak maximum. Again this result is expected because the peak

for AJNDE35 appears around 514 nm so as the amount of AJNDE35 activated increased it was expected that it would contribute more to the spectrum. As was the case in section 5.5 with the multiplexed system of AJNDE16 and the DGEBA-DETA autofluorescence, it appears that the fluorescence spectra of the multiplexed AJNDE16 and AJNDE35 is the result of the superposition of the two individual fluorescence spectra.

The fluorescence images at the bottom of Figure 7.1 display a similar trend to the spectra. Initially the sample exhibits a weak muddy orange fluorescence, but as the exposure time increases the fluorescence begins to turn green and after 90 minutes at 232 °C it is bright green. Another interesting feature of the multiplex system is that in the absence of oxidation the spectra becomes visibly brighter as exposure time increases because of the superposition of the fluorescence of the two probes. This was also observed in the fluorescence measurements. It should also be noted that similar changes in the spectra were observed when observed in the multiplexed samples heat-treated at 204 °C and 218 °C though the exposure time for the changes to occur was much longer than the samples heat-treated at 232 °C.

7.2 Modeling of Multiplexed System

From the results in section 7.1 it is expected that the multiplexed probe system can be modeled as the superposition of the models for AJNDE16 and AJNDE35 developed in section 6.2. The equation for such a multiplex model is given in equation 7.1 below.

$$P_m = A\beta_{16}P_{16}^{\infty} + B\beta_{35}P_{35}^{\infty} \qquad \text{equation 7.1}$$

where P_m is multiplexed system spectra, A and B are the weighting factors of probes AJNDE16 and AJNDE35 respectively.[65] Since measuring A and B separately is not trivial in

the fluorescence spectrum, equation 7.1 can be better utilized expressing the weighting factors as a ratio of the individual weighting factors as seen in equation 7.2.

$$P_m = \beta_{16}P_{16}^{\infty} + r\beta_{35}P_{35}^{\infty} \qquad \text{equation 7.2}$$

Where r is the ratio of the weighting factor terms (i.e. $r = B/A$). Currently the value of r has been found by minimizing the sum of squared residuals of equation 7.2 to the empirical data, but it is believed that it should be possible to find the r value from material properties of the probes and the stoichiometry of two probes in the sample. However, all the factors that affect r have not yet been determined so the value of r must still be determined empirically for now. The r value for the multiplexed system in this study was found to be 1.561. A comparison of the model in equation 7.2 to measured spectra of the multiplexed samples heat-treated for various times at 232 ºC can be seen in Figure 7.2. All spectra were normalized by the maximum intensity of the multiplexed system.

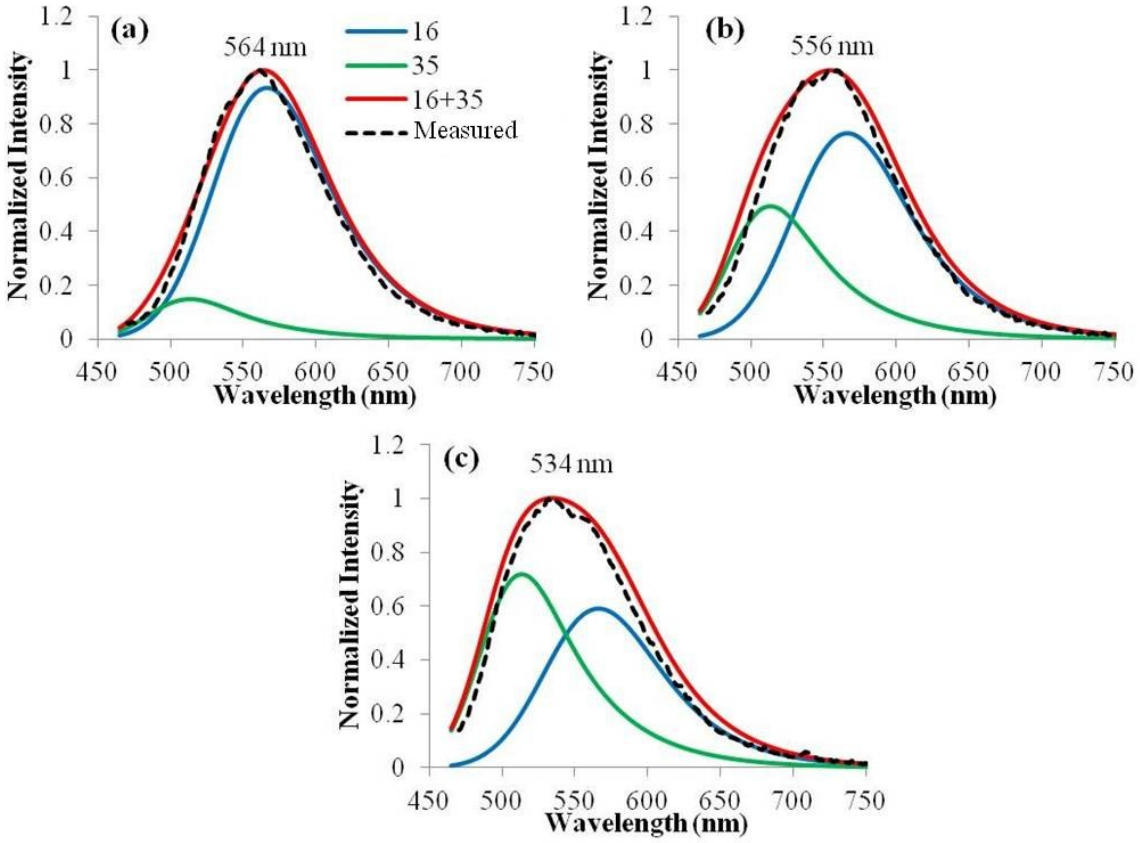

Figure 7.2 Comparison of multiplex model to measurements for different exposure times at 232 °C (a) 5 min (b) 30 min (c) 90 min

From Figure 7.2 it can be seen that the model for the multiplexed system in equation 7.2 does a relatively good job of fitting the measurements and thus validates that the measured fluorescence spectra is formed by the superposition of the fluorescence peaks from AJNDE16 and AJNDE35. The model fails to capture the shoulder that is observed in the measured spectra, but it tends to captures the maximum of the shoulder. Another interesting note is that according to the kinetic models AJNDE16 is fully activated before AJNDE35 reaches 20 % activation meaning that for most of the thermal exposure in the multiplexed system the AJNDE16 peak is essentially an unchanging reference peak.

7.3 Ratiometric Fluorescence and Response Curves

One of the primary reasons for creating a multiplexed system with AJNDE16 and AJNDE35 was to be able to utilize ratiometric fluorescence as a way to quantify the thermal exposure of the part using the measured fluorescence response. In the literature, ratiometric fluorescence systems often have well separated peaks and thus defining the ratiometric response is usually straightforward as taking the intensity of peak 1 and dividing it by peak 2.[63, 79-81] Thus the initial thought was to use the intensities at 514 nm and 565 nm which correspond to the peaks of the individual probes, but this ratio did not turn out to be very accurate. It is believed that the reason for this is that at 514 nm there may be some noise in the fluorescence peak caused by light from the excitation source being recorded by the detector. Since it is very difficult to control the amount of reflection of the excitation, the intensities in the fluorescence spectrum near the excitation peak tend to vary much more significantly than the intensities at higher wavelengths where there is little or no light from the excitation source. With a better filter set for the spectrometer to remove the reflected excitation light, the ratio of I_{514}/I_{565} might work well; however, with the measurement setup used in this study that ratio performed poorly.[82] To avoid the wavelengths were the reflected light might affect the intensity, 540 and 560 nm were chosen as the wavelengths to ratio. These wavelengths were selected because they were wavelengths where change is observed in the spectra throughout the thermal exposure. Simply taking the ratio of I_{540}/I_{560} provided satisfactory results, but the response curves generated for different temperatures had almost no separation for short exposure times. So instead a response function was adapted from the literature and is defined in equation 7.3.[59, 83]

$$F = \frac{(R - R_{min})}{(R_{max} - R)} \qquad \text{equation 7.3}$$

Where R is I_{540}/I_{560}, and R_{min} and R_{max} are the minimum and maximum possible value of R. For the defined R, R_{min} was found to be 0.791 and R_{max} was equal to 1.13. Using this response functions and the model developed in section 7.2, response curves for temperatures ranging from 190.6 °C to 232.2 °C (390 °F to 450 °F) were generated with intervals between curves ~ 2.7-2.8 °C (~5 °F). A plot of the response curves for the temperature range described above can be seen in Figure 7.3. It should be noted that the points in the plot are not measurements but F values determined using the multiplexed system model.

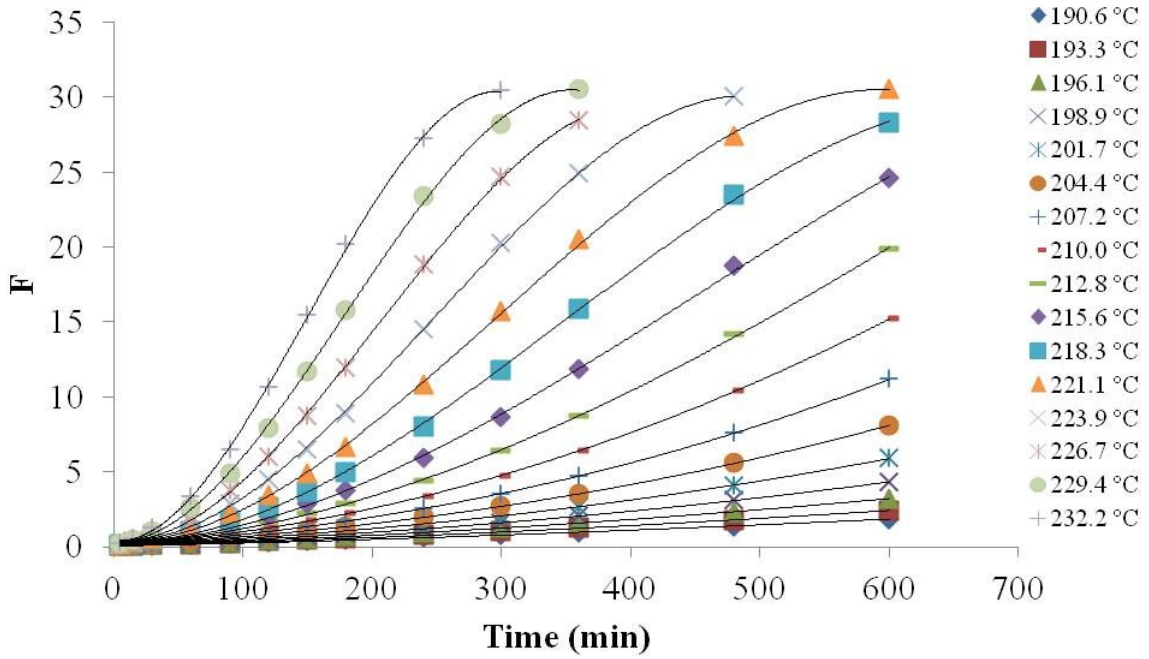

Figure 7.3 Response curves for thermal exposure for temperatures ranging from 190.6 °C to 232.2 °C

All the response curves were generated by fitting the F-values generated using the multiplexed system model in equation 7.2 with third order polynomials and the R^2 values were greater than 0.99. It should be noted the curves were limited to have a maximum value of F less than 30, because when F is greater than 30 the curve begins to plateau as it approaches full

activation of both AJNDE16 and AJNDE35 and this causes the quality of the fit to decrease. While this may seem like a limitation of the response curves if you compare the time-temperature combinations where F is greater than 30 with the SBS strength retention values in Figure 1.1, it can be seen that the amount of thermal exposure to reach that F value is usually sufficient to cause enough damage to the composite where ultrasound can start to detect it. Thus technically the damage would no longer be considered to be in the ITD range which the probes are designed for. This shows that this multiplexed system exhibits a relatively good measure of the endpoint of the ITD region which is one of the key parameters when choosing a TTI for a specified application.[51] The coefficients for the polynomial fits can be seen in Table 7.1.

Table 7.1 Coefficients for response curves fit to polynomial at^3+bt^2+ct+d

Temperature (°C)	a	b	c	d
198.9	$1.12(10^{-9})$	$5.51(10^{-6})$	.00343	.0408
201.7	$2.79(10^{-9})$	$7.53(10^{-6})$	.00422	.0405
204.4	$4.81(10^{-9})$	$1.10(10^{-5})$	.00508	.0422
207.2	$5.47(10^{-9})$	$1.79(10^{-5})$	.00580	.0511
210.0	$-7.22(10^{-10})$	$3.26(10^{-5})$	.00591	.0787
212.8	$-2.60(10^{-8})$	$6.31(10^{-5})$	.00452	.1411
215.6	$-8.63(10^{-8})$	$1.18(10^{-4})$	.00102	.255
218.3	$-1.35(10^{-7})$	$1.61(10^{-4})$	.00223	.230
221.1	$-3.16(10^{-7})$	$2.77(10^{-4})$	-.00373	.362
223.9	$-5.39(10^{-7})$	$4.00(10^{-4})$	-.00606	.405
226.7	$-9.36(10^{-7})$	$5.79(10^{-4})$	-.00898	.445
229.4	$-1.39(10^{-6})$	$7.44(10^{-4})$	-.00393	.350
232.2	$-2.36(10^{-6})$	$1.06(10^{-3})$	-.00650	.386

It should also be pointed out that obtain reasonably good accuracy with the response curves that it is necessary to have such small increments as ~2.7-2.8 °C between curves because the measurements are so sensitive to temperature that if this increment is much larger a significant amount of error can be introduced if the temperature of the exposure falls between two response curves. As an example, assume a value of F equal to 7 was measured and that the temperature range was somewhere between 218.3 °C and 223.9 °C. For a value of F equal to 7

the 218.3 °C and 223.9 °C response curves would correspond to correspond to 314 min and 218 min respectively. So a difference of 5.6 °C can change the estimated time for the measurement by almost 100 min. It should be noted that the higher the measured F value is, the greater the spacing between the response curves. This trend also leads to a higher variance in estimates from response curves at lower temperature. This has to do the difference in the slope of the tangent line to response curves. When the slope is large a small change in the measured F value only causes a small change in the estimate, but at lower slopes found in the lower temperature curves a small change in the F value causes a much bigger change in the estimate. However, considering that the ITD develops at a much slower rate at the lower temperatures, the higher magnitude of the variance in the estimate at low temperature is not as significant as the same amount of variance at high temperatures. For example an error of 10 min at 232 °C where ITD develops in less than 1 hour is much more significant than an of error of 10 min at 204 °C where it takes up over 8 hours to reach the same damage level as 232 °C.

Another issue is that the response curves still have poor separation between the curves for short exposure times especially at lower temperatures and so the accuracy in this region is also poor. This can be seen in Figure 7.4, which is a zoomed in version of Figure 7.3 for $t \leq 100$ min.

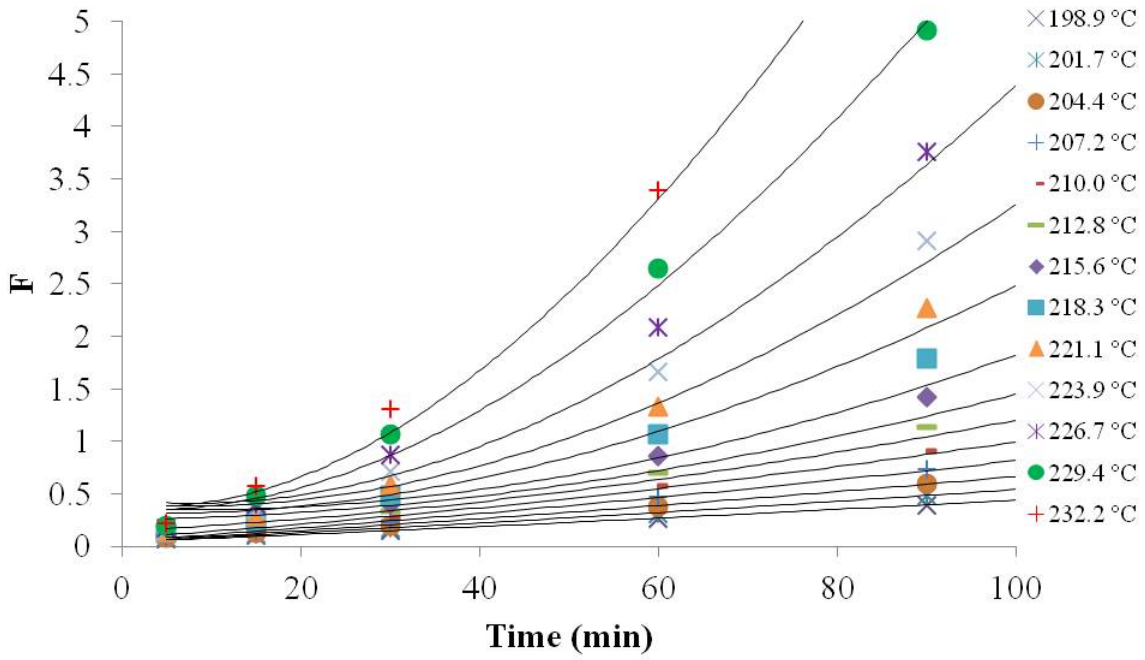

Figure 7.4 Response curves for thermal exposure for t ≤ 100 min

The accuracy in this region isn't too much of a concern for TTI designed to find ITD though because again when comparing the thermal exposures that cause the F values less than 0.5 to the SBS strength retention, it is not expected that much damage will occur for those exposures. As it has been mentioned previously, the onset of ITD is not formally defined in the literature, but from comparing the response curves with the SBS strength data in Figure 1.1, it appears that around an F-value of 1 is when the damage starts to become significant. It should be noted that the F value does not necessary correspond to the SBS values though as it only represents a relative activation level of the two probes.

7.4 Application of Multiplexed System as a TTI for ITD of CFRP

Currently there are two ways that the response curves can be utilized for a TTI system. The first is to define a reference temperature and then use that responsive curve and a measured F value to determine the estimated time at the exposure. A given F value is an equivalent state

that is independent of the thermal loading path to reach that state. Thus the estimated time from the response curve would represent the time at defined temperature to reach that state since the actual thermal history is likely unknown. Whether or not this corresponds to an equivalent state of damage in the composite for all temperature and time combinations remains to be investigated. In the second method, a time value is defined (e.g. 1 hour) and the effective temperature is determined. This approach has been taken when classifying samples measured for ITD using FTIR measurements.[33]. In either case an equivalent state of thermal exposure is defined and the results can be compared to calibration sets for thermal damage in order to evaluate the how damaged in the part is. In this section both methods will be demonstrated.

7.4.1 Set Temperature

In order to evaluate the multiplexed system, the epoxy was applied as a coating to an already cured composite panel. The panel was then subjected to localized heating to generate a thermal gradient such that a range of temperatures could be evaluated on approximately the same time scale. One of the panels for the first method can be seen in Figure 7.5a. The fluorescence image was taken with a white light source with a 435 nm bandpass filter over the source. The dashed box in the figure indicates where the heating blanket was located and the superimposed colored circles represent the locations where thermocouple and fluorescence measurements were taken. The thermocouple data and associated fluorescence spectra can be seen in Figure 7.5b and Figure 7.5c respectively.

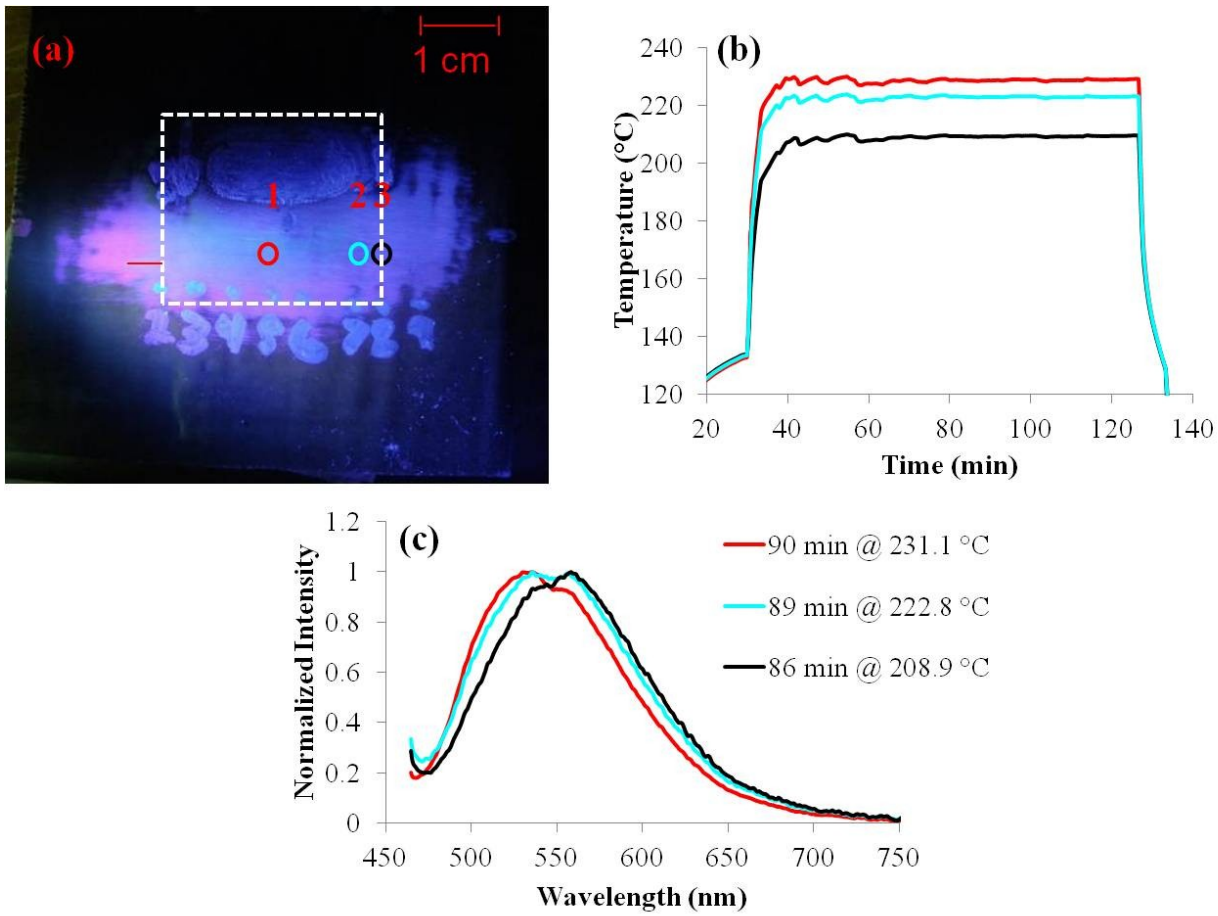

Figure 7.5 Multiplexed coating sample subjected to localized heating for ~90 min (a) fluorescence image (b) thermocouple measurements (c) fluorescence measurements

From the fluorescence image in Figure 7.5a, it can be seen that the fluorescence emission varies significantly near the edge of the where the blanket was placed. Outside the fluorescence is the orange characteristic of AJNDE16 and inside the fluorescence is green which is indicative that a significant amount of AJNDE35 has been activated. A yellowish fluorescence can be seen in between the orange and green fluorescence which is likely an intermediate state where both AJNDE16 and AJNDE35 are both contributing significantly to the spectra. Based on knowledge of the kinetics and the temperatures measured with the thermocouples these results were expected. Near the center of the heating blanket the temperature was relatively high (~ 231 °C) thus it would be expected that both probes would respond. At the edge of the heating blanket the

thermal gradient began to appear and the temperature starts to drop rapidly to below 200 °C where only AJNDE16 would be expected to activate enough to be observed at the exposure time of ~ 90 min. The difference in the fluorescence is also seen in fluorescence measurements in Figure 7.5c and confirms this analysis.

To demonstrate utilizing the multiplex system as a TTI by defining a set temperature, the exposure was estimated at the 3 locations indicated by the circles in Figure 7.5a. Three temperature response curves were selected and the estimated time at those temperatures was found for each point. It should be noted that the temperatures selected were chosen specifically to be close to the temperature measurements of the thermocouples at each of the locations to demonstrate the accuracy of the TTI. The bold value represents the estimated exposure time for the response curve closest to the thermocouple at that location.

Table 7.2 Estimated exposure times using set temperature response curves

Loc.	I540/I560	F value	$t_{232.2}$ (min)	$t_{221.1}$ (min)	t_{210} (min)	TC measurement
1	1.084	6.37	**87.6**	173	359.1	~90 min @ 231.1 °C
2	1.009	1.802	41.9	**83.6**	156.7	~89 min @ 222.8 °C
3	.994	0.823	24.4	49.7	**85.6**	~86 min @ 208.9 °C

The most interesting feature in Table 7.2 comes when comparing the estimated times for the temperature response curve closest to the thermocouple measurement at that location. For all the locations the best time estimate is within ~ 1°C and 5 minutes of the actual measurement. This shows the multiplex system has great accuracy. It is interesting to note that the accuracy could potentially be improved as well. The spot size of excitation light was approximately 2.5 mm which was much bigger than the area the thermocouple was measuring and the fluorescence is likely more of an average of the fluorescence area around the thermocouple. By reducing the beam size it may be possible to obtain more accurate measurements. It should also be noted that

some of the error is located in the response curves as well since they were generated from the kinetic models which were shown to have a small amount of error in them. Thus collecting more kinetic data and improving the model would be another possible way to improve the accuracy.

7.4.2 Set Time

For the set time demonstration of the TTI, another panel was the multiplexed TGDDM-MMCA coating was locally heated this time for ~ 147 min. The thermocouple measurements and the fluorescence spectra measured at the location where the thermocouples were positioned are shown in Figure 7.6.

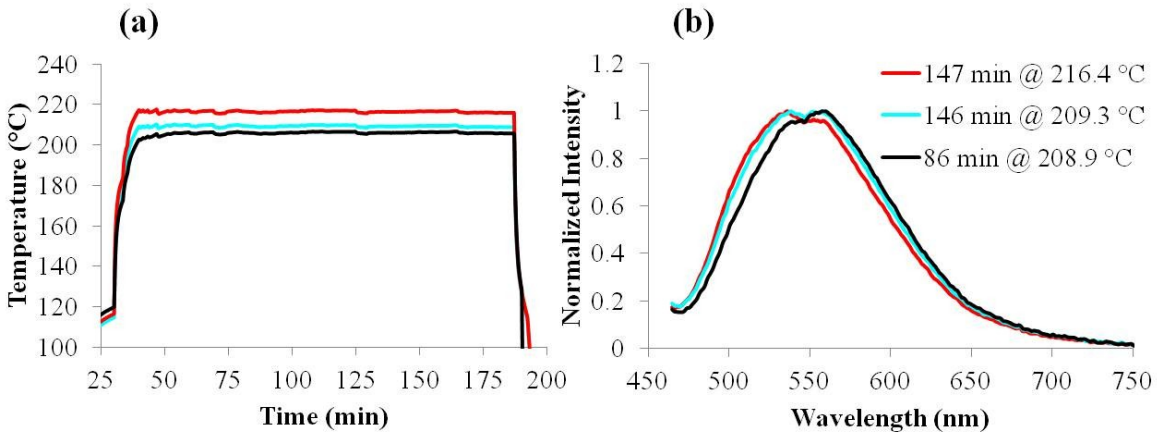

Figure 7.6 Multiplex coating subjected to localized thermal exposure for ~147 min (a) fluorescence spectra (b) thermocouple measurements

The fluorescence spectra in Figure 7.6b is very similar to that seen in Figure 7.5c although for this exposure there appears to less activation of AJNDE35 at the maximum temperature. The temperatures estimated by using the measured F values and a set time of 147 min are shown in Table 7.3 This time was specifically chosen to match the experimental conditions to display the accuracy of the multiplex TTI. Five measurements were taken at each location and the average and standard deviation of those measurements is shown in the table.

Table 7.3 Estimated exposure temperatures using a set time of 147 min

Location	I540/I560	F value	T_{147} (°C)	TC Measurement
1	$1.031 \pm .006$	2.715 ± 0.245	215.5 ± 0.9	~147 min @ 216.4 °C
2	$1.001 \pm .003$	1.775 ± 0.072	210.8 ± 0.5	~146 min @ 209.3 °C
3	$0.955 \pm .004$	0.992 ± 0.053	203.8 ± 0.7	~142 min @ 205.7 °C

From Table 7.3, it can be seen that the estimated temperatures compare very favorably to the thermocouple measurements with the estimated temperatures being less than 2 °C away from the measured temperature. Again these results indicate the great potential that the multiplexed system of AJNDE16 and AJNDE35 have as TTI for detecting ITD in CFRP.

7.5 Summary

A multiplexed system was made by doping both fluorescent thermal damage probes AJNDE16 and AJNDE35 into a TGDDM-MMCA matrix. For short exposure times the multiplexed system exhibited a fluorescence peak around 564 nm that was very close to the peak of probe by itself. As the exposure time increased another peak began to develop around 538 nm and continued to blue-shift with thermal exposure. It was proposed that the fluorescence spectrum of the multiplexed system was formed by the superposition of the fluorescence of the two probes and this was confirmed by the modeling. A response function was defined using a ratiometric fluorescent measurement R which was defined as I_{540}/I_{560}. Using this ratio, temperature response curves were generated using the model. The accuracy of the response curves was assessed by locally heating composite panels with the multiplexed TGDDM-MMCA coating and measuring the fluorescence at areas along the thermal gradient. The TTI was used by defining a set time or set temperature and predicting the unknown quantity using the response curves and the measured R value. In both cases the estimates were found to very accurate, thus demonstrating the capability of the multiplex system for use as a TTI.

8. CONCLUSIONS AND FUTURE WORK

8.1 Conclusions

Incipient thermal damage (ITD) of carbon fiber reinforced-composite (CFRP) represents a significant issue for use of CFRP in aircraft. ITD has been shown to reduce matrix dominated properties such as short beam shear (SBS) strength by almost 20 % before it can be detected by common inspection techniques like ultrasound. This research has focused on using fluorescent probes that respond to thermal exposure as a means of detecting ITD in composites. Two thermal damage probes were synthesized and designated AJNDE16 and AJNDE35. When the thermal probe is exposed to a significant thermal exposure the organic molecule decomposes into two molecules, the activated probe molecule and a volatile bi-product. This decomposition restores a conjugation bridge in the backbone of the probe that causes the fluorescence of the probe to shift to a longer wavelength which acts as an indicator that a thermal exposure has occurred. The fluorescence of both probes was observed after thermal exposure in a TGDMM-MMCA epoxy matrix (121 °C). In the Toray 3900 (TGDDM-DDS) matrix (177 °C cure), the AJNDE16 probe was found to activate during the cure and subsequently no change in the fluorescence was observed after thermal exposure. AJNDE35 worked as expected in the Toray 3900 matrix. A carbon fiber composite with AJNDE16-doped Hysol 9390 (TGDDM-MMCA) matrix was also demonstrated and the probe-doped composite was found to behave similarly to the probe-doped epoxy samples. AJNDE16 was also demonstrated in a room temperature cure DGEBA-DETA epoxy matrix coating that was applied to a CFRP panel. This system had an interesting fluorescence response as the fluorescence of AJNDE16 combined with the

autofluorescence of the DGEBA-DETA matrix, which acted like another thermal probe, to give a fluorescence emission gradient when the coating was exposed to a localized thermal event.

This was interesting because it indicated a potential method to quantify the extent of the thermal damage which was not feasible with just a single probe. The only quantity of a single thermal damage probe that changes with increasing thermal exposure is the fluorescence intensity as more of the probe activates. However, outside of strict laboratory conditions, fluorescence intensity measurements are very difficult to reproduce. Thus a single probe is only truly capable of indicating that a thermal exposure has occurred. A multiplexed system that combines two probes; however, provides the opportunity to utilize ratiometric fluorescence where the ratio of the intensity of both probes can be utilized to characterize the rate of change in the system to determine the extent of thermal exposure. Quantifying the amount of thermal exposure makes it possible to estimate the damage caused by the thermal exposure. This information can used to guide a repair of a CFRP composite with ITD.

The main issue found with the application of the probes was that oxidation of the matrix during thermal exposure was found to quench the fluorescence of the probes. This was attributed to the increased absorbance of the matrix which prevented the probes from being excited and/or the emitted fluorescence escaping from the matrix. However, if the thin oxidation layer is removed from the surface by sanding the fluorescence was restored. In addition, in the event of a localized thermal exposure even if some of the fluorescence emission is quenched by oxidation of the matrix the fluorescence should still be observable because of the thermal gradient generated by a localized heating event. The probes have also exhibited excellent temporal stability under ambient laboratory conditions. Once activated, the probes have been shown to

still strongly fluorescence for more than two years. The probes also were found not to activate at ambient conditions thus limiting the chance of a false positive inspection.

The kinetics of both probes AJNDE16 and AJNDE35 were both measured and fit to a first order phenomenological rate equation. From the kinetic measurements the apparent activation energies for AJNDE16 and AJNDE35 were calculated. As expected the apparent activation energy of AJNDE16 (104 kJ/mol) was less than that of the more thermally stable AJNDE35 (128 kJ/mol). A kinetic model was generated for both probes that fit the measured data relatively well.

A multiplexed system combining probes AJNDE16 and AJNDE35 in a TGDDM-MMCA was also introduced. The resulting fluorescence spectrum for the multiplexed samples was found to be formed by the superposition of the spectra of the individuals and the relative amount of each probe active. Using ratiometric fluorescence a response function (called F) was defined and the response curves were generated for various temperatures. The response curves were found to have lose accuracy at low temperatures and short exposure times ($F \leq 0.5$) and also in the case of long term exposure ($F \geq 30$). In both cases these inaccuracies were not considered detrimental to the multiplex systems ability to perform as a TTI. For the short term exposure case, little damage to the composite was expected to occur in this region and in the long term exposure case the damage would likely be significant enough that it could be detected by ultrasound. The capabilities of the multiplexed system as a TTI were demonstrated by coating CFRP panels with the multiplexed epoxy and locally heating those panels. The abilities of the multiplex coating as a TTI was shown by two separate methods, one where the temperature was set and the exposure time was estimated from the response curves and the reverse case where the time was set and temperature was estimated. In both cases, the multiplexed coating was found to be exceptionally

accurate in predicting values measured by thermocouples. This demonstrated the great potential of the multiplexed fluorescent thermal damage probe systems as a TTI for detecting ITD in CFRP.

8.2 Future Work

8.2.1 Improvement and Optimization of TTI

While the multiplexed system of AJNDE16 and AJNDE35 worked relatively well as TTI there are some potential improvements that could be made to the system. The first potential improvement may be to optimize the molar ratio of AJNDE16 and AJNDE35 in the multiplexed system. In this dissertation only a 1:1 molar ratio of AJNDE16 and AJNDE35 was utilized. By varying the ratio of the probes it should be possible to increase or decrease the observed spectral changes which could potentially lead to better accuracy and/or changing the response time of the system to fit a specific application.

Another issue that still needs to be resolved is to determine how to determine the weight factor r in equation 7.2 without fitting the data to the experimental measurements. Having this capability would be very useful when trying to optimize the molar ratio of the probes used since the effects of changing the molar ratio could be examined by running simulations with the model rather than having to run time and material consuming experiments. From literature the measured fluorescence intensity should be a factor of the intensity of the excitation source, the fluorescence quantum yield, the absorbance at the excitation wavelength, concentration of the probes, and some geometry and instrumentation factors.[36, 84] It is expected that the r value should represent the weighting (intensity ratio) of the peaks of the two probes after complete activation. Since this is essentially the ratio of the peaks of AJNDE16 and AJNDE35 at

maximum intensity, the geometry and instrumentation factors would be cancelled out in the ratio since they would be the same for both probes. Thus it should be possible to define an r value using only the material properties such as quantum yield and absorbance and the molar ratio of the probes. By further characterizing these parameters it may possible to determine r without relying on fitting empirical data.

In chapter 6, it was shown that there was a small amount of error between the kinetic models for AJNDE16 and AJNDE35 and the empirical measurements. One of the potential issues may be that only three temperatures were used to determine the apparent activation energy for both probes. Since the rate constant k (equation 1.1) used in the model requires the activation energy to calculate the accuracy of the activation energy may have affected the results. By measuring the kinetics of the probes at more temperatures it may be possible to refine the activation energy values and in doing so obtain a better fit of the models to the data. Since the response curves were generated using the model, this may improve the accuracy of the response curves as well.

Another potential path to improve the usability of the TTI is to replace the spectrometer measurements with image analysis techniques such that a wide area could be inspected very quickly by imaging the fluorescence and then analyzing the color of the emitted fluorescence.[2, 30, 82] This would potentially make the inspection process significantly quicker than using a spectrometer. It is unknown how image analysis may affect the accuracy of the measurements so there may be a trade off in terms of speed and accuracy. However, it may also be possible to optimize the molar ratio of the probes to improve the spectral shifts for image analysis.

In cases where a part is only thermally exposed once, there is the potential to be able to determine both the time and temperature of the exposure without assuming an effective value for

one of the variables. As it was seen in the localized exposure experiments in sections 5.6 and 7.4, the steady-state temperatures in the thermal gradient have relative close exposure times. As mentioned before there is no way to determine both the time and temperature of the exposure from a single F-value measurement since it represents an equivalent activation states for the probes and is independent of thermal history. However, if two or more measurements are made at different points along the thermal gradient it should be possible to find a common exposure time between the measurements which would determine the exposure time. The temperature curves intersected by these measurements would then give the temperatures at those locations. Thus both the time and the temperatures could potentially be resolved if they are both unknown.

8.2.2 Effect of Matrix on Fluorescence Properties of Probes

It was shown in section 4.3 that doping the thermal damage probes into an epoxy matrix causes a significant blue-shift of the fluorescence emission peak compared to the probe without a matrix. This blue-shift has a significant impact on the design of probes as both AJNDE16 and AJNDE35 were designed to emit at longer wavelengths than was observed in the probe-doped matrices. Another issue that has been found is that the quantum yield of the probes changes significantly in different matrices as well. The quantum yield (Φ) and λ_{max} of probes AJNDE16a and AJNDE35a doped in the epoxy matrices is given in Table 8.1 Quantum yield and λ_{max} of AJNDE16a and AJNDE35a in epoxy matrices. The quantum yield measurements were taken using an excitation wavelength of 430 nm. The quantum yield measurements were provided by collaborator Jeffrey Yang.

Table 8.1 Quantum yield and λ_{max} of AJNDE16a and AJNDE35a in epoxy matrices

Probe	DGEBA-DETA		TGDDM-MMCA		Toray 3900	
	Φ	λ_{max}	Φ	λ_{max}	Φ	λ_{max}
AJNDE16a	30.6 %	560 nm	22.9 %	563 nm	N/A	N/A
AJNDE35a	16.8 %	510 nm	13.9 %	510 nm	11.6 %	514 nm

The blue-shifting of the fluorescence emission in the matrix can be caused by several factors including the polarity and free volume of the matrix.[38, 73, 75] Interactions between the probe and the matrix may also alter the non-radiative decay rates of the fluorescence thus affecting the quantum yield of the probe.[38, 75] These factors will need further study to help elucidate how these matrix properties affect the emission of the probes in the matrix.

8.2.3 Characterize New Thermal Damage Probes

There are several issues with the probes that could be addressed to improve the performance going forward. As described in section AJNDE16 is not compatible with some epoxies like Toray 3900 because it can activate during the cure. The synthesis of AJNDE35 is very expensive and the process may be difficult to scale up production for industrial applications. In addition, AJNDE16 and AJNDE35 may not be an ideal for a multiplex system because of the significant overlap in the fluorescence emission spectra. It may be easier to observe and measure changes in the fluorescence if there is greater separation of the fluorescence emission of the peaks. Also some study on the degradation kinetics of the epoxy need to be performed so that the kinetics of the probe activation can be better designed to match the degradation process. In order to address these issues, new probes are being developed to improve the scalability, emission wavelength, quantum yield of the probes, and kinetic matching of the probes to the degradation. After the design and synthesis of these new probes is completed, the fluorescence

emission, kinetics, and suitability to use in a multiplexed TTI system with other probes will need to be characterized.

9. ACKNOWLEDGEMENTS

The author would like to thank the Boeing Company's University Research Program for funding this project, under project #BL8DL (Witness Surface Coatings Project). The author would also like to thank his Ph.D advisor Dr. Brian Flinn; co-PI on the project Dr. Alex Jen, co-researchers Dr. Zhengwei Shi, Dr. Sei-Hum Jang, Dr.Ryan Toivola. Jeffrey Yang, and Burny Lai for all the help and guidance they provided. The author would also like to thank the other Flinn group members Gary Weber, Ashley Tracey, Curtis Hickmott, Dana Rosenbladt, David Pate, and Tamar Sisneros for their support. Last, but not least the author would like to thank his family and friends who helped him through some of the rough times in my graduate studies.

10. WORKS CITED

1. Sathish S, Welter JT, Jata KV, Schehl N, and Boehnlein T. *Review of Scientific Instruments* 2012;83(9):11.
2. Fisher WG, Storey JME, Sharp SL, Janke CJ, and Wachter EA. *Applied Spectroscopy* 1995;49(9):1225-1231.
3. Taylor DM and Lin KY. *Journal of Aircraft* 2003;40(5):971-976.
4. Rose N, Lebras M, Bourbigot S, and Delobel R. *Polymer Degradation and Stability* 1994;45(3):387-397.
5. Macan J and Ivankovic M. *Progress in Polymer Degradation and Stability Research*: Nova Science Publishers, Inc., 2008.
6. Buch X and Shanahan MER. *Journal of Applied Polymer Science* 2000;76(7):987-992.
7. Musto P, Ragosta G, Russo P, and Mascia L. *Macromolecular Chemistry and Physics* 2001;202(18):3445-3458.
8. Patterson-Jones JC and Smith DA. *Journal of Applied Polymer Science* 1968;12(7):1601-1620.
9. Musto P. *Macromolecules* 2003;36(9):3210-3221.
10. Damian C, Espuche E, and Escoubes M. *Polymer Degradation and Stability* 2001;72(3):447-458.

11. Buch X and Shanahan MER. *International Journal of Adhesion and Adhesives* 2003;23(4):261-267.
12. Mailhot ND, Morlat-Therias S, Bussiere PO, and Gardette JL. *Macromolecular Chemistry and Physics* 2005;206(5):585-591.
13. Mailhot N, Morlat-Theias S, Ouahioune M, and Gardette JL. *Macromolecular Chemistry and Physics* 2005;206(5):575-584.
14. Anderson BJ. *Polymer Degradation and Stability* 2011;96(10):1874-1881.
15. Bellenger V and Verdu J. *Journal of Applied Polymer Science* 1983;28(9):2677-2688.
16. Tsotsis TK. *Journal of Composite Materials* 1995;29(3):410-422.
17. Schieffer A, Maire JF, and Leveque D. *Composites Science and Technology* 2002;62(4):543-549.
18. Street KN, Russell AJ, and Bonsang F. *Composites Science and Technology* 1988;32(1):1-14.
19. Leveque D, Schieffer A, Mavel A, and Maire JF. *Composites Science and Technology* 2005;65(3-4):395-401.
20. Tandon GP and Ragland WR. *Composites Part A-Applied Science and Manufacturing* 2011;42(9):1127-1137.
21. Tandon GP and Pochiraju KV. *Journal of Composite Materials* 2011;45(4):415-435.
22. Bowles KJ. *Journal of Composites Technology & Research* 1999;21(3):127-132.
23. Bowles KJ, Jayne D, Leonhardt TA, and Bors D. *Journal of Advanced Materials* 1994;26(1):23-32.
24. Bowles KJ, Madhukar M, Papadopoulos DS, Inghram L, and McCorkle L. *Journal of Composite Materials* 1997;31(6):552-579.
25. Rouquie S, Lafarie-Frenot MC, Cinquin J, and Colombaro AM. *Composites Science and Technology* 2005;65(3-4):403-409.
26. LeBras M, Rose N, Bourbigot S, Henry Y, and Delobel R. *Journal of Fire Sciences* 1996;14(3):199-234.
27. Buch X and Shanahan MER. *Polymer Degradation and Stability* 2000;68(3):403-411.
28. Lesnikovich AI and Levchik SV. *Journal of Thermal Analysis* 1983;27(1):89-94.
29. Levchik SV, Levchik GF, and Lesnikovich AI. *Thermochimica Acta* 1985;92(SEP):157-160.
30. Fisher WG, Meyer KE, Wachter EA, Perl DR, and Kulowitch PJ. *Materials Evaluation* 1997;55(6):726-729.
31. Sathish S, Welter J, Reibel R, and Buynak C. *Review of Quant. Nondest. Eval.* 2006;25:1015-1018
32. Smith B. *Fundamentals of Fourier Transform Spectroscopy*: CRC Press, Inc., 1996.
33. Shelley PH, Vahey PG, Werner GJ, and Seelenbinder J. *Proceedings of SAMPE Annual Technical Conference*, May 23-26, 2011. Long Beach, CA, United states.
34. Dara IH, Ankara A, Akovali G, and Suzer S. *Journal of Applied Polymer Science* 2005;96(4):1222-1230.
35. Matzkanin G and Hansen G. *Heat Damage in Graphite Epoxy Composites: Degradation, Measurement, and Detection*. 1998.
36. Valeur B. *Molecular Fluorescence Principles and Applications*: Wiley-VCH Verlag GmbH, 2001.
37. Rigail-Cedeno A and Sung CSP. *Polymer* 2005;46(22):9378-9384.

38. Olmos D, Aznar AJ, Baselga J, and Gonzalez-Benito J. *Journal of Colloid and Interface Science* 2003;267(1):117-126.
39. Pucci A, Bizzarri R, and Ruggeri G. *Soft Matter* 2011;7(8):3689-3700.
40. Hu JM and Liu SY. *Macromolecules* 2010;43(20):8315-8330.
41. Sing C, Kunzelman J, and Weder C. J. *Materials Chemistry* 2009;19:104-110.
42. Crenshaw BR, Kunzelman J, Sing CE, Ander C, and Weder C. *Macromolecular Chemistry and Physics* 2007;208(6):572-580.
43. Kinami M, Crenshaw BR, and Weder C. *Chemistry of Materials* 2006;18(4):946-955.
44. Kunzelman J, Gupta M, Crenshaw BR, Schiraldi DA, and Weder C. *Macromolecular Materials and Engineering* 2009;294(4):244-249.
45. Crenshaw BR, Burnworth M, Khariwala D, Hiltner A, Mather PT, Simha R, and Weder C. *Macromolecules* 2007;40(7):2400-2408.
46. Tang L, Whalen J, Schutte G, and Weder C. *ACS Applied Materials & Interfaces* 2009;1(3):688-696.
47. Wu D, Wang YJ, Chen JC, Ye XQ, Wu QM, Liu DH, and Ding T. *Food Control* 2013;34(1):230-234.
48. Tsironi T, Stamatiou A, Giannoglou M, Velliou E, and Taoukis PS. *LWT-Food Science and Technology* 2011;44(4):1156-1163.
49. Lee BS and Shin HS. *Food Science and Biotechnology* 2012;21(5):1483-1487.
50. Galagan Y and Su WF. *Food Research International* 2008;41(6):653-657.
51. ASTM. F1416-96. Standard Guide for Selection of Time-Temperature Indicators 1996 (2003).
52. Schwartz M. *Encyclopedia of Smart Materials*, Volumes 1-2: John Wiley & Sons, 2002.
53. Yam KL. *Wiley Encyclopedia of Packaging Technology* (3rd Edition). John Wiley & Sons, 2009.
54. Gentili D, Durso M, Bettini C, Manet I, Gazzano M, Capelli R, Muccini M, Melucci M, and Cavallini M. *Scientific Reports* 2013;3.
55. Samat A and Guglielmetti R. *Chromogenic Materials, Thermochromic*. *Kirk-Othmer Encyclopedia of Chemical Technology*: John Wiley & Sons, 2000.
56. Azizian F, Field AJ, and Heron BM. *Dyes and Pigments* 2013;99(2):432-439.
57. Inouye M, Tsuchiya K, and Kitao T. *Angewandte Chemie-International Edition in English* 1992;31(2):204-205.
58. Yamamoto S, Furuya H, Tsutsui K, Ueno S, and Sato K. *Crystal Growth & Design* 2008;8(7):2256-2263.
59. Demchenko AP. *Journal of Fluorescence* 2010;20(5):1099-1128.
60. Wang FW, Lowry RE, and Fanconi BM. *Polymer* 1986;27(10):1529-1532.
61. Heyes AL, Seefeldt S, and Feist JP. *Optics and Laser Technology* 2006;38(4-6):257-265.
62. Natrajan VK and Christensen KT. *Measurement Science & Technology* 2009;20(1).
63. Barilero T, Le Saux T, Gosse C, and Jullien L. *Analytical Chemistry* 2009;81(19):7988-8000.
64. Bur AJ, Vangel MG, and Roth SC. *Polymer Engineering and Science* 2001;41(8):1380-1389.
65. Chandrasekharan N and Kelly LA. *Journal of the American Chemical Society* 2001;123(40):9898-9899.
66. Creton R. *Developmental Brain Research* 2004;151(1-2):33-41.

67. Yu WM, Sandoval RM, and Molitoris BA. *American Journal of Physiology-Renal Physiology* 2007;292(6):F1873-F1880.
68. Strong AB. *Fundamentals of Composite Manufacturing: Materials, Methods, and Applications*: Society of Manufacturing Engineers, 2008.
69. Calado VMA and Advani SG. *Processing of Composites*. Cincinatti, OH: Hanser Gardener, 2000.
70. *Applied Polymer Science: 21st Century*: Elsevier Science Ltd., 2000.
71. Allen NS, Binkley JP, Parsons BJ, Phillips GO, and Tennent NH. *Polymer Photochemistry* 1982;2(2):97-107.
72. Allen NS, Binkley JP, Parsons BJ, Phillips GO, and Tennent NH. *Polymer Photochemistry* 1982;2(5):389-393.
73. Song JC and Sung CSP. *Macromolecules* 1993;26(18):4818-4824.
74. Paik HJ and Sung NH. *Polymer Engineering and Science* 1994;34(12):1025-1032.
75. Lin KF and Wang FW. *Polymer* 1994;35(4):687-691.
76. Sung CSP, Pyun E, and Sun HL. *Macromolecules* 1986;19(12):2922-2932.
77. Oxtoby D, Gillis, H., Nachtrieb, N. *Principles of Modern Chemsitry*, 4th ed.: Saunders College Publishing, 1999.
78. Kalambet Y, Kozmin Y, Mikhailova K, Nagaev I, and Tikhonov P. *Journal of Chemometrics* 2011;25(7):352-356.
79. Peng XJ, Yang ZG, Wang JY, Fan JL, He YX, Song FL, Wang BS, Sun SG, Qu JL, Qi J, and Yang M. *Journal of the American Chemical Society* 2011;133(17):6626-6635.
80. Zhu HJ, Zhang W, Zhang K, and Wang SH. *Nanotechnology* 2012;23(31).
81. Peng X, Wu Y, Fan J, Tian M, and Han K. *Journal of Organic Chemistry* 2005;70(25):10524-10531.
82. Yousuf A and Kulowitch P. *Proceedings of ASEE Annual Conference* June 18- June 21, 2000. St. Louis, MO, United states: 1447-1455.
83. Grynkiewicz G, Poenie M, and Tsien RY. *Journal of Biological Chemistry* 1985;260(6):3440-3450.
84. Sung SPS, Chin IJ, and Yu WC. *Macromolecules* 1985;18(7):1510-1512.